A STUDY ON PROTEIN AND DNA ANALYSIS BY CAPILLARY ELECTROPHORESIS

by

Asuman Nevra ÖZER

BS. in Ch.E., Boğaziçi University, 1997

Submitted to the Institute for Graduate Studies in
Science and Engineering in partial fulfillment of
the requirements for the degree of
Master of Science
in
Chemical Engineering

Boğaziçi University

1999

ACKNOWLEDGMENTS

The research presented in this thesis was conducted at the Chemical Engineering Department of the Boğaziçi University between September 1997 and June 1999 supervised by Assoc. Prof. Dr. Kutlu Ülgen and Prof. Dr. Betül Kırdar.

I am very much grateful to my supervisor Assoc. Prof. Dr. Kutlu Ülgen for all her kindness, moral support and friendly encouragement throughout both my undergraduate and graduate studies and this research. I am indebted to Prof. Dr. Betül Kırdar for all the help, motivation and guidance she has given and for evaluation of my thesis. I feel fortunate to have the chance of working with these great supervisors.

I am obliged to Prof. Dr. Zeynep İlsen Önsan for her precious comments on my work and for her guidance throughout my academic studies in the department. I also thank Prof. Dr. Dilek Çalgan and Assoc. Prof. Dr. Belma Özbek for the time they devoted to reading and commenting on my thesis.

I would like to express my gratitude to Mitch Halloran in Düzen Laboratories in Ankara for his hospitality and precious time devoted to my unlucky experiments and for all the information and comments he supplied whenever I was confused. I also benefited greatly from the valuable suggestions of Tuncer Onay from the Biology Department.

Heartfelt thanks are due to Eko and Bern for their interest in my work and their everlasting support and help I will always appreciate. More than thanks are needed to express my feelings to all my beloved friends, either close or faraway but always with me, either in the lab or outside or whirling under my three stars, some offering suggestions and helping me out, some being the most tolerant and understanding during my neurotic times and making me laugh when I cry, some making this work harder but me more ambitious. Nothing would have been possible without the "joie de vivre" they bring into my world.

Finally, this thesis is dedicated to my parents whom I owe everything and my brother, my dear bodyguard.

ABSTRACT

The aim of this research was to establish a method for the analysis of several proteins and DNA using capillary electrophoresis. Bovine serum albumin, human serum proteins and some restriction enzymes namely Taq1, EcoR1, Pst1 were analysed by capillary zone electrophoresis in fused silica capillary columns. Entangled solution capillary electrophoresis by applying dynamic coating with the use of a run buffer containing non-cross linked polyacrylamide and capillary gel electrophoresis in polyacrylamide gel-filled columns were performed for the separation of the 491 bp and 488 bp PCR amplified DNA fragments from Turkish cystic fibrosis carriers. The effect of various parameters such as the use of different buffer systems, capillary dimensions, detector wavelengths, polarity modes, applied voltage, sample injection modes and sample loading amounts on the analytical parameters were evaluated. The optimum wavelength for the detection of proteins was 214 nm. Highest voltages possible should be used for the fastest and most efficient separation. The use of a shorter capillary column resulted in faster migration, less zone broadening and narrower peaks. The TBE buffer used for the analysis of restriction enzymes was found to be not suitable while the most appropriate buffer system for the analysis of human serum proteins was Dolnik's buffer. For the analysis of DNA fragments, optimization of the dynamic coating procedure or static coating of the capillary column with linear polyacrylamide should be developed.

ÖZET

Bu çalışmada, bazı proteinler için bir kapiler elektroforez metodu geliştirmek amacıyla, sığır albumini, insan serum proteinleri, Taq1, EcoR1, Pst1 restriksiyon enzimleri ve polimeraz zincir reaksiyonlarıyla amplifiye edilmiş DNA kısımları silika kapiler kolonlarda analiz edildi. Lineer poliakrilamid içeren tampon çözeltiyle dinamik kaplama ve jel dolu kapiler kolonlar kullanılan jel elektroforez metotları, 491 ve 488 baz çiftine sahip kistik fibroz taşıyıcısı Türk hastalardan alınmış DNA parçalarını ayrıştırmak için kullanıldı. Değişik tampon çözeltileri, kolon boyutları, dedektör dalga boyu, polarite, voltaj, örnek injeksiyon modu ve miktarının analitik parametreler üzerindeki etkileri incelendi. Hızlı ve verimli ayrıştırma için mümkün olan en yüksek voltajda çalışmanın ve proteinler için en uygun dalga boyunun 214 nm olduğu gözlendi. Kısa kolon kullanımı erken protein çıkışına, daha az bant genişlemesine ve dar piklere sebep oldu. TBE tampon çözelti sisteminin restriksiyon enzimleri için uygun olmadığı bulundu. Serum proteinleri içinse Dolnik çözeltisinin kullanımının verimli olduğu görüldü. DNA kısımlarının incelenmesinde, dinamik kaplama metodunun optimizasyonu veya lineer poliakrilamidle statik kaplama metodunun geliştirilmesine karar verildi.

TABLE OF CONTENTS

Page

Page

LIST OF FIGURES

Page

Page

Page

Page

LIST OF TABLES

LIST OF ABBREVIATIONS

abs	absorbance
AU	absorbance unit
bp	base pair
BSA	bovine serum albumin
CE	capillary electrophoresis
CF	cystic fibrosis
CFTR	cystic fibrosis transmembrane conductance regulatory
CGE	capillary gel electrophoresis
CIEF	capillary isoelectric focusing
CITP	capillary isotachophoresis
CZE	capillary zone electrophoresis
Da	daltons
dH_2O	distilled water
DNA	deoxyribonucleic acid
dNTP	2'-deoxynucleoside 5'-triphosphate
DTT	dithiothreitol
EDTA	ethylenediaminetetraaceticacid
Elc.	electromigration
Exp	Experiment
HCl	hydrochloric acid
HPCE	high performance capillary electrophoresis
HPLC	high performance liquid chromatography
Hyd.	Hydrostatic injection
I.D.	inner diameter
IEF	isoelectric focusing
KCl	potassium chloride
kDa	kilodaltons
kV	kilovolts
mAU	mili-absorbance unit
MBE	moving-boundary electrophoresis

MEKC	micellar electrokinetic chromatography
min	minutes
mV	milivolts
NaCl	sodium chloride
nm	nanometers
PA	polyacrylamide
PAGE	polyacrylamide gel electrophoresis
PCR	polymerase chain reaction
RE	restriction enzyme
s	seconds
SDS	sodium dodecyl sulphate
S/N	signal-to-noise ratio
TBE	Tris-Borate-EDTA
TEMED	N,N,N',N'-tetramethylethylenediamine
UV	ultraviolet
V	volts
ZE	zone electrophoresis
λ	detector wavelength (nm)

1. INTRODUCTION

The emergence of a new biotechnological industry utilizing recombinant DNA techniques for the production of highly specialized biomolecules has increased the demand for sophisticated analytical instrumentation and methodologies. In the biotechnological and pharmaceutical industries, these analytical instruments and methods are used for the identification of chemicals and structures, control of purity and assay of potency. Biomolecules such as proteins, nucleic acids and polysaccharides are often present in very small quantities and sample sizes are often limited, requiring highly sensitive and selective separation techniques. The same is true for the analysis of complex samples of biological origin, i.e. in clinical and diagnostic applications. Miniaturized, microcolumn separation techniques, such as micro-HPLC, capillary gas chromatography or capillary electrophoresis (CE) are particularly suitable for the detection of analytes in very small (micro) volumes (Schwartz, 1992).

Capillary electrophoresis (CE) is a fine example of optimizing the transport mechanisms in order to yield highly efficient separations. The high efficiency of high performance capillary electrophoresis (HPCE) gives the opportunity to improve the peak capacity of the separation. That is the ability to better separate complex mixtures or for simple mixtures, separate them very rapidly. Peak symmetry by high performance capillary electrophoresis tends to be excellent. With the absence of a stationary phase, factors that contribute to peak tailing are minimized (Weinberger, 1998).

High performance capillary electrophoresis offers a novel format for liquid chromatography and electrophoresis which:

1. employs capillary tubing within which the electrophoretic separation occurs;
2. utilizes very high electric field strengths, often higher than 500 V/cm;
3. uses modern detector technology such that the electropherogram often resembles a chromatogram;
4. has efficiencies in the order of capillary gas chromatography or even greater;

5. requires minute amounts of sample;
6. is easily automated for precise quantitative analysis and ease of use;
7. consumes limited quantities of reagents;
8. is applicable to the widest selection of analytes compared to any other analytical separation technique.

The purpose of this research was to establish a method for the analysis of several proteins such as bovine serum albumin, human serum proteins, restriction enzymes Taq1, EcoR1, Pst1 and PCR amplified DNA fragments from Turkish cystic fibrosis carriers using capillary electrophoresis. The factors affecting analytical parameters such as migration time, peak height and peak shape were studied. The effect of the use of different buffer systems, capillary dimensions, detector wavelengths, polarity modes, applied voltage, sample injection modes and sample loading amounts on the analytical parameters were investigated.

2. THEORETICAL BACKGROUND

2.1 Basic Electrophoretic Separation Modes

Electrophoresis is defined as the transport of electrically charged compounds in solution under the influence of an electric field. It includes a great number of systems involving either differential or equilibrium gradient methods. They are all based on one of the four electrophoretic modes, namely moving-boundary electrophoresis (MBE), zone electrophoresis (ZE), isotachophoresis (ITP) and isoelectric focusing (IEF). All electrophoretic processes are fundamentally unique and they can all be carried out in the same electrophoretic equipment (Kuhn and Hoffstetter-Kuhn, 1993).

2.1.1 Zone Electrophoresis

For zone electrophoresis, the column and the electrode reservoirs have to be filled with the carrier electrolyte, which conducts the electric current and provides the buffering capacity (Figure 2.1). The sample, consisting of a mixture of anions and cations, is introduced into this continuous buffer system at one end of the tube as a sharp initial zone. This zone represents the only discontinuity of the system. Under the influence of the electric field, the ionic species of the carrier electrolyte and of the sample migrate to the corresponding electrode, cations toward the cathode and anions toward the anode, respectively. Due to its high concentration the carrier electrolyte determines the physical properties such as conductance and pH throughout the capillary. The influence of the sample can be neglected. Therefore the sample components migrate independently from the carrier electrolyte with their specific velocities. After some time, they will separate into distinct zones if their differences in net mobilities are high enough. Their relative position and their shapes continuously change with time. Thus, no steady-state is reached in ZE (Kuhn and Hoffstetter-Kuhn, 1993).

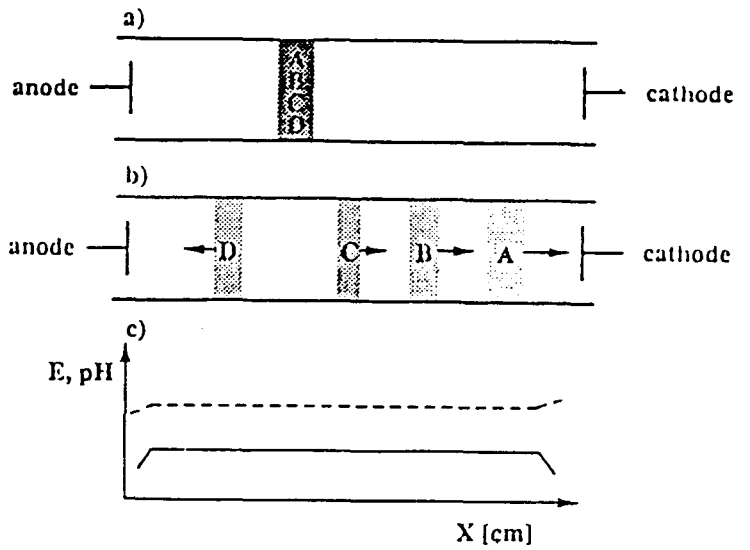

FIGURE 2.1. Principle of zone electrophoresis. a) initial state, b) differential migration of the distinct sample zones, c) profile of field strength (*plain line*) and pH (*dashed line*) across the separation chamber (Kuhn and Hoffstetter-Kuhn, 1993).

ZE can be carried out either as a one phase process in free solution or in combination with a solid support medium or a second liquid phase. In the latter cases, separation is not only governed by electrophoretic migration, but also by molecular sieving or partitioning between two phases (Grossman and Soane, 1991).

2.1.2 Isotachophoresis

In isotachophoresis a small quantity of sample is introduced at the interface of a discontinuous buffer system, consisting of a leading (L) and a terminating (T) electrolyte. In Figure 2.2, the separation of three cationic species (A, B, C) in a narrow-bore tube is simulated. The tube and the cathode reservoir are filled with the leading electrolyte whose cations must have a higher mobility than the cations that have to be separated. Additionally, the anions of the leader should possess a buffer capacity at the pH at which the sample is separated. The anode reservoir is filled with the terminating electrolyte which

must possess a lower mobility than the cationic species of the sample (Figure 2.2.a) (Kuhn and Hoffstetter-Kuhn, 1993).

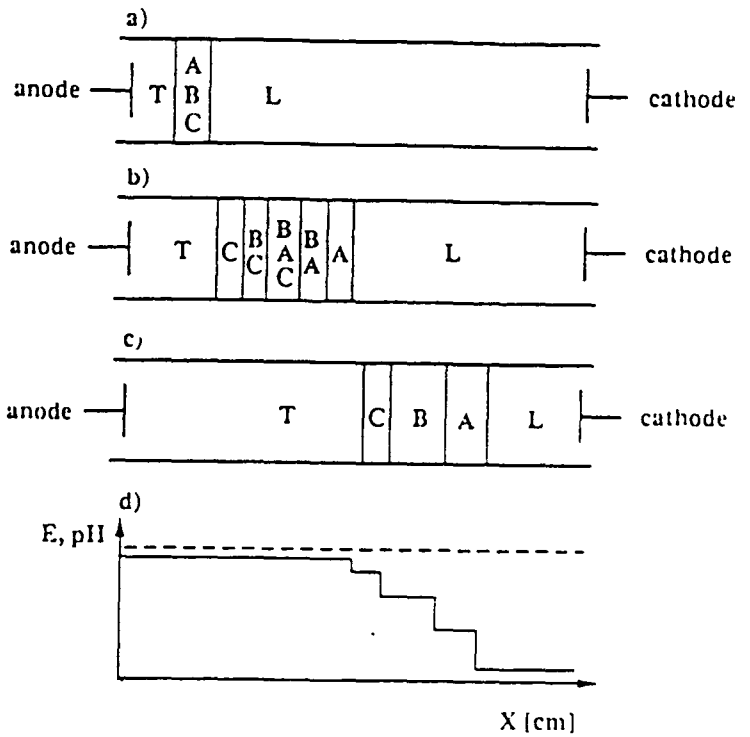

FIGURE 2.2. Principle of isotachophoresis. a) initial state, b) intermediate state, c) steady-state, d) profile of field strength (*plain line*) and pH (*dashed line*) across the separation chamber (Kuhn and Hoffstetter-Kuhn, 1993).

If voltage is applied, the cationic compound with the highest mobility (A) will migrate faster, leaving behind those with lower mobilities (B and C). This results in two mixed zones in front of and behind the original sample zone (Figure 2.2.b). Due to their higher mobilities the cations of the leading electrolyte can never be passed by sample cations. The terminating cations, however, are not able to pass the cationic compounds of the sample. Hence, the sample zones are sandwiched between leader and terminator. In order to maintain the transport of the current through the system, the mixed sample zones are separated further, until each zone contains only one cationic species (Figure 2.2.c). No further changes occur and a steady state has been reached. All zones must migrate

connected to each other like a moving train with the same velocity as the leading cation, because no background electrolyte is present that could transport the electric current, if they were released. The electric field strength shows a stepwise profile along the capillary (Figure 2.2.d) (Kuhn and Hoffstetter-Kuhn, 1993).

For the separation of anionic components the leading electrolyte possessing the highest mobility has to be filled into the anode reservoir and the terminating electrolyte, which must possess a lower mobility than the sample, into the cathode reservoir. The separation takes place according to the same principle, but the migration is directed towards the anode (Weinberger, 1998)

2.1.3 Isoelectric Focusing

Isoelectric focusing is limited to the separation of amphoteric substances, because the sample components are not separated due to their differences in net mobility as in the other electrophoretic modes, but due to their different isoelectric points (pI), where the pI is that pH at which an ampholyte has zero net charge. At that pH they are present mainly in the zwitterionic form and do not migrate when they are exposed to an electric field. At lower pH, they will be positively charged and migrate to the cathode. If the pH is higher than their pI, they will be negatively charged thus migrate towards the anode. In general, separation takes place in a linear pH gradient across the separation chamber (Figure 2.3) (Zhu et al., 1989).

The pH gradient is generated by a mixture of carrier ampholytes which have isoelectric points ranging from the acidic to the basic range in close proximity to each other and possess a good buffering capacity. The ampholyte solution, commonly a mixture of polyamino polycarboxylic acids, is placed in the separation chamber. The anode compartment is filled with an acidic solution, whereas the cathode compartment contains a base. If voltage is applied, H_3O^+ ions migrate to the cathode and OH^- ions to the anode.

The ampholytes migrate according to their charge and pI towards the corresponding electrodes and buffer the migrating H_3O^+ and OH^- ions (Figure 2.3.a). The local pH is given by the particular carrier ampholyte whose charge is balanced by the H_3O^+ and OH^- concentration, respectively. A sample consisting of three amphoteric substances is introduced to this prebuilt pH gradient (Figure 2.3.b). The sample can also be dissolved directly in the solution of carrier ampholytes, before the pH gradient is generated. In both cases, the separation mechanism is the same. Each ampholyte migrates towards the position where pH is equal to its pI. At this position its velocity becomes zero, and the component will be concentrated into a narrow zone (Figure 2.3.c). As in ITP, the system is able to correct zone broadening effects: if the compound changes its position by diffusion, it will be charged again, thus migrating back to the point where its velocity is zero (Kuhn and Hoffstetter-Kuhn, 1993).

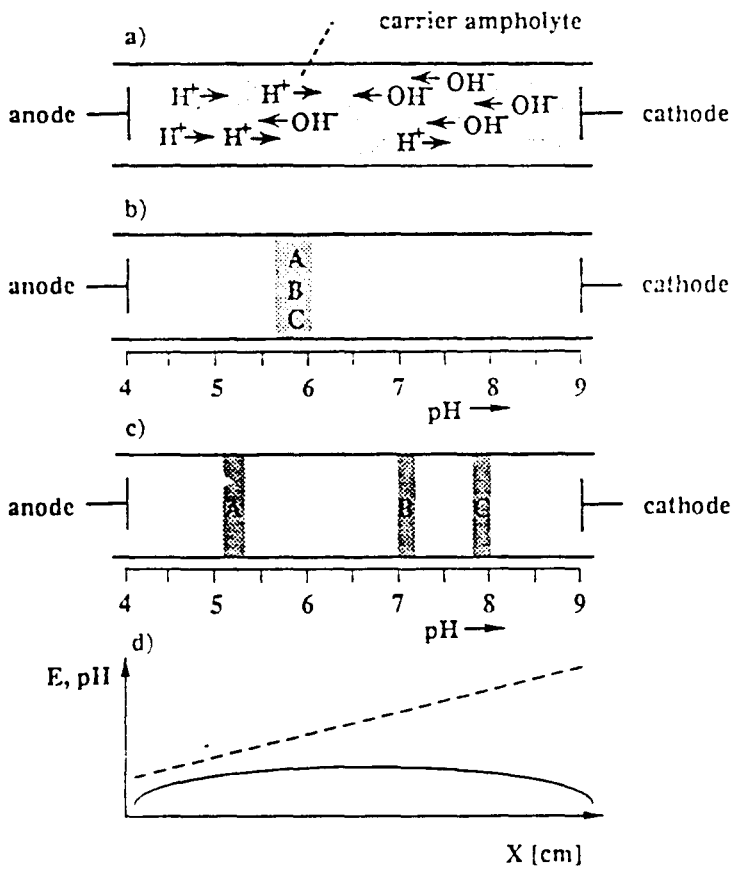

FIGURE 2.3. Principle of isoelectric focusing. a) generation of the pH gradient, b) sample introduction, c) steady-state, d) profile of field strength (*plain line*) and pH (*dashed line*) across the separation chamber (Kuhn and Hoffstetter-Kuhn, 1993).

2.2 Set-up for Capillary Electrophoresis

All electrophoretic modes can be carried out, in principle, using the same equipment, which consists of five units: the anode and the cathode reservoirs with the corresponding electrodes, the separation chamber, the injection system and the detector. The basic instrumental set-up to accomplish capillary electrophoresis is depicted in Figure 2.4. A capillary tube filled with the buffer solution is placed between two buffer reservoirs. The electric field is applied by means of a high voltage power supply which can generate voltages up to 30 kV (Weinberger, 1998). Injection of the analytes is performed by replacing one buffer reservoir by the sample vial. A defined sample volume is introduced into the capillary by either hydrodynamic flow or electromigration. An on-column detector is located at the end of the capillary which is opposite to the injection side.

If the uncoated open-tube fused silica capillary is used as the separation chamber, as is mostly the case in CZE, two electrokinetic actions occur under the influence of the electric field. First, electrophoresis of the ions takes place, secondly, electroosmosis, which takes place due to the immovable charge of the capillary walls being effective from the basic to weak acid pH range. Separation, however, is based solely on electrophoresis while electroosmosis causes a liquid transport analogous to a mechanical pump. Because the electroosmotic flow in aqueous solution is mostly directed toward the cathode, the sample is injected at the anode. The sample components migrate with different migration velocities, depending on their charge densities, towards the corresponding electrodes. They are all carried through the detection system by the electroosmotic flow, which is higher than the migration velocities of the ions (Kuhn and Hoffstetter-Kuhn, 1993).

If electrophoresis is carried out in the absence of electroosmotic flow, injection is accomplished at the electrode with the same sign as the charged compounds to be separated. In practice this can easily be achieved by changing the polarity of the electrodes (Cheng and Mitchelson, 1994).

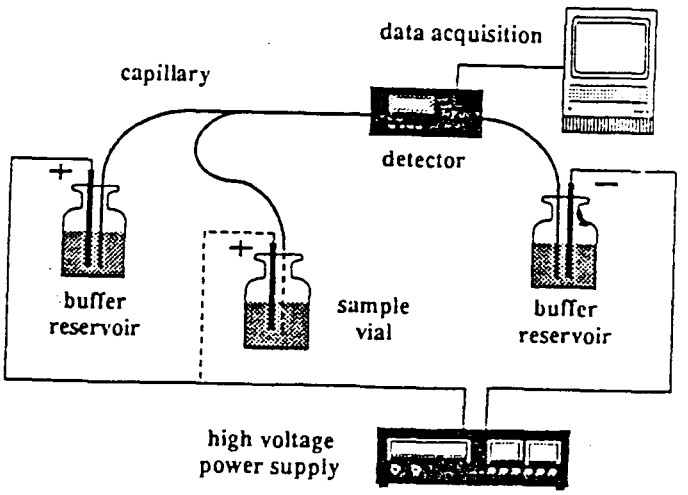

FIGURE 2.4. Instrumental set-up of a capillary electrophoresis system (Kuhn and Hoffstetter-Kuhn, 1993).

Most commercial instruments use on-column UV-VIS absorbance or fluorescence detection. The detector response is recorded versus the migration time. The output which is analogous to a chromatogram obtained in HPLC is called an electropherogram. A computer connected to the detector allows data acquisition and interpretation (Weinberger, 1998).

2.3 Theory of Electrophoretic Migration

Electrophoretic migration of ions or charged particles is obtained by harnessing electrical forces along the axis of an electric field gradient. The electrophoretic migration shows itself macroscopically as a conduction of electric current in a solution under the influence of an applied voltage following Ohm's law.

$$U = R \times I \tag{2.1}$$

where U is the electric potential (Volts), R is the electric resistance of the electrolyte (Ohms) and I is the electric current (Amperes). The resistance R of the solution is the reciprocal to the conductance L which can be measured by a conductometer. The conductance depends on the geometry of the measuring device, the ionic species and the electrolyte concentration. In practice the measured conductance L is related to the specific conductance κ by dividing the cell constant according to

$$L = \kappa \times K^{-1} \tag{2.2}$$

where L is the measured conductivity in Siemens (S), κ is the specific conductance (S/cm) and K is the cell constant (1/cm) (Kuhn and Hoffstetter-Kuhn, 1993).

If the specific conductance is divided by the concentration c, the equivalent or molar conductance Λ becomes

$$\Lambda = \frac{K}{c}\left[cm^2\Omega^{-1}mol^{-1}\right] \tag{2.3}$$

In practice, equivalent weights instead of molecular weights of the ions are usually taken into account to allow a comparison of the conductive properties of electrolyte solutions. For this purpose the molarity of an ion has to be divided by the stoichiometric number (Schwartz et al., 1992).

According to the first Kohlrausch law, anions and cations contribute independently to the conductance, which means that the equivalent conductance Λ is the sum of the ionic equivalent conductances of the cations (λ^+) and the anions (λ^-). For strong (completely dissociated) 1:1 electrolytes

$$\Lambda = \lambda^{+} + \lambda^{-} \tag{2.4}$$

where the ionic equivalent conductances are in $cm^2\Omega^{-1}mol^{-1}$. The equivalent conductance should be independent of concentration according to (2.3). This is only true at infinite dilution. For strong electrolytes, the second Kohlrausch law describes empirically the influence of the concentration on the equivalent conductance:

$$\Lambda_c = \Lambda_0 - k\sqrt{c} \tag{2.5}$$

where Λ_c is the equivalent conductance at a concentration c, Λ_0 is the limiting equivalent conductance, c is the electrolyte concentration (M) and k is a constant ($M^{-1/2}$). Ionic interactions are responsible for the fact that the equivalent conductance decreases with increasing electrolyte concentration (Kuhn and Hoffstetter-Kuhn, 1993).

In the case of weak electrolytes, the equivalent conductance Λ_c is strongly affected by the dissociation of the ions. The quotient of the equivalent conductance measured at a concentration c and the limiting equivalent conductance is equal to the dissociation degree α :

$$\frac{\Lambda_c}{\Lambda_0} = \alpha \tag{2.6}$$

α describes the degree of dissociation and is defined as the ratio of the concentration of the dissociated ion to the total concentration of the analyte. α depends both on the pH and on the concentration of the electrolyte solution. Ostwald's law describes the relationship

between the dissociation constant K_c, the concentration of the electrolyte solution c and the equivalent conductance:

$$K_c = \frac{\Lambda_c^2}{(\Lambda_0 - \Lambda_c)\Lambda_0} c \tag{2.7}$$

Since K_c and Λ_0 are constant, this relationship shows the influence of the electrolyte concentration on Λ_c. The equivalent conductance decreases with increasing concentration (Kuhn and Hoffstetter-Kuhn, 1993).

For weak electrolytes ionic interactions do not play such an important role as for strong electrolytes, because the concentration dependence of Λ_c is more affected by the degree of dissociation. Nevertheless, for an exact description of all factors, the right side of (2.6) has to be multiplied by the so-called coefficient of the conductance f_A (Bae and Soane, 1993).

If a charged compound is dissolved in an electrolyte solution, the macroscopically measured conductance of the solution does not provide any information about its migration behavior. In electrophoretic separations, however, the electrophoretic behavior of the charged analyte is more important than that of the whole solution. When the migration of a charged compound in an electrolyte solution at infinite dilution, where no ionic interactions occur, is considered, the charged component i is accelerated by the electric force F_e in a homogeneous electric field.

$$F_e = z_i \times e_0 \times E \tag{2.8}$$

where z_i is the charge number of component i, e_0 is the elemental charge in Coulomb ($C=1.602x10^{-19}$ A.s) and E is the electric field strength (V/cm).

In a viscous hydrodynamic medium the drag force F_d which acts on the moving species i is proportional to its migration velocity v_i^0 and the Newtonian viscosity η of the medium.

$$F_d = k \times \eta \times v_i^0 \tag{2.9}$$

where k is a constant (cm), η is the Newtonian viscosity of the solution (Pa.s) and v_i^0 is the migration velocity of component i at infinite dilution (cm/s). If the acceleration caused by the electric force F_e is counterbalanced by the drag force F_d, the charged species i moves with a constant migration velocity which is given by

$$v_i^0 = \frac{z_i e_0}{6\pi\eta r_i} E \tag{2.10}$$

The hydrodynamic or Stokes radius r_I of the ion i represents the radius of the solvated or, in aqueous solution, hydrated form of the ion. The conductances increase in the opposite direction to that expected when there is no hydration (Kuhn and Hoffstetter-Kuhn, 1993).

According to (2.10), the migration velocity is proportional to the electric field strength. The proportionality factor is called the absolute or limiting electrophoretic mobility μ_i^0. The migration velocity as well as the electrophoretic mobility can have

negative or positive values depending on the sign of the charge number z_i. μ_i^0 is related to the migration velocity by division by the electric field strength.

$$\mu_i^0 = \frac{v_i^0}{E} = \frac{z_i e_0}{6\pi\eta r_i}\left[cm^2V^{-1}s^{-1}\right] \tag{2.11}$$

The absolute electrophoretic mobility μ_i^0 represents the average velocity of a charged species per unit of electric field strength at zero concentration. For a given ion, μ_i^0 is only dependent on the viscosity of the medium. The influence of temperature on the electrophoretic mobility has its origin almost completely in the change in the solvent viscosity with temperature which can be expressed by

$$\eta = C.e^{\frac{E_A}{RT}} \tag{2.12}$$

where C is a constant (Pa.s), E_A is the activity energy for the viscous flow (J/mol), R is the molar gas constant (8.314 J/mol.K) and T is the temperature in degrees Kelvin (Kuhn and Hoffstetter-Kuhn, 1993).

Since the viscosity drops exponentially with increasing temperature, the electrophoretic mobility is increased exponentially with the temperature. In a first approximation for small ΔT values, however, the change in mobility with temperature can be calculated by

$$\mu_{T_2} = \mu_{T_1}\left(1+\alpha.\Delta T\right) \tag{2.13}$$

where α is about 0.02 K^{-1} for aqueous solutions. Thus, as rule of thumb, the mobility increases with rising temperature approximately 2 per cent per one degree Kelvin (Weinberger, 1998).

μ_i^0 is a characteristic constant for a given species in a certain solvent at constant temperature and is proportional to the equivalent conductance at infinite dilution.

$$\Lambda_0 = \lambda_0^+ + \lambda_0^- = \left(\mu_i^{0+} + \mu_i^{0-}\right)F \tag{2.14}$$

where F is the Faraday constant equal to 96,485 C/mol (Kuhn and Hoffstetter-Kuhn, 1993).

The phenomenon of electrostatic interactions in electrolyte solutions has been treated extensively by Debye, Hückel and Onsager and is based on the fact that an ion is always surrounded by oppositely charged counterions. These counterions forming the so-called ionic atmosphere are responsible for the action of two additional forces slowing down the ionic species, namely the electrophoretic retardation F_{ret} and the relaxation effect F_{rel}. this is illustrated in Figure 2.5. The electrophoretic retardation is caused by the fact that the central ion does not migrate in a stationary environment as is assumed by Stokes law. Since the counterions move in the opposite direction to the central ion, the friction force is higher resulting in a decrease of the mobility. Additionally the directed movement of the central ion permanently deforms the ionic atmosphere. The charge density of the ionic atmosphere in front of the central ion is always somewhat lower than behind it. Coulomb forces between the ions tend to rebuild it in its proper arrangement, which takes a finite time. During this relaxation time the central ion is slowed down by the electrical force F_{rel} acting in the opposite direction to its migration (Weinberger, 1998).

The higher the electrolyte concentration, the stronger are the electrostatic interactions not only between the ions of the electrolyte solution, but also between the charged analyte and its counterions. The easiest way to consider the influence of the ionic atmosphere on

the mobility is to exchange the theoretical charge by the smaller effective charge and the hydrodynamic radius by the effective radius of the ion including its atmosphere of counterions (Kuhn and Hoffstetter-Kuhn, 1993).

$$\mu_i = \frac{Q_{eff}}{6\pi\eta R} \tag{2.15}$$

where μ_I is the effective electrophoretic mobility ($cm^2/s.V$), Q_{eff} is the efective charge of the ion (C) and R is the total radius of the ion (cm). As a consequence, if ionic interactions occur, the effective mobility will always be lower than the absolute mobility. According to (2.3) and (2.14) the effective mobilities of all components i are related to the specific conductance of the solution κ as follows:

$$\kappa = F.\sum_{i=1}^{n} c_i \mu_i \tag{2.16}$$

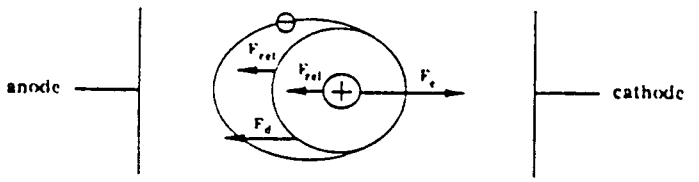

FIGURE 2.5. Forces acting on a charged species in an electrolyte solution (Kuhn and Hoffstetter-Kuhn, 1993).

Especially for colloids and particles where electrophoretic migration is induced as a result of the surface charge caused by adsorbed ions, another definition of the electrophoretic mobility has been developed based on the Debye-Hückel theory of the diffuse double layer at the surface of charged particles,

$$\mu_i = \frac{\zeta.\varepsilon}{4\pi\eta} \tag{2.17}$$

where ζ is the zeta potential (Volts) and ε is the permittivity (dielectric constant) of the medium equal to $4\pi\varepsilon_0\varepsilon_r$ (F/m). In the ideal case, the mobility defined by (2.17) is independent from the size and shape of the particle. In general, this equation should be used for the electrophoretic mobility of particles that are large compared to the thickness of their double layer (Kuhn and Hoffstetter-Kuhn, 1993).

2.4 Determination of Effective Mobility

Calculation of the ionic mobilities using (2.11), (2.15) or (2.17) is very difficult or even impossible. However, μ_I can be calculated from an electropherogram as illustrated in Figure 2.6 which shows a typical separation pattern achieved by CZE in open fused silica tubes in the presence of electroosmotic flow (EOF).

The sample has been injected at the anodic end of the capillary. The migration of the sample components through the detector cell is recorded versus time. The sample consists of a cationic component (1), an anionic component (2) and a neutral substance which moves with the velocity of the electroosmotic flow and serves as an electroosmotic flow marker (EOF marker). If the electroosmotic flow velocity is higher than the velocity of the

anionic compound, a simultaneous detection of cations, anions and neutral species is possible as illustrated in Figure 2.7 (Kuhn and Hoffstetter-Kuhn, 1993).

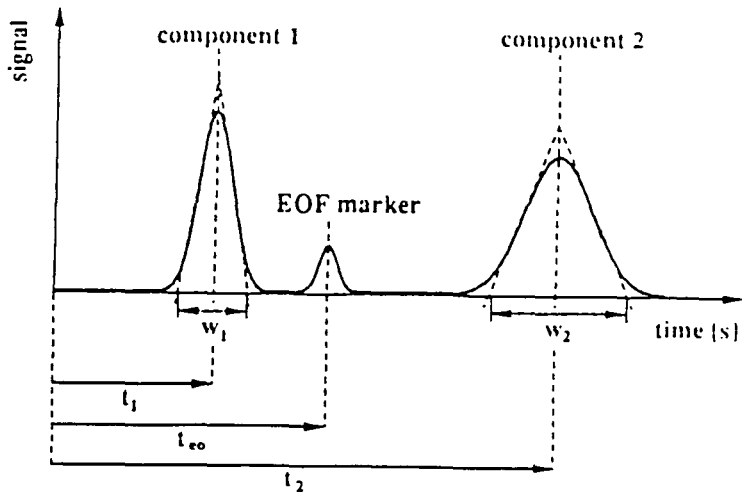

FIGURE 2.6. Schematic diagram of a capillary electrophoretic separation (Kuhn and Hoffstetter-Kuhn, 1993).

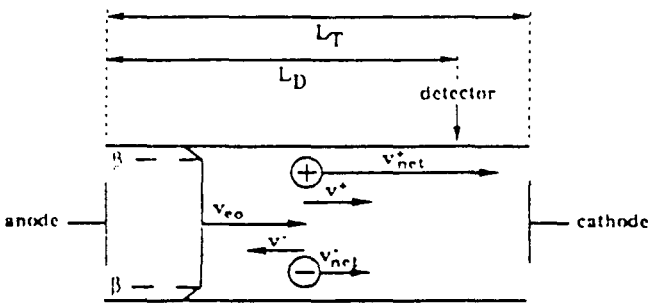

FIGURE 2.7. Schematic representation of the migration of cations and anions in the presence of electroosmosis (Kuhn and Hoffstetter-Kuhn, 1993).

The net velocity $v_{i(net)}$ of component i is to be calculated by dividing the length of the capillary from the injection point to the detector L_D by the migration time t_i. The

electrophoretic velocity v_i can be calculated from the net velocity and the electroosmotic flow velocity v_{eo} as follows:

$$v_i = v_{i(net)} - v_{eo} = \frac{L_D}{t_i} - \frac{L_D}{t_{eo}} \left[cm.s^{-1}\right] \tag{2.18}$$

where L_D is the capillary length to detector or effective capillary length (cm), t_i is the migration time of component i (s), t_{eo} is the migration time of the EOF marker (s), $v_{i(net)}$ is the net velocity of component i (cm/s) and v_{eo} is the electroosmotic flow velocity (cm/s) (Jorgenson and Lukacs, 1981).

v_i takes negative values in the case of anions since v_{eo} is higher than $v_{i(net)}$. Thus, the signs indicate the relative direction of the flow velocity and the electrophoretic or electroosmotic velocity. In practice, however, the negative sign is often neglected. The effective electrophoretic mobility of component i is then given by

$$\mu_i = \frac{v_i}{E} = \frac{v_i L_T}{V} \left[cm^2 V^{-1} s^{-1}\right] \tag{2.19}$$

where L_T is the distance between the electrodes or the total capillary length (cm). If CE is performed in the absence of the electroosmotic flow, where v_i is equal to $v_{i(net)}$, the following simplified equation can be used instead of (2.18) and (2.19) (Jorgenson and Lukacs, 1981).

$$\mu_i = \frac{v_i}{E} = \frac{L_D L_T}{t_i V} \left[cm^2 V^{-1} s^{-1}\right] \tag{2.20}$$

2.5 Electroosmosis

Electroosmosis or also known as "electroendosmosis" is one of the oldest electrokinetic effects discovered. It is a basic phenomenon in all electrophoretic separation processes. It can be described as the relative motion of a liquid to a fixed charge surface caused by an electric field. This motion is also called electroosmotic flow (EOF). The magnitude and the direction of the resulting electroosmotic flow depend on the composition of the capillary and the nature of the solute within the tube. Empirically it was found that the phase with the higher dielectric constant is positively polarized versus the other. Because of its extremely high dielectric constant, water is usually positively polarized in comparison to the fused silica surface. Hence, if an electric field is applied across the fused silica capillary, the mobile ions of the solution migrate with their hydrate water towards the cathode resulting in a flow of the whole solution (Weinberger, 1998).

In a pressure-driven flow system such as HPLC, frictional forces at the liquid-solid boundaries cause a strong pressure drop across the capillary. These forces result in a laminar or parabolic flow profile. As a consequence, a cross-sectional velocity gradient occurs within the capillary resulting in a velocity profile such that the velocity vector is highest in the middle of the tube and goes toward zero approaching the walls (Figure 2.8.a). In electrically-driven systems the liquid flow caused by electroosmosis shows a plug profile because the driving force is uniformly distributed along the capillary. Consequently, a uniform velocity vector across the tube occurs. Only in the double layer region, very close to the capillary surface, the flow velocity approaches zero (Figure 2.8.b). Zone broadening caused by the laminar flow profile in HPLC is therefore negligible in CZE (Kuhn and Hoffstetter-Kuhn, 1993).

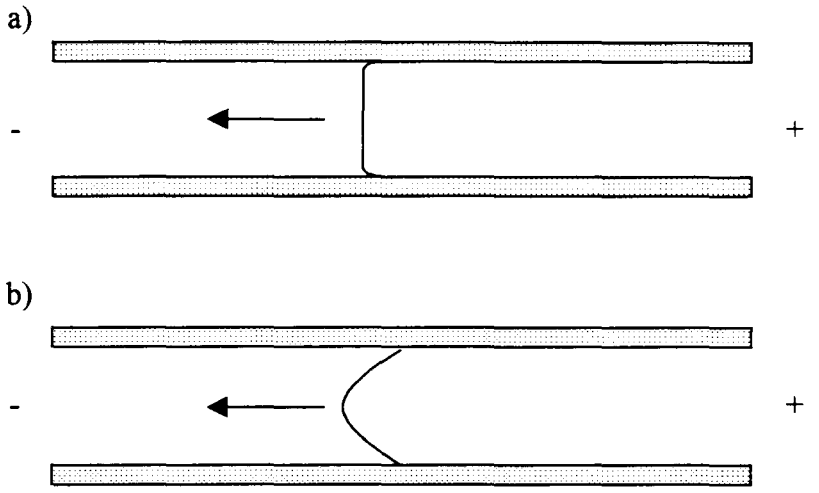

FIGURE 2.8. Capillary flow profiles. a) pressure-driven systems, b) electrically-driven systems (Weinberger, 1998).

The reason for the relative motion of the buffer solution can be found in the nature of the capillary surface. When silica is in contact with an aqueous solution, its surface hydrolyzes to form silanol surface groups. These groups may be positively charged, neutral or negatively charged, depending on the pH value of the surrounding electrolyte solution. Counterions tend to adsorb onto the silica wall by electrostatic attractions to balance the surface charge. According to Stern's model, a rigid double layer of adsorbed ions is superposed by a diffuse double layer allowing diffusion of ions by thermal motion. This double layer system causes an electrical potential at the interface between silica surface and electrolyte solution. Within the rigid double layer the potential decreases linearly away from the surface and the potential of the diffuse double layer known as the zeta potential drops exponentially away from the surface. The thickness of the rigid layer lies in the molecular range, assuming that a monomolecular layer of counterions is adsorbed. As a consequence, the electrophoretic mobilities of analytes decrease with increasing ionic strength of the solution (Kuhn and Hoffstetter-Kuhn, 1993).

The fused silica capillaries that are typically used for separations have ionizable silanol groups in contact with the buffer contained within the capillary. The pI of fused

silica is about 1.5. The degree of ionization is controlled mainly by the pH of the buffer (Weinberger, 1998).

The electroosmotic flow is defined by

$$v_{eo} = \frac{\varepsilon\zeta}{4\pi\eta}E \tag{2.21}$$

where ε is the dielectric constant, η is the viscosity of the buffer and ζ is the zeta potential of the liquid-solid interface (Kuhn and Hoffstetter-Kuhn, 1993).

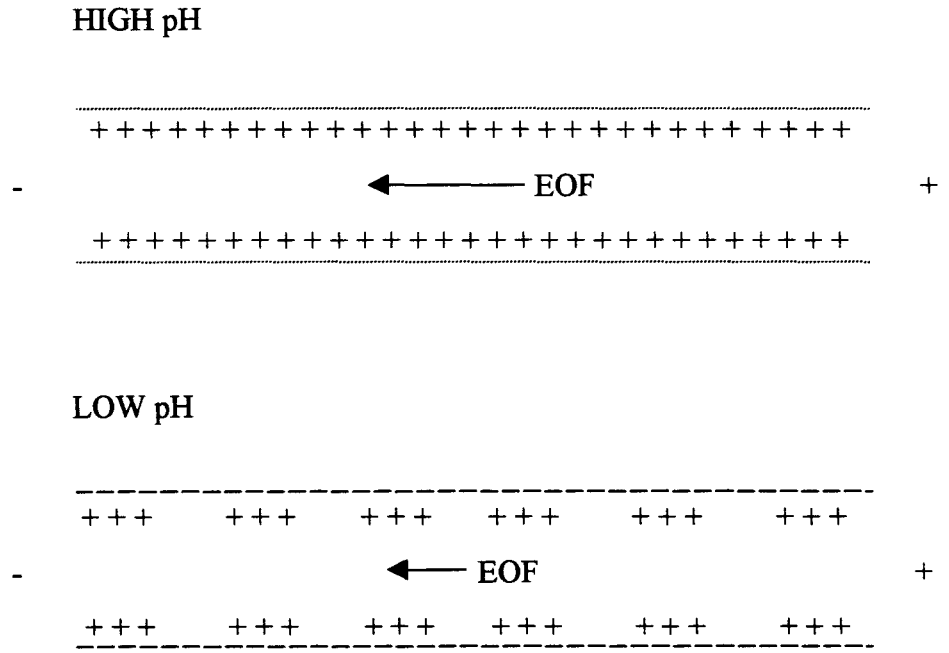

FIGURE 2.9. Electroendosmotic flow (Weinberger, 1998).

For the calculation of electrophoretic mobilities from the migration time and the electroosmotic flow, the velocity of the EOF has to be precisely known. The simplest way is to choose the "water" dip indicating the migration of the former injection plug and being equal to the EOF displacement. The "water" dip appears in the electropherogram because the sample solution often has a lower UV absorbance than the electrolyte system resulting in a negative UV signal. On the other hand, if the UV absorbance of the signal is higher than that of the buffer solution, a positive system peak can be observed at the site of the former injection plug. A more precise approach is to inject a neutral marker into the capillary that migrates with the electroosmotic velocity. From the migration time to the detector and the capillary length, the EOF can be calculated. The neutral marker has to fulfill some requirements. The compound must be water soluble, neutral over a wide pH range and no adsorption on the capillary walls must occur. Additionally it should show a high UV absorbance in order to allow small amounts to be injected. Benzyl alcohol, riboflavin and with restrictions mesityl oxide, acetone and benzene have been described as well suited for this purpose. However, the EOF marker has to indicate the real EOF displacement. If the marker is attracted by the capillary surface or partially charged by complexation with the carrier electrolyte, it will be slower or faster than the real flow (Jorgenson and Lukacs, 1981).

There have been several approaches to the proper control of the electroosmotic flow with particular emphasis on its reduction or elimination. To some extent buffer additives can be used to modify dynamically the capillary surface. Cationic surfactants like cetyltrimethylammonium bromide (CTAB) and related homologous compounds are claimed to be reagents which are able to change the sign of the surface charge by adsorption. Depending on the concentration, the EOF slows down and even reverses in the opposite direction. The addition of organic modifiers such as alcohols or hydrophilic linear polymers also leads to a reduction of EOF. As an alternative to dynamic coating, polymers like polyacrylamide are covalently bound to the silica to eliminate entirely the EOF, with the additional benefit of minimizing the adsorption of proteins to the capillary wall. Finally, gel-filled capillaries are another approach to minimize electroosmosis (Hjerten, 1985).

2.6 Performance Criteria

Analytical separations are performed to obtain, in a reasonable short time, information, both qualitative and quantitative, about the composition of a sample. This information is only provided, if the separation technique exhibits satisfactory performance. Factors are derived which allow the performance to be quantified using parameters like efficiency and resolution.

2.6.1 Efficiency

The efficiency of the electrophoretic system is gauged by the number of theoretical plates N achieved by the capillary. Experimentally, N can be calculated from an electropherogram using one of the following equations:

$$N = 16\left(\frac{t}{w}\right)^2 \tag{2.22}$$

$$N = 5.54\left(\frac{t}{w/2}\right)^2 \tag{2.23}$$

where t is the migration time of the component, w is the temporal peak width at the baseline (Kuhn and Hoffstetter-Kuhn, 1993).

The second equation above is preferred if the peak of interest shows a tailing. To compare different separation systems with respect to separation efficiency, the plate number is often referred to a capillary length of one meter (Jorgenson and Lukacs, 1981).

During migration through the capillary, molecular diffusion occurs leading to peak dispersion, σ^2, calculated as

$$\sigma^2 = 2D_m t = \frac{2D_m L^2}{\mu_{ep} V} \tag{2.24}$$

where D_m (cm^2/s) is the diffusion coefficient of the solute. The number of theoretical plates is given as

$$N = \frac{L^2}{\sigma^2} \tag{2.25}$$

Substituting the dispersion equation into the plate count equation yields

$$N = \frac{\mu_{ep} V}{2D_m} \tag{2.26}$$

The dispersion (σ^2) in this simple system is assumed to be time related diffusion only (Jorgenson and Lukacs, 1981). The equation indicates that macromolecules such as proteins and DNA, which have small diffusion coefficients (D) will generate the highest number of theoretical plates. In addition, the use of high voltages will also provide for the greatest efficiency by decreasing the separation time. The practical voltage limit with today's technology is about 30 kV. The practical limit of field strength (one could use very short capillaries to generate high field strength) is Joule heating. Joule heating is a consequence of the Ohmic resistance of the buffer to the flow of electricity (Weinberger, 1998).

2.6.2 Resolution

The resolution R between two species is given by the expression

$$R_s = \frac{1}{4}\frac{\Delta\mu_{ep}\sqrt{N}}{\mu_{ep}+\mu_{eo}} \tag{2.27}$$

where $\Delta\mu$ is the difference in mobility between the two species, μ is the average mobility of the two species and N is the number of theoretical plates. If the plate count equation is substituted

$$R_s = 0.177\Delta\mu_{ep}\sqrt{\frac{V}{(\mu_{ep}+\mu_{eo})D_m}} \tag{2.28}$$

This expression indicates that increasing the voltage is not an effective means of improving resolution (Jorgenson and Lukacs, 1981). To double the resolution, the voltage must be quadrupled. Since the working range of voltage is 10-30 kV, Joule heating limitations are quickly approached. The key to high resolution is to increase $\Delta\mu_{ep}$. The control of mobility is best accomplished through selection of the proper mode of capillary electrophoresis coupled with selection of the appropriate buffers (Weinberger, 1998).

The resolution between two peaks in an electropherogram can be calculated as follows:

$$R = \frac{2(t_2 - t_1)}{w_1 + w_2}, \text{where } t_2 \geq t_1 \qquad (2.29)$$

Resolution definition contains two terms, one expressing the efficiency and the other representing the selectivity of the separation system. The separation factor in CE is defined by the ratio of the migration times of the components. Selectivity is the most critical factor for the optimization in CE; method optimization in terms of selectivity is limited to modifications of the electrolyte system (Quesada, 1997).

2.7 Factors Influencing Performance

2.7.1 Fundamental Dispersive Effects

Band broadening in capillary electrophoresis is the result of a number of effects which all contribute additively to the spreading of a zone. Supposing Gaussian peak shapes, the band broadness can be expressed by the variance σ^2. The total variance is the sum of variances due to the particular sources of dispersion such as diffusion, adsorption, Joule heating, electrophoretic dispersion, injection, the width of the detection zone and other effects (Jorgenson and Lukacs, 1981).

In CE separated molecules pass the detector cell with different velocities. The time that sample compounds with different electrophoretic mobilities require to pass the detector is not the same for all compounds. Variations in temporal width may arise solely from differences in electrophoretic mobilities (Kuhn and Hoffstetter-Kuhn, 1993).

2.7.1.1 Diffusion. In CE a sample is supposed to be injected as a sharp zone into the tube. During migration through the capillary the profile of the sample zone is broadened

due to directed diffusion. Simultaneously to the broadening of the band the maximal absorbance of the zone decreases with the migration time (Kuhn and Hoffstetter-Kuhn, 1993).

2.7.1.2 Adsorption. As the diameter of the capillary decreases, the tendency for adsorptive interactions between the solutes and the fused silica surface is increased, especially at high field strength. Band broadening in tubes of small diameters and elevated voltages is higher than theoretically expected, even if thermal effects can be neglected (Jorgenson and Lukacs, 1981).

Wall adsorption can be minimized by choosing the buffer pH such that analyte and silica have the same charge sign. Hence wall adsorption tendencies are supressed by Coulombic repulsion (Kuhn and Hoffstetter-Kuhn, 1993).

Dynamic capillary coatings involve the use of buffer additives to reduce adsorption. Buffers containing high salt concentrations minimize adsorption of proteins to the silica by an ion exchange mechanism. Zwitterions are used to prevent adsorption, they do not contribute significantly to conductivity even at high concentrations but compete strongly for the active surface sites. Cationic surfactants are especially useful to reduce adsorption of cationic proteins. Non-ionic surfactants can be used to dynamically coat deactivated capillaries (Schwartz et al., 1992).

A more sophisticated possibility for reducing adsorption is represented by the surface treatment of the silica by static coating (Hjerten, 1985).

2.7.1.3 Joule Heating. The production of heat in HPCE is the inevitable result of the application of high field strengths. Two major problems arise from heat production. These are the temperature gradients across the capillary and the temperature changes with time due to ineffective heat dissipation (Weinberger, 1998).

The rate of heat generation in a capillary can be approximated as follows:

$$\frac{dH}{dT} = \frac{iV}{LA} \tag{2.30}$$

where L is the capillary length and A is the cross-sectional area. Since i=V/R and R=L/kA where k is the conductivity, then

$$\frac{dH}{dt} = \frac{kV^2}{L^2} \tag{2.31}$$

The amount of heat generated is proportional to the square of the field strength. Either decreasing the voltage or increasing the length of the capillary has a dramatic effect on the heat generation. Using low conductivity buffers is also helpful in this regard (Weinberger, 1998).

Temperature gradients across the capillary are a consequence of heat dissipation. Since heat is dissipated by diffusion it follows that the temperature at the center of the capillary should be greater than at the capillary walls. Since viscosity is lower at higher temperatures, it follows that both EOF and solute mobility will increase as well. Mobility for most ions increases by 2 per cent per degree K. The result is a flow profile that resembles hydrodynamic flow and bandbroadening occurs (Figure 2.10).

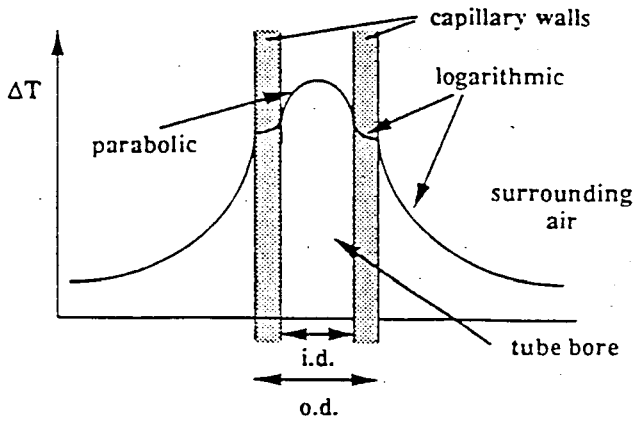

FIGURE 2.10. Schematic representation of the temperature profile as a result of current flow across a capillary with an electrolyte solution (Kuhn and Hoffstetter-Kuhn, 1993).

The thermal conductance of the fused silica is double the conductance of water which means that heat is more effectively conducted across the capillary than through the liquid (Zhu et al., 1989).

Operating with narrow diameter capillaries improves the situation for two reasons: the current passed through the capillary is reduced by the square of the capillary radius and the heat is more readily dissipated across the narrower radial path (Weinberger, 1998).

The resulting thermal gradient is proportional to the square of the diameter of the capillary, which can be approximated from the following equation:

$$\Delta T = 0.24\frac{Wr^2}{4K} \tag{2.32}$$

where W is the power, r is the capillary radius, and K is the thermal conductivity (Weinberger, 1998).

The second problem is ineffective heat dissipation. If heat is not removed at a rate equal to its production, a gradual but progressive temperature rise will occur until equilibrium is reached. Depending on the specific experimental conditions, imprecision in migration time will result due to variance in both EOF and solute mobility. Narrow diameter capillaries help heat dissipation but effective cooling systems like forced air are required to ensure heat removal (Rush et al., 1991).

2.7.1.4 Electrophoretic Dispersion. The electrophoretic or electromigration dispersion is responsible for the peak asymmetry frequently observed in CZE. Two factors are responsible for peak broadening: the difference in specific conductance κ between the sample and the buffer zone and the concentration ratio of the sample constituent to the buffer's coion c_S/c_B. Both factors have their origin in mobility differences between sample and coion. If the ratio c_S/c_B is low enough, the conductivity change between sample and buffer zone is negligible and the carrier electrolyte determines the conductivity and the pH along the whole separation compartment. The concentration distributions resulting from the combination of the two effects of differences in conductivities and mobilities of sample and buffer solutions are summarized on Table 2.1. If, on the other hand, the sample concentration becomes too high, electrophoretic dispersion manifests itself in sample overloading of the electrolyte system. as long as the ratio does not exceed 10^{-2} the mobility and concentration of the counterion does not affect the separation (Kuhn and Hoffstetter-Kuhn, 1993).

The phenomenon of the concentration of a highly diluted sample at the boundary between sampling and separating compartments is called sample stacking. It is used in CZE to improve detection sensitivity and to narrow the length of the sample zone leading to an increase of the theoretical plate numbers (Waters Corporation, 1995).

TABLE 2.1. Impact of the ratio of the conductivity of the sample solution κ_S to the conductivity of the buffer solution κ_B (Kuhn and Hoffstetter-Kuhn, 1993).

	$\kappa_S > \kappa_B$	$\kappa_S = \kappa_B$	$\kappa_S < \kappa_B$
$\mu_S^+ < \mu_B^+$	Dilution peak tailing	Peak tailing	Concentration peak tailing
$\mu_S^+ = \mu_B^+$	Dilution		Concentration
$\mu_S^+ > \mu_B^+$	Dilution peak fronting	Peak fronting	Concentration peak fronting

2.7.1.5 Sample Injection Width. The injection width of the sample is the most extrinsic contribution to band broadening. If the sample is introduced into the capillary as a rectangular pulse the variance due to injection is

$$\sigma^2 = \frac{I^2}{12} \tag{2.33}$$

where I is the width of the initial sample pulse (cm). The length of the injection plug is the most significant factor in respect to peak broadening, if the injection length is several times the diffusion width for the species in the zone. Therefore, the number of theoretical plates N varies linearly with the applied voltage, only in the case of very small injection lengths (Jorgenson and Lukacs, 1981).

Peak efficiency dramatically decreases with increasing injection times and thus with increasing sample zone lengths. The injection time should be as short as possible depending on the detector performance, and moderate stacking conditions and low applied potentials should be employed during the stacking period. Moderate stacking means that

the conductivity of the sample solution should only be slightly lower than that of the buffer zone (Kuhn and Hoffstetter-Kuhn, 1993).

2.7.2 Operational Parameters

2.7.2.1 Field Strength. Since both the electroosmotic and electrophoretic migration velocities are directly proportional to the field strength, the use of the highest voltages possible will result in the shortest times for the separation. The theory predicts that short separation times will give the highest efficiencies since diffusion is the most important feature contributing to bandbroadening. The limiting factor here is Joule heating (Rush et al., 1991).

Rational methods development should remove any arbitrary selection of experimental parameters. This approach should be valuable during validation and any subsequent reexamination of experimental variables. To apply this to voltage optimization, it is best to perform an Ohm's plot to note when a deviation from linearity occurs. There is no need to perform a run; the capillary is just filled with buffer and voltage is changed while recording the current. This data is useful in evaluating the heat removal capacity of different instruments as well (Weinberger, 1998).

2.7.2.2 Capillary Dimensions. The choice of capillary dimensions has an effect on several factors such as migration time and resolution, detection sensitivity, heat dissipation and adsorption (Pande et al., 1992).

The most common and useful capillaries range from 25-75 μm. From the standpoint of resolution, the narrower the capillary inner diameter, the better the separation. Narrow capillaries yield poorer limits of detection due to detector pathlength and sample loadability. Narrow capillaries are also more prone to clogging. As long as samples and buffers are filtered through < 0.5 μm filters, clogging is seldom a problem in the above

mentioned size range. The impact of Joule heating becomes evident in larger diameter capillaries. The EOF increases dramatically at high buffer concentrations. This is contrary to what is normally expected as the buffer concentration is elevated. The decreased viscosity due to heat buildup provides for this perturbation (Jorgenson and Lukacs, 1981).

Increasing the capillary length gives proportional increases in the number of theoretical plates provided the field strength is kept constant. For example, if a 20 cm capillary is run at 15 kV, a 40 cm capillary should be run at 30 kV. Longer capillary would not improve the plate count further since constant field strength cannot be maintained; only the run time would increase (Weinberger, 1998).

With the longer migration time the separation efficiency and the peak resolution improve for the longer capillary. Shorter capillaries show lower electrical resistance and cause higher currents. While the surface area for dissipation of Joule heating decreases, the generation of heat is enlarged by the increased power of the system. High electroosmotic flows require long capillaries to maintain the resolution (Kuhn and Hoffstetter-Kuhn, 1993).

2.7.2.3 Temperature. The mobility equation previously described contains a viscosity term. Since viscosity is a function of temperature, precise temperature control is important. As the temperature increases, the viscosity decreases thus the electrophoretic mobility increases as well. Some buffers like Tris are known to be pH sensitive with temperature. For complex separations like peptide maps, even small pH shift can alter the selectivity (Weinberger, 1998).

Operating at elevated temperature is also common for several reasons. It aids methods development since elevating the temperature will speed the analysis. Often, this is done rather than shortening the capillary. Higher temperatures can help overcome solubility problem. When separating molecules that can undergo conformational changes, the impact of temperature must always be considered. In some cases, conformers are

separable at low temperatures. Protein unfolding is frequently observed at elevated temperatures (Rush et al., 1991).

Conformational changes result in effective charge or hydrodynamic shape changes which can result in variations in migration time and peak shape. This leads to asymmetric peaks and sigmoidal mobility plots versus temperature in the transition region. The broadened or multiple peaks do not necessarily mean that a protein sample is impure (Schwartz et al., 1992). Subambient temperature control (4 °C) is suggested (Kuhn and Hoffstetter-Kuhn, 1993).

Operating at low temperatures can also be useful. At sub-ambient temperature, buffer viscosity is higher resulting in lower currents. This permits the use of more concentrated buffers which can increase the loading capacity. This feature can be useful when performing fraction collection (Weinberger, 1998).

2.7.3 Electrolyte System

- The buffer system should have no negative effect on the separation.
- A higher buffer capacity over a broad pH range must be guaranteed.
- The pH should show a low variation with temperature.
- In the case of UV/VIS absorbance as detection mode, the buffer should show low UV absorbance at the wavelength of interest.
- The mobility of the buffer ion should be similar to the analytes to minimize electrophoretic dispersion.
- The electrophoretic mobility of the counterion should be as low as possible to minimize heat generation and to allow high voltages to be applied (Kuhn and Hoffstetter-Kuhn, 1993).

2.7.3.1 pH. The pH value of the electrolyte solution in CE is the most important separation parameter for changing the selectivity of the system. In general, separation in electrophoresis is based on differing mobilities of the analytes, which in turn depend on their size and net charge. The size of an ion is related to the molecular mass and the degree of hydration depending again on factors like ionic strength and polarity of the solution. The net charge of the ion is dependent on the degree of ionization given by the pK value of the acid or basic functional group and the pH of the solution. In the particular case where the substances to be separated are entirely charged over the pH range of interest, variation of the pH does not influence the net charge of the ions. This holds usually for ions of strong acids or bases. If, however, the ionizable functional groups of the analytes are weak acids or bases, the pH of the electrolyte shows a strong influence on the net charge (Pande et al., 1992).

2.7.3.2 Choice of Buffer. Most buffer systems have sufficient buffer capacity only in a limited pH range. Due to the logarithmic definition of pH, buffer capacity decreases by a factor of 10 for every pH unit away from the pK. Particularly useful are those buffers having a high buffer capacity at simultaneously low conductance resulting in a low current and heat generation (Kuhn and Hoffstetter-Kuhn, 1993).

2.7.3.3 Ionic Strength. The ionic strength of the buffer influences not only the EOF but also indirectly the viscosity of the medium. The viscosity is dependent on the temperature and as a result, there is a dependence on the capillary diameter. With a short capillary, with increasing buffer concentration, the migration times uniformly increase. With a longer capillary, the migration times first increase then decrease. The decrease in migration time is a consequence of Joule heating causing a reduction in the buffer viscosity. There is also the impact of buffer concentration on peak width as well. The sharper peak widths at the higher buffer concentrations are due to a phenomenon known as stacking (Weinberger, 1998).

In practice, when working at high field strengths, variation of the ionic strength induces several effects, i.e. temperature increase and viscosity changes, which in turn

influence the mobility. While EOF is only slightly decreased with rising buffer concentration, the migration time of the analytes declines with increasing buffer concentration. In addition, higher resolutions are obtained with increasing buffer concentration which can be caused by a better suppression of electrophoretic dispersion. The mobilities of the solutes increase continuously with higher ionic strengths while the electroosmotic mobility decreases (Kuhn and Hoffstetter-Kuhn, 1993).

2.8 Instrumentation

2.8.1 Injection

From the theoretical point of view the sample should be injected as an infinite small volume into the capillary to minimize the initial zone broadness of the analytes. There are two fundamental ways to introduce the sample into the capillary: hydrodynamic and electrokinetic injection (Waters Corporation, 1995).

When the capillary is placed in the sample, it is important that the injection commence immediately and the capillary should be moved to the run buffer after injection not to allow errors and band broadening due to capillary action and siphoning. The injection zone width should be kept as small as possible to prevent reduction in efficiency and resolution. The injection buffer must be miscible with the run buffer and must not cause precipitation. The ionic strength of the injection buffer should be lower than that of the run buffer. If the injection buffer differs greatly from the run buffer from the standpoint of additives, or the injection buffer has an ionic strength greater than the run buffer, then only small injections should be made (Weinberger, 1998).

2.8.1.1 Hydrodynamic Injection. For hydrodynamic injection a pressure drop has to be applied along the capillary either by high pressure at the injection side, or by vacuum at the detector side, or by hydrostatic pressure by utilizing gravity (Zhu et al., 1989).

The hydrodynamic injection volume is a linear function of the applied pressure difference along the capillary and its duration. The injection volume can be calculated by Poiseuille's law for liquid flow through a circular tube:

$$V_i = \frac{\Delta p.\pi.r^4.t}{8\eta.L_T} \tag{2.34}$$

where V_i is the injection volume (m^3), Δp is the pressure difference (Pa), r is the inner radius of the capillary (m), t is the injection time (s), η is the viscosity (Pa.s) and L_T is the total capillary length (m) (Kuhn and Hoffstetter-Kuhn, 1993).

If sample injection is accomplished by gravity the pressure difference is given by the hydrostatic pressure which is defined as

$$\Delta p = \rho.g.\Delta h \tag{2.35}$$

where ρ is the density of the sample solution (kg/m^3), g is the gravitational acceleration (9.80665 $N.kg^{-1}$) and Δh is the height difference between liquid levels of sample and buffer vials (m). The sample volume introduced by hydrodynamic flow can be manipulated by varying the injection time and/or the pressure difference (Kuhn and Hoffstetter-Kuhn, 1993).

There are several advantages of hydrodynamic injection. The amount of material injected to the capillary is fixed, provided the sample viscosity and temperature are controlled and there is no quantitative discrimination during the injection process (Weinberger, 1998).

2.8.1.2 Electrokinetic Injection. This injection mode is based on the fact that voltage causes electrophoretic and electroosmotic movement. If voltage is applied for a short interval of time, sample is introduced into the capillary due to electrophoretic migration. If, additionally, electroosmotic flow occurs, a sample volume will be introduced into the column. The injected sample is volume is then given by

$$V_i = v_{eo}.\pi.r^2.t \tag{2.36}$$

The quantity of a species i introduced into the capillary (M) by electromigration is

$$Q_i = \frac{(\mu_i + \mu_{eo}).\pi.r^2.V.c_i.t}{L_T} \tag{2.37}$$

Thus, the quantity introduced into the capillary can be controlled by varying the voltage and/or the introduction time (Jorgenson and Lukacs, 1981).

Hydrodynamic injection is preferable over electrokinetic injection. However, the latter mode is preferred if discrimination of the component of interest from contaminants is desired, or if polyacrylamide gel-filled capillaries are used, or if a concentrating of a component from a diluted sample solution is desired (Kuhn and Hoffstetter-Kuhn, 1993).

The main advantage of electrokinetic injection is trace enrichment. If the EOF is low, it is possible to inject only anions or cations into the capillary. It is critical that the injection buffer be of constant ionic strength or the voltage drop at the point of injection varies causing serious quantitative errors (Weinberger, 1998).

2.8.2 Detection

On-capillary detection is generally required for CE since construction of a post-capillary flow cell is not practical considering the minuscule dimensions of the capillaries. The detected peak widths are a function of chromatographic processes and are not related to the peak velocity past the flow cell. In CE, the migration velocity of solutes through the capillary is a function of each solute's electrophoretic and electroosmotic components. Since detection occurs on-capillary, these forces are operative as the solute is transiting the detection window. Thus, slower moving components spend more time migrating past the detector window compared to their more rapidly moving counterparts (Weinberger, 1998).

In terms of the kind of signal which is obtained, two main types of detectors can be distinguished: non-selective and selective detectors. Whereas non-selective detectors measure differences in physical properties of the analyte relative to that of the whole solution, selective detectors measure a specific property of the analyte. Unselective detectors, including refractive index (RI), conductometric and indirect detection methods, commonly exhibit lower sensitivities and dynamic ranges, but they are more universal than selective detectors, including UV/VIS absorbance, fluorescence, mass spectrometry (MS), Raman, electrochemical and radiometric detectors (Kuhn and Hoffstetter-Kuhn, 1993).

In order to compare detection systems with respect to their performance or to evaluate the best detection system for a specific separation, the criteria used are sensitivity (response factor), detection limit, noise, linear (dynamic) range, response index and time constant (response time). The sensitivity or response factor refers to input/output and is

given by the ratio of a measured signal (current, voltage, absorbance, etc.) to an amount (weight or moles of substance). High frequencies arise from incomplete grounding or from the signal amplification system and can usually minimized by filtering. Low frequencies occur due to temperature variations, impurities of the background electrolyte or air bubbles. Instead of sensitivity and noise, the signal-to-noise ratio (S/N) together with the detection limit of a special substance is often used to characterize detector sensitivity (Wahlbroehl and Jorgenson, 1984).

2.8.2.1 UV/VIS Absorbance Detection. Owing to its sensitivity to a wide range of compounds and functional groups and its ease of use, UV/VIS absorbance is the most popular detection principle, although it suffers from low sensitivity compared to other detection modes developed for capillary separation systems. By UV/VIS absorbance, substances ring can be registered if they provide at least one of the following functional groups: bromine, iodine or sulphur; two conjugated double bonds; a double bond vicinal to an atom having a single electron pair; a carbonyl group; an aromatic ring (Kuhn and Hoffstetter-Kuhn, 1993).

The wavelength which can be used to detect absorbing analytes are dependent on the light source and the kind of photometer. In practice, the wavelengths commonly used are 190 and 200 nm for all kinds of analytes, 210 and 214 nm for peptides and proteins, 254 nm for aromatic compounds, 280 nm for proteins and 260 nm for nucleic acids (Waters Corporation, 1995).

2.8.3 Capillary Column

Capillaries with an internal diameter of 25-75 μm are usually employed. Fused silica is the material of choice due to its UV transparency, high thermal conductance, durability (when polyamide coated) and zeta potential. Functionalized and gel-filled capillaries are also available (Weinberger, 1998).

Capillaries in bulk can be purchased from several suppliers. For a capillary preparation, a ruler, a cutter (diamond cutter or silicon wafer), butane lighter, methanol and a tissue are required. The procedure is as follows:

1. The polyamide coating is nicked near the edge of the capillary as squarely as possible. The ends of the capillary are gently pulled at the cut until it breaks. The desired length is measured from the cut end, taking into account the length from the detector to the buffer reservoir, and cut again.
2. The separation length of the capillary is measured and a length of about 2-3 mm is flamed with butane lighter. The burnt polyamide is cleaned with a tissue moistened with methanol. The capillary can now be inserted into the instrument taking care not to bend the now fragile detector window.
3. The capillary is washed for 15 minutes with 1 N sodium hydroxide, 0.1 N sodium hydroxide and run buffer each. The detector side reservoir is changed to run buffer. The system is now ready to run.

The base conditioning procedure is important to ensure the surface of the capillary is fully charged. For some methods it is necessary to regenerate this surface with 0.1 N sodium hydroxide and extreme cases, 1 N sodium hydroxide. The regeneration procedure is frequently necessary if migration times change on a run to run basis. This is most common when using buffers in the pH 4-6 region. Regeneration is seldom necessary below pH 3 and above pH 9 except as a daily startup procedure (Weinberger, 1998).

Not all attempts to store a fused silica capillary are successful. Capillaries are prone to clogging from dried buffer residues. While this is not too serious for naked silica, capillary damage can be costly when using chemically modified capillaries (Weinberger, 1998). To prevent the damage of the capillary during storage, it is rinsed with bistilled water to remove the running buffer for a few minutes, nitrogen or air is blown through the capillary and then it is removed from the instrument (Kuhn and Hoffstetter-Kuhn, 1993).

2.8.4 Sample Collection

CE as it is normally practiced has both the inlet and outlet of the capillary immersed in buffer reservoirs to complete a closed circuit. Thus, sample zones are directly discharged into the outlet reservoir, which hinders sample collection. Among the approaches to overcome this problem are the use of a programmable fraction collector consisting of a collector tray and three digital linear actuators to allow precise movement (Rose and Jorgenson, 1988), completion of the electrical circuit in the capillary prior to its outlet by using a membrane assembly at the exit (Cheng et al., 1992), use of detection close to the end of capillary and a sheath liquid at the exit to allow continuous collection (Müller et al., 1995), development of a coaxial capillary flow cell that allows electrical connection (Chiu et al., 1995).

2.9 Techniques

Besides ongoing efforts in the area of CZE in the presence of electroosmotic flow a broad variety of other CE techniques matching the needs of special analytical problems have been developed (Kuhn and Hoffstetter-Kuhn, 1993). As a continuation of free-zone electrophoresis, Hjerten introduced CZE in coated capillaries where adsorption as well as electroosmosis are eliminated and separation of proteins which tend to absorb strongly on glass surfaces is accomplished (Hjerten, 1985). Micellar electrokinetic chromatography (MEKC) was presented to facilitate the separation of uncharged compounds by CE. Use of polyacrylamide gel-filled capillaries started and then capillary gel electrophoresis (CGE) for the separation of proteins and nucleic acids to combine the very high resolution of gel electrophoresis with the sample instrumental set-up of CZE predestined for automation and on-line detection was introduced (Kuhn and Hoffstetter-Kuhn, 1993).

2.9.1 Capillary Coating in Capillary Zone Electrophoresis

The capillary surface can be coated dynamically by adding additives such as surfactants, zwitterionic salts or hydrophilic linear polymers to the buffer system. This procedure is advantageous because of its simplicity and low cost but reproducible dynamic coating is difficult to achieve and changes in the buffer composition alter the coating conditions. Also, disturbing interactions with the analytes may occur (Kuhn and Hoffstetter-Kuhn, 1993).

The coating procedure of the inner walls of capillary columns with a monomolecular polymer layer is based on the use of a bifunctional group in which one group reacts specifically with the glass wall and the other with a monomer taking part in the polymerization process. Examples of such bifunctional compounds are vinyltriacetoxysilane, vinyltrichlorosilane, methylvinyldichlorosilane, vinyltri(β-methoxyethoxy)silane and γ-methacryloxypropyltrimethoxysilane, where one or two of the methoxy, acetoxy, methoxyethoxy or chloro groups react with the silanol groups in the glass wall, whereas the acryl or vinyl groups with acryl or vinyl monomers to form a polymer, e.g. non-cross-linked polyacrylamide, poly(vinylpyrrolidone), poly(vinyl alcohol). Non-covalently attached polymer is then removed simply by rinsing with water. this procedure gives a thin, well defined monomolecular layer of a polymer covalently bound to the glass wall. This coating procedure is applied specifically to polyacrylamide coatings. About 80 µl of γ-methacryloxypropyltrimethoxysilane were mixed with 20 ml with water, which had been adjusted to pH 3.5 by acetic acid. This silane solution was sucked up into the capillaries. After reaction at room temperature for one hour the silane solution was withdrawn. The columns were washed with a deaerated 3 or 4 per cent (w/v) acrylamide solution containing 1 µl TEMED and 1 mg potassium persulphate per ml solution. After 30 minutes the excess of (not attached) polyacrylamide was sucked away and the columns were rinsed with water. most of the water in the columns was removed by aspiration and the remainder by drying in an oven at 35 °C (Hjerten, 1985).

2.9.2 Capillary Gel Electrophoresis

The gel-filled capillaries are difficult to manufacture with sufficiently large pores, tend to undergo problems with matrix contraction, and often are subject to complications associated with air bubbles, which automatically decrease the electric current in the circuit (Gelfi et al., 1994c). Nevertheless, gel-filled capillaries have proven useful in high-resolution separation of oligonucleotides or of smaller double-stranded DNA (dsDNA) fragments. Polymer-network capillaries owing to their wider range of pore sizes offer comparable or better separations to the gel-filled capillaries. They are, however, restricted by the viscosity of the buffer-polymer mixtures, making it difficult to completely fill the capillaries (Srinivasan et al., 1993).

Cross-linked polyacrylamide has been used as a sieving medium for CGE separations of proteins. However, the sensitivity is not optimal for protein analysis because the polyacrylamide gel interferes with the UV absorbance detection of proteins at 214 nm. Linear, i.e. non-cross-linked, polyacrylamide was used as a sieving medium for proteins. This low viscosity medium is advantageous in that capillary gels are easily prepared and are easily replaceable, they can be rinsed out of the capillary. Linear polymers such as celluloses and polyethylene glycols have also been used for other separations requiring sieving in CE (Schwartz et al., 1992).

Gels with small pore sizes, e.g. 6 per cent T, 5 per cent C, possess a greater size selectivity for short oligonucleotide chains. A gel with medium pore size, e.g. 3 per cent T, 5 per cent C, allows one to separate a broader molecular weight range of oligonucleotides. To compensate for the lower resolving power of the larger pore size for short nucleotide chains, the effective column length has to be increased. Thus, good separation is achieved, but at the expense of longer analysis times. An increase of the pore size can be achieved by reducing the amount of crosslinking agent for a given per cent T. If the pore size is too low the analytes are totally excluded from the capillary. If, on the other hand, the pores are too large, the analytes move freely through the capillary and no molecular sieving occurs. It is

therefore necessary to select appropriate gel concentrations for particular samples (Kuhn and Hoffstetter-Kuhn, 1993).

Sample injection in CGE can only be performed electrokinetically. The samples migrate into the capillary according to their mobility. In the case of nucleic acids, the injected amount is independently of their different size and sequence. This lack of discrimination between analytes during electrokinetic injection is in contrast to the discrimination found in CZE and is based on their equal effective mobilities in free solution (Waters Corporation, 1998).

At present, DNA fragments are analysed by two major capillary electrophoresis approaches: a polymer-network capillary separation system and a capillary-gel separation system. The polymer-network system is based on buffers containing additives that create a gel-like matrix inside the capillary. The migrating DNA fragments interact with the dynamic pores of this matrix resulting in separations based on size. The capillary-gel system on the other hand, uses an in situ polymerized acrylamide gel cross-linked to the walls of the capillary. Fixed pores in the gel retard migration of the DNA fragments in a manner similar to that in slab gels and, consequently, results in separations based on size (Srinivasan et al., 1993).

3. MATERIALS

3.1 Chemicals

All chemicals and solutions used in this study were from Merck (Germany) or Sigma (USA) unless stated otherwise in the text. The instant films (667) were from Polaroid (USA).

The samples analysed by capillary electrophoresis were bovine serum albumin (fraction V); human serum provided by Düzen Laboratories in Ankara; restriction enzymes Taq1 from Promega (USA), EcoR1 from Promega (USA) and Pst1 from New England Biolabs (USA); μPAGE $pd(A)_{25\text{-}30,40\text{-}60}$ oligonucleotide standard from Waters (USA).

The water used in the experiments was high-grade water distilled from a Millipore water distillation apparatus before use.

3.2 Buffers and Solutions

3.2.1 Polyacrylamide Gel Electrophoresis Buffers

Acrylamide-bisacrylamide mixture (30:0.8)

Acrylamide	29.2 g
N'N'-bis-methylene-acrylamide	0.8 g
dH_2O	to 100 ml

Sample buffer

0.5 M Tris-HCl pH 6.8	1 ml
Glycerol	0.8 ml
10%(w/v) SDS	1.6 ml
2-β-mercaptoethanol	0.4 ml
0.05%(w/v) Bromophenol blue	0.2 ml

Electrophoresis Separating Gel (10%)

1.5 M Tris-HCl pH 8.8	2.5 ml
Acrylamide/Bis (30:0.8)	3.33 ml
10%(w/v) SDS	100 µl
10% Ammonium persulfate	50 µl
TEMED (N,N,N',N'-tetramethylethylenediamine)	5 µl
dH_2O	to 10 ml

Electrophoresis Stacking Gel (5%)

0.5 M Tris-HCl pH 6.8	2.5 ml
Acrylamide/Bis(30:0.8)	1.7 ml
10%(w/v) SDS	100 µl
10% Ammonium persulfate	50 µl
TEMED	10 µl
dH_2O	to 10 ml

5X Running Buffer

Tris-base	15 g
Glycine	72 g
SDS	5 g
dH_2O	to 1 L

Stain

Coomassie blue R-250	0.1%
Methanol	40%
Acetic acid	10%

Destain

Isopropanol	25%
Acetic acid	10%

Fixing

Acetic acid	7%

SDS Molecular Weight Markers

Myosin	205 kDa
β-Galactosidase	116 kDa
Phosphorylase b	97.4 kDa
Albumin, bovine	66 kDa
Albumin, egg	45 kDa
Carbonic Anhydrase	29 kDa

3.2.2 Buffers and Solutions used in PCR

MDE Buffer

Tris-HCl (pH 8.3)	100 mM
KCl	500 mM
$MgCl_2$	17.5 mM
Gelatin	0.01 %

Oligonucleotide Primers for the Amplification of Exon 10 of CFTR Gene

10i5: F 5'- GCA GAG TAC CTG AAA CAG GA -3'

10i3: R 5'- CAT TCA CAG TAG CTT ACC CA -3'

3.2.3 Agarose Gel Electrophoresis Buffers

5X TBE (Tris-Borate) Buffer

Tris-base	445 mM
Boric acid	445 mM
EDTA	10 mM

10X Loading Buffer

Bromophenol Blue	2.5 mg
SDS	1% in 1 ml glycerol

3.2.4 Storage Buffers of Restriction Enzymes

Storage Buffer of Taq1

NaCl	400 mM
Tris-HCl (pH 7.4)	10 mM
EDTA (Ethylenediaminetetraacetic acid)	0.1 mM
DTT (Dithiothreitol)	1 mM
BSA	0.5 mg/ml
Triton X-100	0.15 %
Glycerol	50 %

Storage Buffer of EcoR1

KCl	300 mM
Tris-HCl (pH 7.4)	10 mM
EDTA (Ethylenediaminetetraacetic acid)	0.1 mM
DTT (Dithiothreitol)	1 mM
BSA	0.5 mg/ml
Triton X-100	0.15 %
Glycerol	50 %

Storage Buffer of Pst1

NaCl	200 mM
Tris-HCl (pH 7.4)	10 mM
EDTA (Ethylenediaminetetraacetic acid)	0.1 mM
DTT (Dithiothreitol)	1 mM
BSA	0.2 mg/ml
Triton X-100	0.15 %
Glycerol	50 %

3.2.5 Buffers used in Capillary Electrophoresis

TBE Buffer

Tris-base	150 mM
Boric acid	150 mM
EDTA	3 mM
pH	8.25

Borate Buffer

Anhydrous Borax ($Na_2B_4O_7$)	150 mM
pH	8.5

Dolnik's Buffer

N-methyl-$_D$-glucamine	200 mM
ε-amino-n-caproic acid	200 mM
pH	10.2

μPAGE Buffer

Tris-borate	100 mM
Urea	7 M
pH	8.3

3.3 Instrumentation

Capillary zone electrophoresis was performed in Waters Quanta 4000E Capillary Electrophoresis system (Figure 3.1) equipped with 35 cm long x 50 μm I.D. and 60 cm long x 75 μm I.D. fused silica capillary columns. Capillary gel electrophoresis was performed to analyse oligonucleotides and DNA samples with 60 cm long x 75 μm I.D. polyacrylamide gel-filled μ-PAGE columns with 100 mM tris-borate, 7 M urea, pH 8.3 buffer (5 per cent T, 5 per cent C gel). The electrophoresis was carried out under constant voltage with either positive or negative high voltage supply. The capillary columns were rinsed with 0.1 M NaOH and then with deionized water for five minutes prior to and after each run, and automatic purging for five minutes with run buffer prior to each injection was performed. The samples were loaded either by hydrostatic injection (gravity-driven siphoning) or by electromigration injection (application of voltage) and the runs were carried out at 20°C. The parameters such as sample time, sample voltage, run time and run voltage were programmable. The detector wavelength was adjusted by changing the UV filter, the lamp, and/or the window. The detection was carried out by UV absorbance at 214 nm, 254 nm and 280 nm.

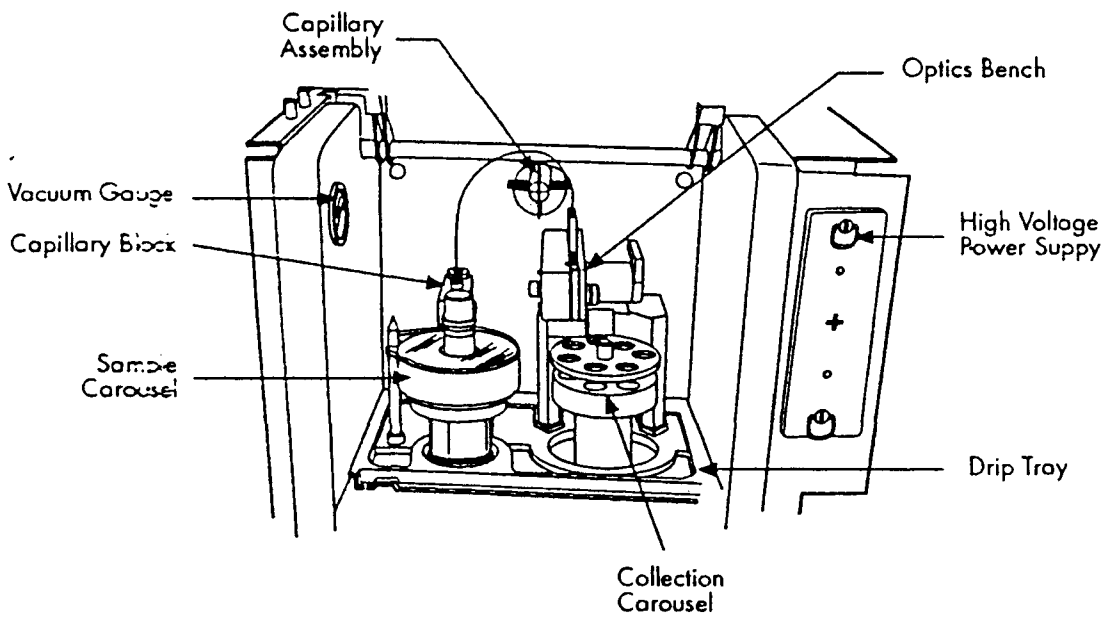

FIGURE 3.1. Separation Compartment of Waters Quanta 4000E Capillary Electrophoresis System.

3.4 Laboratory Equipment

Autoclaves	Eyela, Model MAC-601, Japan
Balances	Precisa 80a-200M, Switzerland
Camera	Direct Screen Instant Camera, Polaroid DS-34
Capillary Electrophoresis	Quanta 4000E, Waters, MA, USA
Deepfreezes	-70°C, GFL, Germany -20°C, Bosch, Germany -20°C, Arçelik, Turkey

Refrigerators	+4°C, Arçelik, Turkey +4°C, Simtel, Turkey
Electrophoresis	Horizon 58, Model200, Horizontal Gel Electrophoresis Apparatus, BRL, USA Miniprotean II, Biorad, England
Gel Drier	Vacuum Drier, BIOMETRA, Germany
Sonicator	Branson Sonifier, VWR Scientific
Spectrophotometer	Lambda 3 UV/VIS, Perkin Elmer Cetus, USA
Thermo-cycler	Thermal Reactor TR1, Hybaid, UK
Transilluminator	Reprostar II, CAMAG, Switzerland

4. METHODS

4.1 Analysis of BSA Sample by SDS-Polyacrylamide Gel Electrophoresis

The purity of the protein was assessed by SDS-polyacrylamide gel electrophoresis under denaturing conditions. Two glass plates and two spacers that were arranged at each side parallel to the two edges of the glass plates were prepared for pouring the gel. The entire length of the two sides and the bottom of the plates were bound with gel sealing tape to make a watertight seal. The required quantity of 10 per cent separating gel was poured without allowing any air bubbles at the bottom. The remaining part of the volume created between two glass plates after pouring the separating gel was at least as long as the teeth of the comb to be placed at the top. This upper part was filled with water before polymerisation of the monomers of acrylamide, which is initiated by TEMED, to prevent formation of a rough surface of polymerised acrylamide and hence distortion of the bands of the protein. Upon hardening, water was discarded and the gel mould was filled completely with 5 per cent stacking gel again containing both acrylamide and TEMED. The comb was then inserted immediately without allowing any air bubbles to become trapped under the teeth. The comb was removed carefully after allowing the stacking gel to polymerise. The gels were then attached to the electrophoresis tank whose reservoirs were previously filled with running buffer.

The protein sample was mixed with sample buffer in 1:1 ratio and subjected to denaturation at 95°C for three minutes. The required volumes of mixture were then loaded to the wells using a micropipette. The electrodes were connected to the power pack (200V) and the gel was run until the marker dyes had migrated the desired distance for effective separation of protein bands. At the end of electrophoresis, the glass plates were detached from each other just after removing spacers without damaging the gel. The gel was then submerged in staining solution for about thirty minutes and then in destaining solution for about thirty minutes at room temperature. The gel was then immersed in fixing solution for

fixing the protein on the gel. After fixing, the gel was transferred onto a filter paper and dried under vacuum for about thirty minutes.

4.2 PCR Amplification of DNA Samples

491-bp fragments of exon 10 of CFTR gene from normal, homozygous and heterozygous Turkish CF patients were prepared by polymerase chain reaction amplification. The PCR reaction mixtures (25 μl) contained MDE reaction buffer (2.5 μl), 25 mM dNTP (0.2 μl), *Taq* DNA polymerase enzyme (1 μl), genomic DNA (1 μl), 25 pmol primers 10i3 and 10i5 (0.5 μl each). Three-step amplifications in the Hybaid thermal cycler were performed using the plate mode and an initial denaturation step at 94 °C for five minutes. The initial denaturation step is followed by thirty cycles of alternating incubations at 94 °C for thirty seconds and 60 °C for two minutes. The reaction ends with four minutes of incubation at 60 °C. After amplification, 5 μl aliquot from each tube was mixed with loading buffer and run on 1.5 per cent agarose gel to check the efficiency of amplification.

4.3 Capillary Electrophoresis

4.3.1 Capillary Zone Electrophoresis of BSA

Sample solution of BSA (5 mg/ml) was prepared by dissolving fraction-V bovine serum albumin in high-grade deionised water. The run buffers were borate buffer, TBE buffer, or Dolnik's buffer which were all degassed by sonication and filtered through 0.45 μm Millipore hydrophilic PVDF filters before each run. Experiments performed for the analysis of BSA by CZE are summarized on Table 4.1.

TABLE 4.1. Experiments performed for the analysis of BSA by CZE.

Exp #	Buffer	Column	High voltage supply	λ (nm)	Injection mode	Sample Voltage (kV)	Sample time (s)	Run voltage (kV)
1	Borate	75μm 60cm	+	214	Hyd.		7	25
2	Borate	50μm 35cm	+	254	Elc.	10	10	10
3	Borate	50μm 35cm	+	254	Elc.	15	10	15
4	Borate	50μm 35cm	+	254	Elc.	20	10	20
5	Borate	50μm 35cm	+	254	Hyd.		15	20
6	Borate	50 μm 35cm	+	254	Hyd.		15	20
7	Borate	50μm 35cm	+	254	Hyd.		15	20
8	Borate	50μm 35cm	+	254	Hyd.		20	20
9	Borate	50μm 35cm	+	254	Elc.	20	20	20
10	Borate	50μm 35cm	+	254	Elc.	15	20	15
11	Borate	50μm 35cm	+	254	Elc.	20	20	20
12	Borate	50μm 35cm	+	254	Elc.	20	20	20
13	Borate	50μm 35cm	+	254	Elc.	20	15	20

TABLE 4.1. continued.

Exp #	Buffer	Column	High voltage supply	λ (nm)	Injection mode	Sample voltage (kV)	Sample time (s)	Run voltage (kV)
14	Dolnik	75μm 60cm	+	214	Hyd.		5	11
15	Dolnik	75μm 60cm	+	280	Hyd.		5	11
16	Borate	75μm 60cm	-	214	Hyd.		7	25
17	TBE	75μm 60cm	+	214	Hyd.		7	25
18	Borate	75μm 60cm	+	214	Hyd.		7	25
19	Borate	75μm 60cm	+	214	Hyd.		7	25
20	TBE	75μm 60cm	-	214	Hyd.		7	25
21	TBE	75μm 60cm	-	214	Hyd.		7	15
22	Borate	75μm 60cm	-	214	Hyd.		7	25
23	Borate	75μm 60cm	+	214	Hyd.		20	20
24	Borate	75μm 60cm	+	214	Elc.	20	20	20
25	Borate	75μm 60cm	-	214	Elc.	20	20	20
26	Borate	75μm 60cm	+	254	Hyd.		20	20

TABLE 4.1. continued.

Exp #	Buffer	Column	High voltage supply	λ (nm)	Injection mode	Sample voltage (kV)	Sample time (s)	Run voltage (kV)
27	Borate	75μm 60cm	+	254	Hyd.		7	25
28	Borate	75μm 60cm	+	254	Elc.	20	20	20
29	Borate	75μm 60cm	+	254	Elc.	20	20	20
30	Borate	75μm 60cm	+	254	Hyd.		7	25
31	Borate	75μm 60cm	+	254	Elc.	20	20	20
32	Borate	75μm 60cm	-	254	Hyd.		7	25
33	Borate	75μm 60cm	+	280	Hyd.		20	20
34	Borate	75μm 60cm	+	280	Elc.	20	20	20
35	Borate	75μm 60cm	+	280	Hyd.		7	25
36	Borate	75μm 60cm	+	280	Elc.	20	20	20
37	Borate	75μm 60cm	+	214	Hyd.		5	11
38	TBE	75μm 60cm	+	214	Hyd.		5	11
39	TBE	75μm 60cm	+	214	Elc.	20	7	25

TABLE 4.1. continued.

Exp #	Buffer	Column	High voltage supply	λ (nm)	Injection mode	Sample voltage (kV)	Sample time (s)	Run voltage (kV)
40	TBE	75μm 60cm	+	214	Elc.	20	20	20
41	TBE	75μm 60cm	-	214	Elc.	20	7	25
42	TBE	75μm 60cm	-	214	Elc.	20	20	20
43	TBE	75μm 60cm	-	254	Hyd.		7	25
44	TBE	75μm 60cm	-	254	Elc.	20	7	25
45	TBE	75μm 60cm	+	254	Hyd.		7	25
46	TBE	75μm 60cm	+	254	Elc.	20	7	25
47	TBE	75μm 60cm	+	254	Hyd.		20	20
48	TBE	75μm 60cm	+	254	Elc.	20	20	20
49	TBE	75μm 60cm	+	280	Hyd.		7	25
50	TBE	75μm 60cm	+	280	Elc.	20	7	25
51	TBE	75μm 60cm	+	280	Hyd.		20	25
52	TBE	75μm 60cm	+	280	Elc.	20	20	25

4.3.2 Capillary Zone Electrophoresis of Restriction Enzymes

The restriction enzymes analysed by CZE were of commercial grade. They were kept in storage buffers. The samples were diluted in high-grade deionised water (1:10) before injection. The storage buffer of Pst1 was also analysed by CZE under the same conditions. TBE buffer was used as the run buffer which was degassed and filtered through 0.45 μm Millipore filters before run. The system was fitted with 60 cm long x 75 μm I.D. capillary and positive high voltage supply. Experiments performed for the analysis of restriction enzymes are summarized on Table 4.2.

TABLE 4.2. Experiments performed for the analysis of RE by CZE.

Exp #	RE Sample	Buffer	λ (nm)	Injection mode	Sample voltage (kV)	Sample time (s)	Run voltage (kV)
1	Taq1	TBE	214	Hyd.		20	20
2	EcoR1	TBE	214	Hyd.		20	20
3	Pst1	TBE	214	Hyd.		20	20
4	Taq1	TBE	254	Hyd.		20	20
5	EcoR1	TBE	254	Hyd.		20	20
6	Pst1	TBE	254	Hyd.		20	20
7	Taq1	TBE	280	Hyd.		20	20
8	EcoR1	TBE	280	Hyd.		20	20
9	Pst1	TBE	280	Hyd.		20	20
10	Pst1	TBE	214	Hyd.		20	11
11	Taq1	TBE	214	Hyd.		20	11
12	Taq1-Pst1 mixture	TBE	214	Hyd.		20	20
13	Storage buffer of Pst1	TBE	214	Hyd.		20	20

4.3.3 Capillary Zone Electrophoresis of Serum Proteins

The serum that was prepared using whole blood drawn from several patients and volunteers was kindly provided from Düzen Laboratories in Ankara. The serum sample was diluted in high-grade deionised water (1:20) before injection. The run buffer used to analyse serum proteins by CZE was Dolnik's buffer prepared as previously described (Dolnik, 1995) and filtered through 0.45 μm Millipore filters before use. The first five experiments listed in the table below were performed with the Biorad capillary electrophoresis system in Düzen Laboratories in Ankara, which was fitted with 60 cm long x 75 μm I.D. capillary and a deuterium lamp detecting at 200 nm, the polarity was switched to normal mode. The serum samples of fourth and fifth individuals were pathological while the others were normal. The last two experiments on table were performed with the Waters Quanta 4000E capillary electrophoresis system to analyse the serum sample of the first individual (P#1). This system was fitted with 60 cm long x 75 μm I.D. capillary and positive high voltage supply. Experiments performed for the analysis of serum proteins are summarized on Table 4.3.

TABLE 4.3. Experiments performed for the analysis of serum proteins by CZE.

Serum Sample	Buffer	λ (nm)	Injection mode	Sample time (s)	Run voltage (kV)
P#1	Dolnik	200	Hyd.	2	11
P#2	Dolnik	200	Hyd.	2	11
P#3	Dolnik	200	Hyd.	2	11
P#4	Dolnik	200	Hyd.	2	11
P#5	Dolnik	200	Hyd.	2	11
P#1	Dolnik	254	Hyd.	5	11
P#1	Dolnik	214	Hyd.	5	11

4.3.4 Entangled Solution Capillary Electrophoresis of PCR Amplified DNA Fragments

Entangled solution capillary electrophoresis (ESCE) was carried out to analyse the DNA samples of Turkish cystic fibrosis patients. Fused silica capillaries were fitted onto the system and dynamic coating with linear polyacrylamide containing buffer was carried out. The run buffer was prepared by adding 6 per cent bis-acrylamide (6 per cent T, 0 per cent C polyacrylamide solution) into the TBE buffer. The runs were performed at negative polarity using the negative power supply and detection was carried out at 254 nm.

4.3.5 Capillary Gel Electrophoresis

Capillary gel electrophoresis (CGE) was performed with 60 cm long x 75 μm I.D. polyacrylamide gel-filled (5 per cent T, 5 per cent C gel) capillary columns filled with μPAGE buffer. The purge cycle feature was disabled since pressure or vacuum should never be applied to the gel. The run buffer used in the analysis of samples with the gel-filled columns was μPAGE buffer which was degassed by sonication and filtered through 0.45 μm Millipore filters before use. Only μPAGE buffer solution had to be used with the gel, other solutions might cause voids to form due to gel expansion or contraction. The system was fitted with the negative high voltage power supply and the UV absorbance was monitored for detection at 254 nm.

The columns were refrigerated (4 °C) and allowed to remain at room temperature for at least two hours before they were cut to the desired length and used for the analysis. The capillary is cut using an appropriate column cutting tool. To assure that no air bubbles become trapped at the tip during cutting, a drop of buffer is put on the scoring point before cutting. The column was cut exactly 7.5 cm from the detection window. Immediately after cutting the ends, the column was installed in the CE instrument and remained in buffer

solution to avoid gel dehydration and consequent bubble formation. For storage after use, the column ends were immersed in the run buffer solution.

Before using the polyacrylamide gel-filled capillary column, it was conditioned at ambient temperature and 100 V/cm (5 kV for the 60 cm capillary which had 50 cm effective length) at negative polarity (injection side = cathode) for five minutes. Then, the applied voltage was increased stepwise to 250 V/cm (12.5 kV) over a period of thirty minutes. The current should be stable at approximately 7-9 μA. In the event of current fluctuations, the applied voltage was stopped and the column was inspected for voids (bubbles). This conditioning procedure was repeated before using a column that has been idle for more than 4 hours.

To check the system and column performance, the μPAGE $pd(A)_{25\text{-}30,40\text{-}60}$ oligonucleotide standard was run at 12.5 kV with negative polarity using electrokinetic injection, 5 seconds at 5 kV. The elution profile was compared to the one shown on the column performance summary sheet.

In order to check the performance of the mercury lamp detecting at 254 nm fitted onto the system, the capillary column was purged with different concentrations of sodium chromate solution that was visible at 254 nm and the absorbance values were recorded.

5. RESULTS AND DISCUSSION

The aim of this work was to establish a method for the analysis of several proteins and DNA using capillary electrophoresis. Bovine serum albumin, human serum proteins and some restriction enzymes namely Taq1, EcoR1, Pst1 were analysed by capillary zone electrophoresis in fused silica capillary columns. Entangled solution capillary electrophoresis was performed for the separation of the PCR amplified DNA fragments from Turkish cystic fibrosis carriers by applying dynamic coating with the use of a run buffer containing non-cross linked polyacrylamide. Capillary gel electrophoresis was also carried out with synthetic standard oligonucleotides in polyacrylamide gel-filled columns. The factors affecting analytical parameters such as migration time, peak height and peak shape were studied. The effect of the use of different buffer systems, capillary dimensions, detector wavelengths, polarity modes, applied voltage, sample injection modes and sample loading amounts on the analytical parameters were investigated.

The peak migration times were measured at the mid-point of the peak base. The peak shapes were dependent on the relative mobility of the sample and of the electrolyte, that is, the non-symmetrical peaks were due to the mobility difference. If the mobility of the electrolyte was higher, tailing was observed. Fronting of the peak occurred when the sample was faster than the electrolyte (Waters Corporation, 1995).

5.1 Capillary Zone Electrophoresis of BSA

5.1.1 Purity of BSA

Before performing the capillary zone electrophoresis, the bovine serum albumin (Fraction V) sample was subjected to electrophoretic analysis under denaturing conditions.

Analysis of the protein on SDS-polyacrylamide gel (5 per cent stacking gel, 10 per cent separating gel) is shown in Figure 5.1. The expected position of BSA relative to standard markers is indicated on the figure.

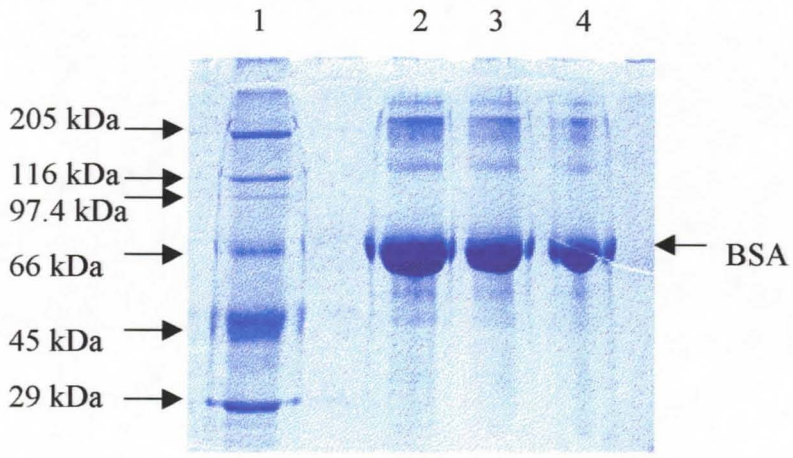

FIGURE 5.1. SDS-PAGE analysis of BSA. Lane 1: SDS molecular weight markers, Lane 2: BSA (5 µl loaded), Lane 3: BSA (3 µl loaded), Lane 4: BSA (2 µl loaded).

The molecular weight of BSA is 66 kDa. The presence of some protein having a molecular weight corresponding to that of dimeric form of BSA and some other impurities could also be observed on SDS gel (Figure 5.1).

5.1.2 Capillary Zone Electrophoresis

In CZE, charged molecules migrate in buffer solution through a capillary under the influence of an applied electric field. The migration of these molecules depends on a number of factors, including the charge to mass ratio of the molecule, the electrical field gradient across the capillary, the pH and ionic strength of the running buffer, and the capillary dimensions. However, proteins get adsorbed onto the walls of uncoated fused silica capillaries. The silica walls have free silanol groups that have a negative charge in

aqueous solutions above a pH value of 2. Proteins can have a net negative charge if the pH of the solutions is adjusted to two units above their isoelectric point. If the protein molecules have a net negative charge, then they should be repelled from the wall surface and their adsorption should be minimized. Protein adsorption can also be decreased by modifying the capillary wall characteristics with coatings, or by using additives in the separation buffer or the sample (Pande et al., 1992).

The sample solution of BSA of 5 mg/ml (pI 4.9) was prepared in high-grade deionized water. The running buffer systems used were borate buffer (pH 8.5), TBE buffer (pH 8.25) and Dolnik's buffer (pH 10.2). Most of the analyses were performed with 60 cm long capillary columns having 75 μm inner diameter while 35 cm long capillary column with 50 μm inner diameter was used in some experiments. UV absorbance was monitored at various wavelengths such as 214 nm, 254 nm and 280 nm. The system was fitted with either positive and negative high voltage power supplies, that is BSA was analysed with both normal and reverse polarity modes. Injections of the samples were either done hydrostatically or by electromigration. The temperature during operation was maintained at 20 °C. The experiments performed for the analysis of BSA were listed on Table 4.1.

The run buffer was degassed by sonication and filtered through 0.45 μm filters. The benefits of degassing were baseline stability and enhanced signal-to-noise ratio, that is the noise was decreased. The migration times for eluting peaks were reproducible and current levels were stable. At high voltages, because of the increase in heat of the capillary and the buffer within it, outgassing might occur inside if the buffer was not degassed.

Before each run, the capillary was rinsed for five minutes with 0.1 M sodium hydroxide, this is flushed out with high-grade deionized water for five more minutes. The time allowed was more than enough to rinse the column thoroughly and obtain a flat baseline. After rinsing, the capillary was purged with the run buffer for five minutes. Small bubbles were observed at the end of the capillary when the purge began and the absorbance changed as the electrolyte passed to the detector, therefore the absorbance value was

adjusted to zero when it stabilized. When the run starts, the system autozeroes the detector and the zero point, that is the absorbance of the baseline, is that of the run buffer. After each run, the capillary was rinsed again with deionized water not to let it dry out with buffer inside.

5.1.2.1 Buffer Systems. The electropherograms of BSA sample using different run buffers are shown in Figures 5.2, 5.3 and 5.4. The buffer systems in these analyses were borate, TBE and Dolnik's buffer respectively. Separations were performed in 60 cm long capillary and the sample was introduced by hydrostatic injection for five seconds at normal polarity using the positive high voltage power supply and detected at 214 nm. The constant run voltage was 11 kV.

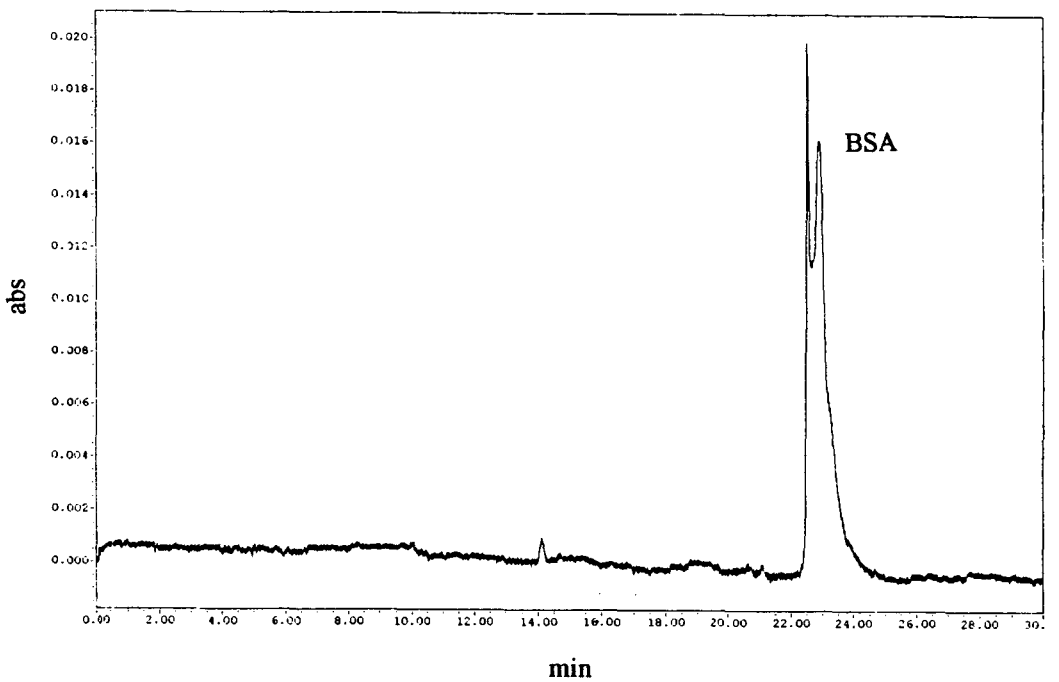

FIGURE 5.2. Electropherogram of BSA.
(Borate, 60 cm column, normal polarity, 11 kV, hydrostatic injection 5 s, 214 nm)

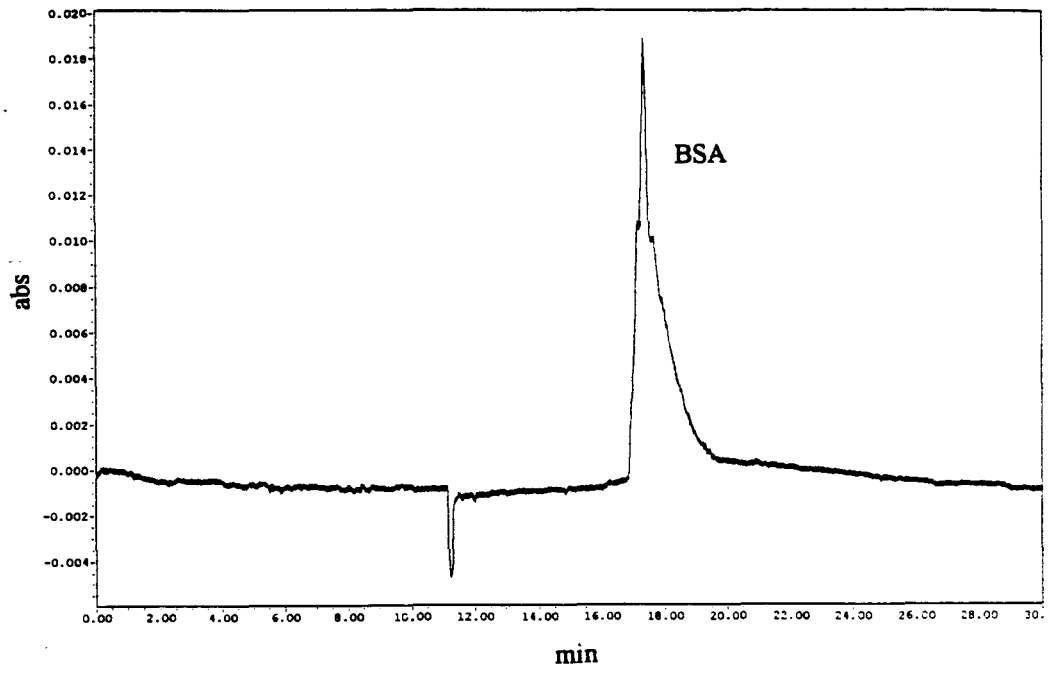

FIGURE 5.3. Electropherogram of BSA.

(TBE, 60 cm column, normal polarity, 11 kV, hydrostatic injection 5 s, 214 nm)

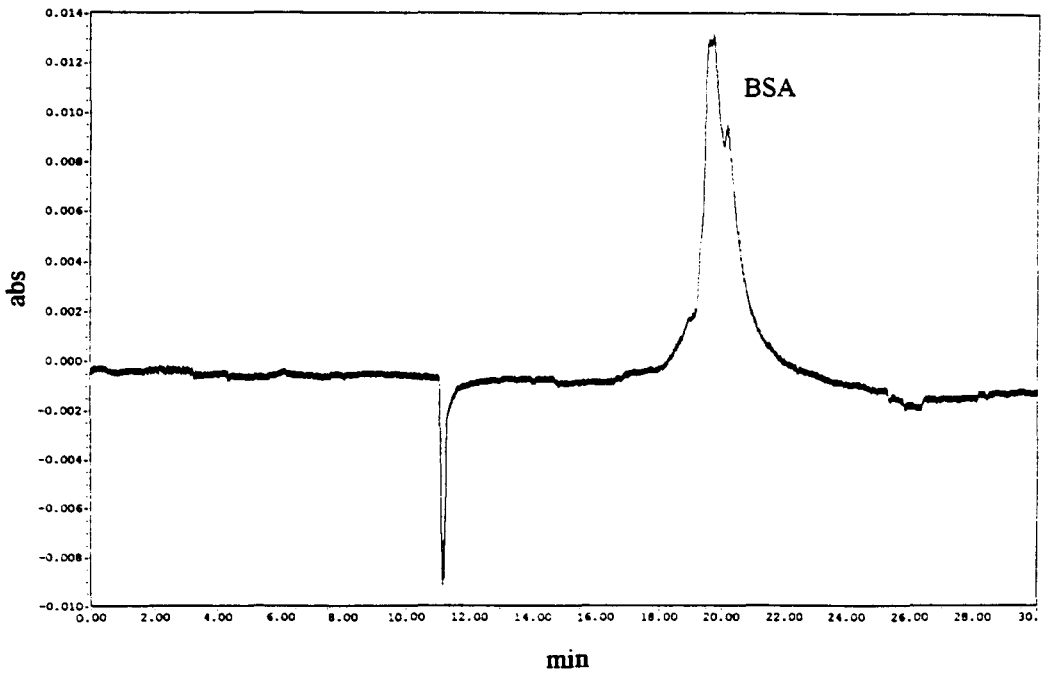

FIGURE 5.4. Electropherogram of BSA.

(Dolnik, 60 cm column, normal polarity, 11 kV, hydrostatic injection 5 s, 214 nm)

The major peak is the albumin that has similar migration times in the runs with TBE and Dolnik's buffer but longer in the one with borate. The small peak migrated about seven minutes before the albumin is in the same form, that is on the negative side with TBE and Dolnik's buffers while it is on the positive side with borate buffer. Since the system autozeroes the detector when the run starts, the zero point is whatever the capillary was purged with, that is the run buffer. The TBE buffer does not only include water, but the Tris, boric acid and EDTA molecules. Dolnik's buffer contains N-MGA and EACA, and borate buffer is just borax. The absorption was measured at 214 nm, in the near UV. The aromatic and polyunsaturated substances absorb well in the near UV, but so do a lot of simple looking organic molecules without extensive conjugated pi-bonds (Halloran, 1999).

After the sample is injected hydrostatically, the starting end of the capillary is filled with BSA. At the beginning of the run, this starting end (anode) moves into the buffer vial, the sample is therefore sandwiched with both ends of capillary inside buffer. When the electric field starts, the charged proteins want to move out of the aqueous zone containing both the sample proteins and other organic molecules, either neutral or charged, in water. The inherent mobility is to move to the anode (or the loading end) away from the detector but the effect of electroendosmotic flow (EOF) is greater in the opposite direction. So, the net movement is towards the cathode where the detector is, and not only the proteins, but also the aqueous zone are swept by EOF towards the detector. When that passes to the detector, if the water, which has a low absorbance at 214 nm, and the other molecules in the aqueous zone do not absorb as well as the sum components that form the buffer, a relative absorbance that is lower than the zero point is seen, i.e. a negative peak. This might explain the case with the TBE and Dolnik's buffers. Molecules containing amine groups are very good absorbers in the near UV (Halloran, 1999). Tris, EDTA, EACA and N-MGA all contain amine groups while borate do not. So when the aqueous zone, carried by EOF, passes the detector, it may contain substances that allow it to absorb better than the borate baseline made as the zero point. Hence no negative peak and possibly a positive one is observed.

When the electropherograms of the two identical runs in Figures 5.5 and 5.6 are compared, the analysis seems reproducible owing to the similar peaks that have equal

values of retention time. The change in the y-axis is only a matter of unit conversion; that is the data collection device reads a signal output of one volt as one absorbance value.

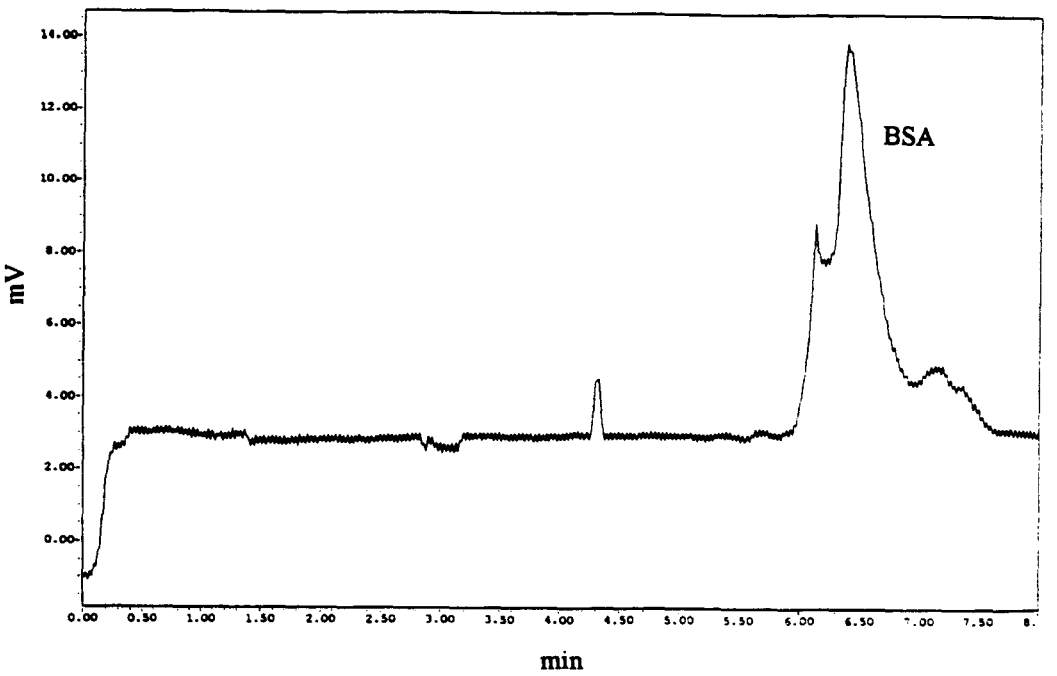

FIGURE 5.5. Electropherogram of BSA.
(Borate, 60 cm column, normal polarity, 25 kV, hydrostatic injection 7 s, 214 nm)

5.1.2.2 UV Absorbance. The optimum wavelength for the detection of BSA was indicated as 214 nm in literature (Pande et al., 1992). Samples were also analysed by monitoring UV absorbance at 254 nm and 280 nm. The zinc lamp was fitted to detect at 214 nm and the mercury lamp was fitted to detect at 254 nm and 280 nm. To configure the detector from 254 nm to 280 nm, the window that covered the lamp was changed. The remarkable difference between the peak height is seen in the electropherograms of runs using different detection wavelengths in Figures 5.7, 5.8 and 5.9. Constant voltage of 20 kV was applied for these analyses in borate buffer by hydrostatic injection of sample in 20 seconds.

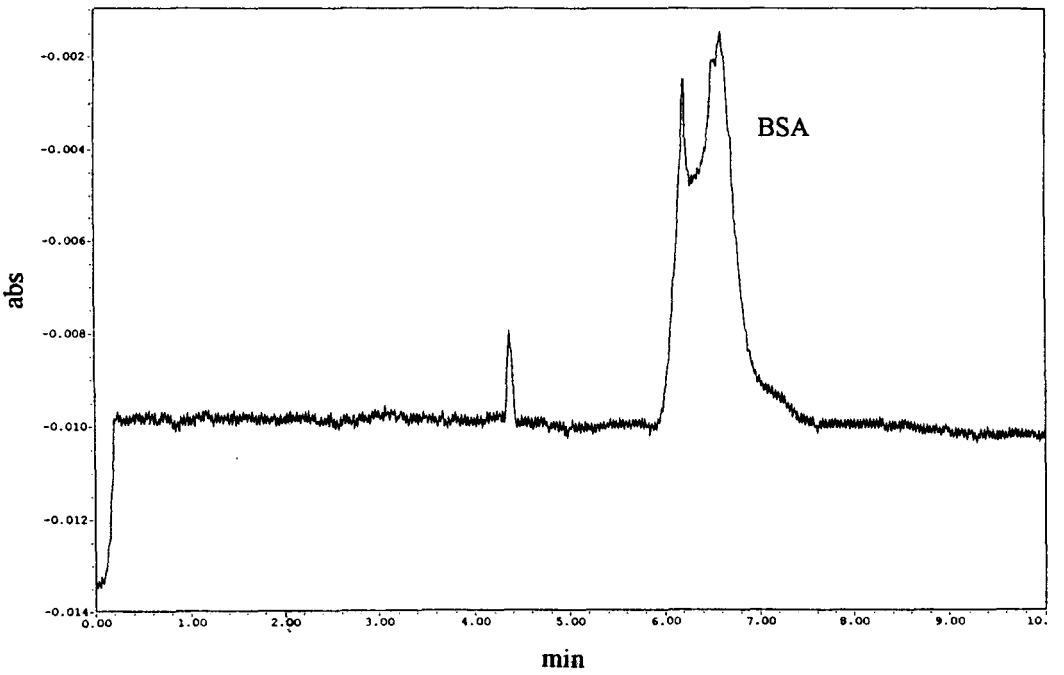

FIGURE 5.6. Electropherogram of BSA.

(Borate, 60 cm column, normal polarity, 25 kV, hydrostatic injection 7 s, 214 nm)

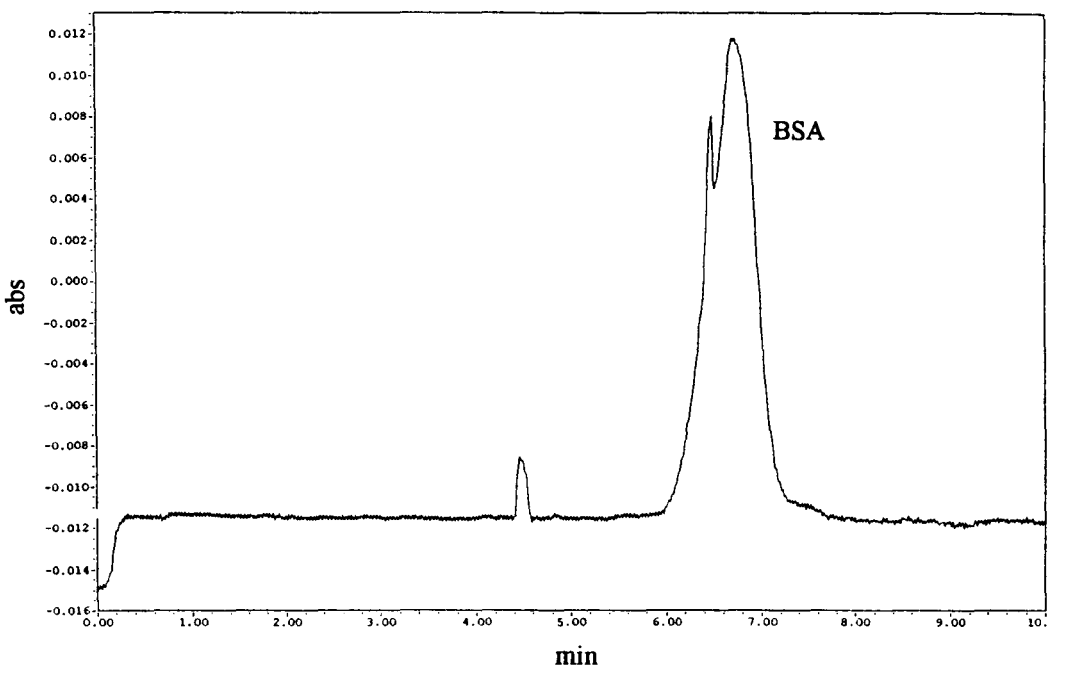

FIGURE 5.7. Electropherogram of BSA.

(Borate, 60 cm column, normal polarity, 20 kV, hydrostatic injection 20 s, 214 nm)

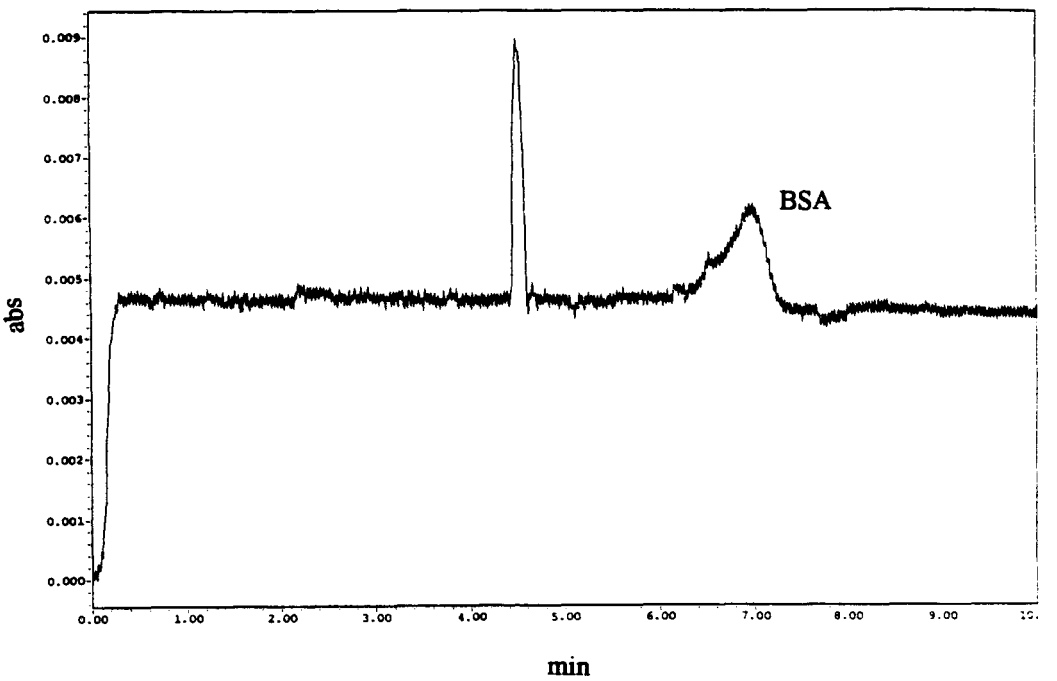

FIGURE 5.8. Electropherogram of BSA.

(Borate, 60 cm column, normal polarity, 20 kV, hydrostatic injection 20 s, 254 nm)

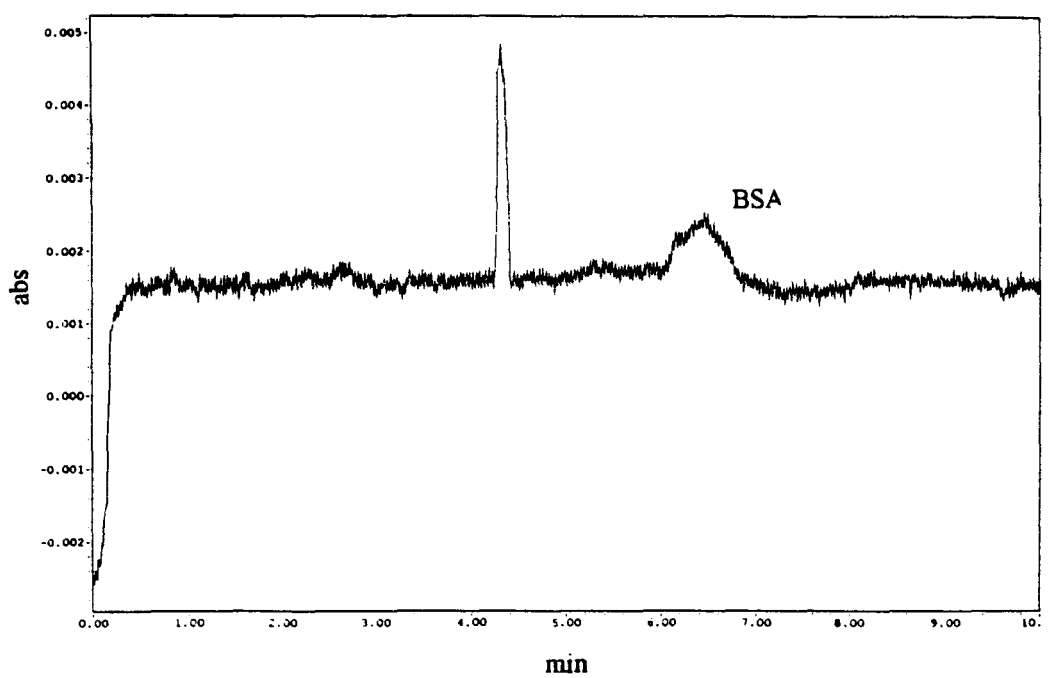

FIGURE 5.9. Electropherogram of BSA.

(Borate, 60 cm column, normal polarity, 20 kV, hydrostatic injection 20 s, 280 nm)

BSA is mostly absorbed at 214 nm since the second peak belonging to BSA is highest on Figure 5.7 although injected sample had the same concentration. The electropherograms detected at 254 nm and 280 nm are almost alike. Similar results were also obtained with TBE buffer (Figures 5.10, 5.11 and 5.12).

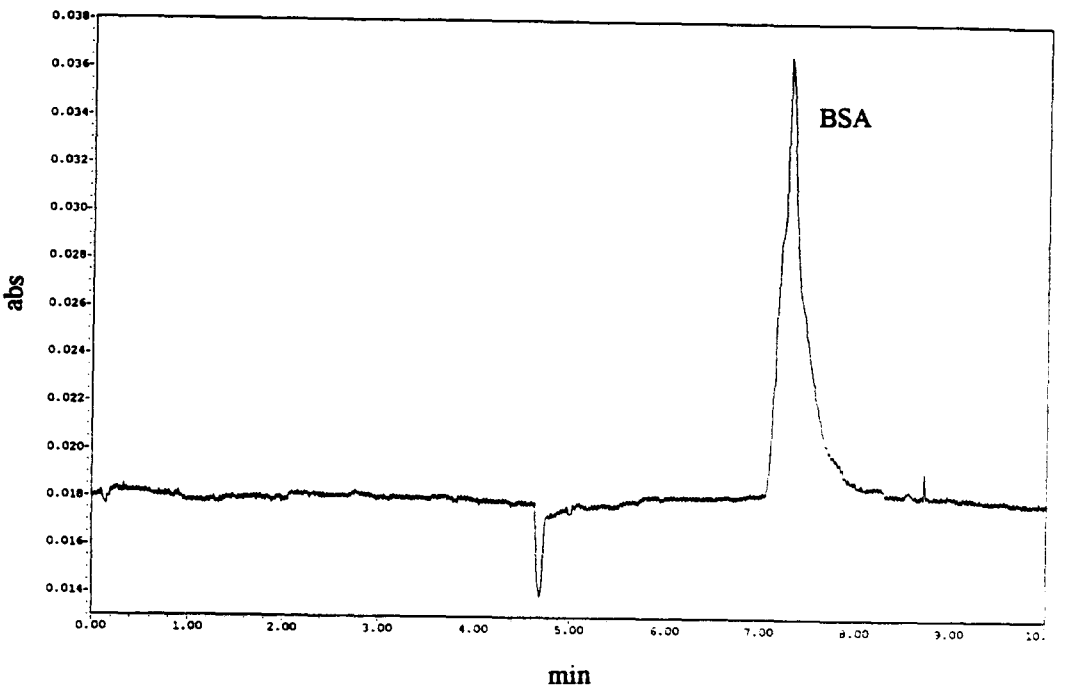

FIGURE 5.10. Electropherogram of BSA.
(TBE, 60 cm column, normal polarity, 25 kV, hydrostatic injection 7 s, 214 nm)

The first peak is on the positive side with the TBE buffer at 254 nm (Figure 5.11) or 280 nm (Figure 5.12) while it was observed on the negative side at 214 nm. This might be because of the higher absorbance of the components in the aqueous zone than the buffer at 254 or 280 nm. The absolute absorbance (absolute height) of the first peak remains approximately the same at all wavelengths. The area of this peak remains constant in different experimental conditions with BSA. As the proteins move out of the aqueous zone, each protein forms its own zone of different mobility. These separate zones are measured independently against the baseline. The aqueous zone forming the first peak might have nothing in it that moves or forms a separate zone, it might be carried only by the electroosmotic force and thus its volume might never change during loading.

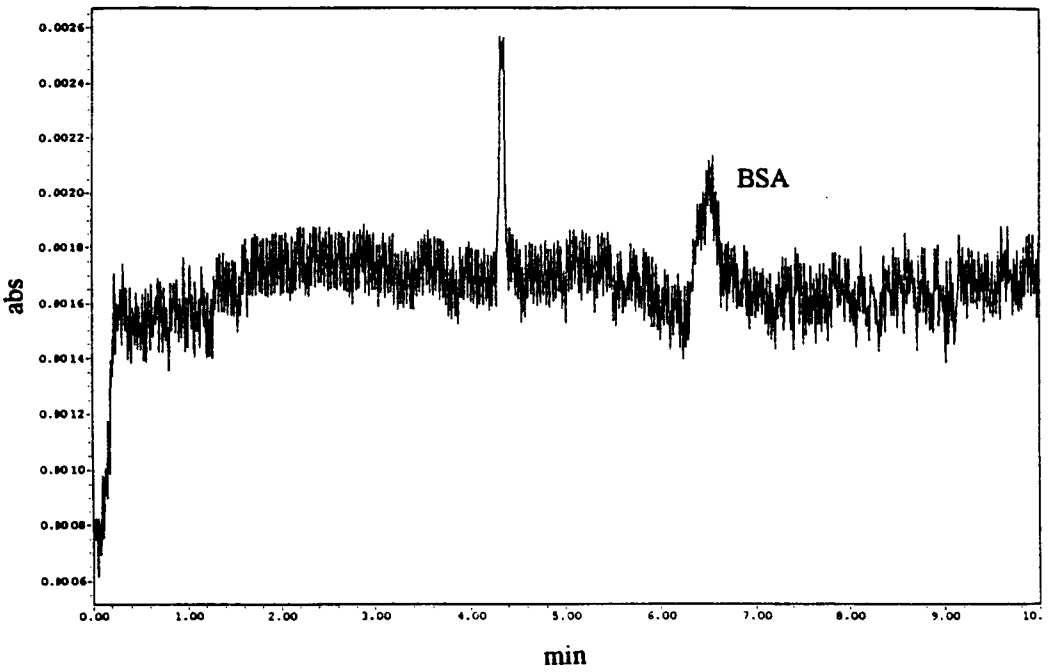

FIGURE 5.11. Electropherogram of BSA.

(TBE, 60 cm column, normal polarity, 25 kV, hydrostatic injection 7 s, 254 nm)

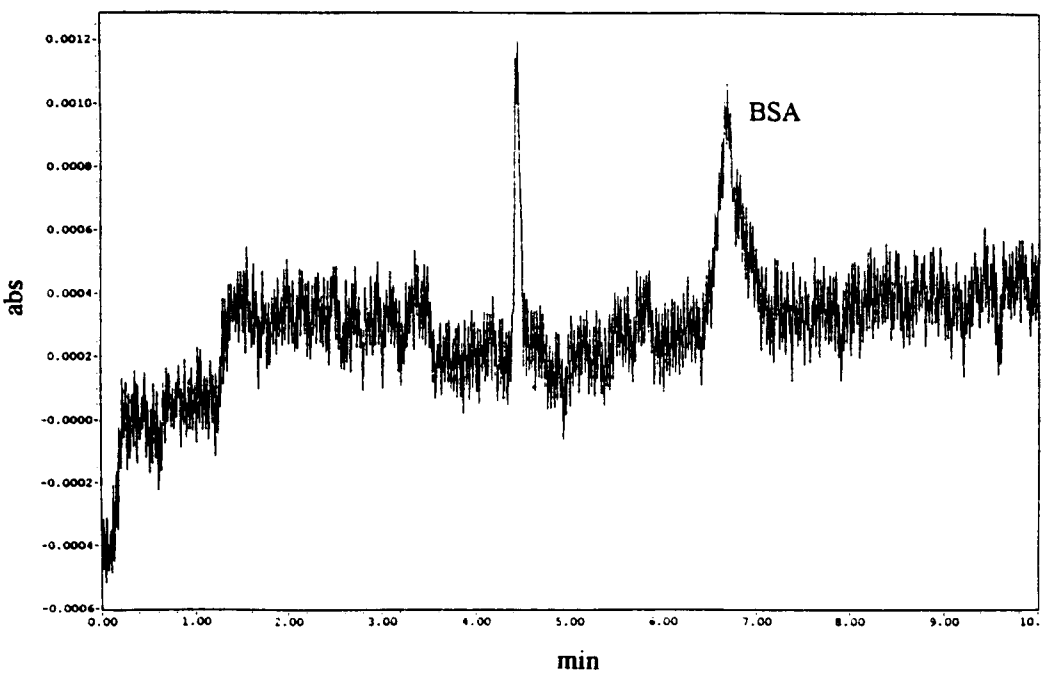

FIGURE 5.12. Electropherogram of BSA.

(TBE, 60 cm column, normal polarity, 25 kV, hydrostatic injection 7 s, 280 nm)

BSA could not be detected at 254 nm or 280 nm when Dolnik's buffer was used. The electropherograms consisted of a very noisy baseline when the sample was run at 11 kV under the same conditions as in the run of Figure 5.4 where a nice peak shape was obtained.

5.1.2.3 Effect of Capillary Column Size. The total length and the effective length of capillary influence the migration time and the peak shape. At constant voltage, the longer the capillary, the smaller is the electrical field gradient (V/cm). This leads to slower migration, greater zone broadening, and wider peak (Pande et al., 1992). 35 cm long capillary column with an inner diameter of 50 μm was used in the analysis of BSA run in borate buffer at 20 kV by hydrostatic injection of 20 seconds, the detection was at 254 nm (Figure 5.13). The electropherogram obtained under same experimental conditions but using 60 cm long column with an inner diameter of 75 μm is illustrated in Figure 5.8.

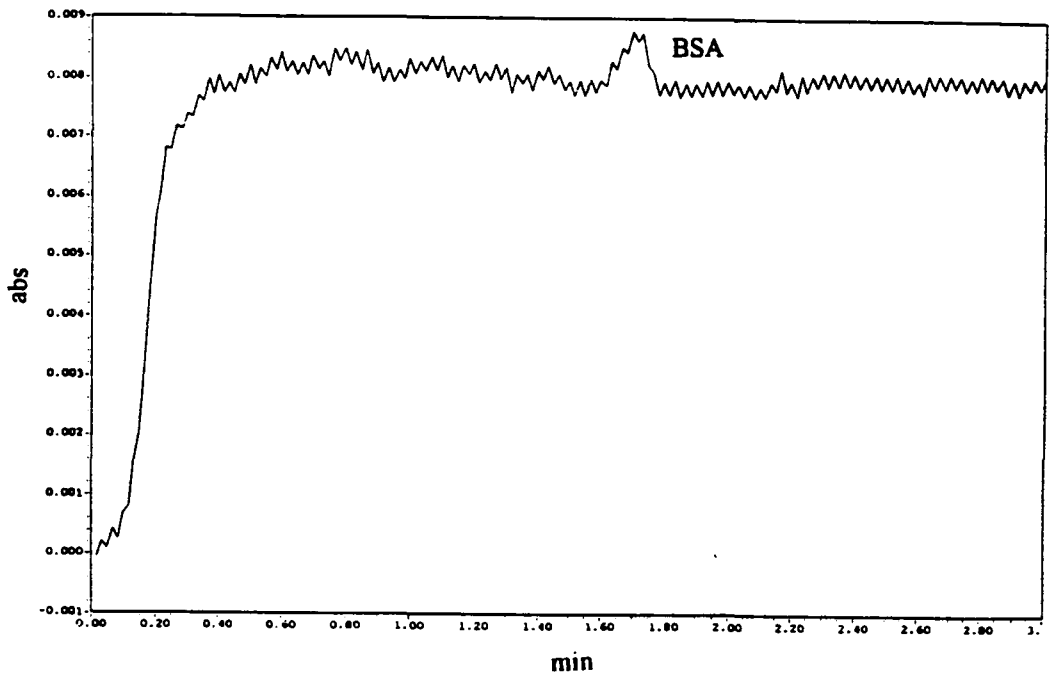

FIGURE 5.13. Electropherogram of BSA.
(Borate, 35 cm column, normal polarity, 20 kV, hydrostatic injection 20 s, 254 nm)

It is reported that the use of longer capillaries gives results in a proportional increase in the number of theoretical plates provided the field strength is kept constant (Weinberger, 1998). As expected, the protein migrated in a shorter time in the shorter capillary. Only one peak, which belongs to BSA, can be observed after the run in shorter column while with the longer column, besides the major BSA peak having approximately the same absorbance of the one in the short column, one more peak occurs before that. This secondary earlier peak probably contains the components in the aqueous zone other than BSA already mentioned.

The small inside diameter of capillaries allows efficient dissipation of the heat generated by the application of high voltages. The principal difficulty lies in the limited ability to dissipate heat generated in the electrophoretic process. It is reported as heat is generated uniformly throughout the medium but is only removed at the inner surface and ends of the tube. Once thermal equilibrium is established, there is a parabolic temperature gradient across the column. Electrophoretic mobility increases as the temperature of the medium is increased. Solutes in the warmer center of the column migrate faster while those at the wall migrate more slowly, resulting in zone broadening. The most effective way to minimize this effect is to reduce the column radius. The radial position of individual solute molecules is constantly changed by diffusion. In a column of reduced radius a solute molecule diffuses back and forth across the radius more often and thus is less likely to spend an abnormally large fraction of time in any one particular portion of the radius. Thus reduction in radius not only reduces radial temperature differences but also diminishes the impact of any temperature differences that remain (Jorgenson and Lukacs, 1981).

5.1.2.4 Effect of Run Voltage. Since both the electroosmotic and electrophoretic migration velocities are directly proportional to the field strength, the use of highest voltages possible would result in shortest times for the separation. Short separation times would give the highest efficiencies since diffusion is the most important feature contributing to band broadening. The limiting factor is Joule heating (Weinberger, 1998). Therefore, for high separation efficiency in terms of time, use of highest voltages possible is suggested.

The electropherograms in Figures 5.2, 5.7 and 5.6 show the runs in borate buffer performed at 11 kV, 20 kV and 25 kV respectively. The other experimental conditions are not fixed, e.g. the heights of the peaks are different due to different amounts of sample load, which will be discussed in the next section. Application of higher voltage decreases the retention time of the sample. This decrease in retention time is very slightly observed between the runs with 20 and 25 kV but the protein migrates much more slowly when voltage is decreased to almost half of its value.

The analysis time is proportional to the square of the column length and inversely proportional to the applied voltage, it appears that high voltages applied to short tubes would generate the greatest number of theoretical plates in the shortest length of time (Jorgenson and Lukacs, 1981).

5.1.2.5 Effect of Injection Time. The amount of sample loaded to the capillary column was changed by setting an appropriate value for the sample time. Peak height increases as the sample loaded to the system is increased, this can be observed in the electropherograms in Figures 5.12 and 5.14. Runs were performed in TBE buffer at 25 kV followed at 280 nm. The height of the second peak that belongs to BSA is higher in Figure 5.14 where the sample was injected hydrostatically for 20 seconds compared to the run in Figure 5.12 with 7 seconds of sample time.

5.1.2.6 Effect of Sample Injection Mode. Two methods of sample introduction were used in the experiments; hydrostatic injection and electromigration injection. During hydrostatic injection, the system placed the injection end of the capillary (and the electrode, although no current is applied) in the sample solution and raised the sample vial to a level 9.6 cm higher than that of the electrolyte at the collection end, creating a pressure differential between each end of the capillary. During injection by electromigration, the capillary and electrode were immersed in the sample and voltage was applied for a specific time.

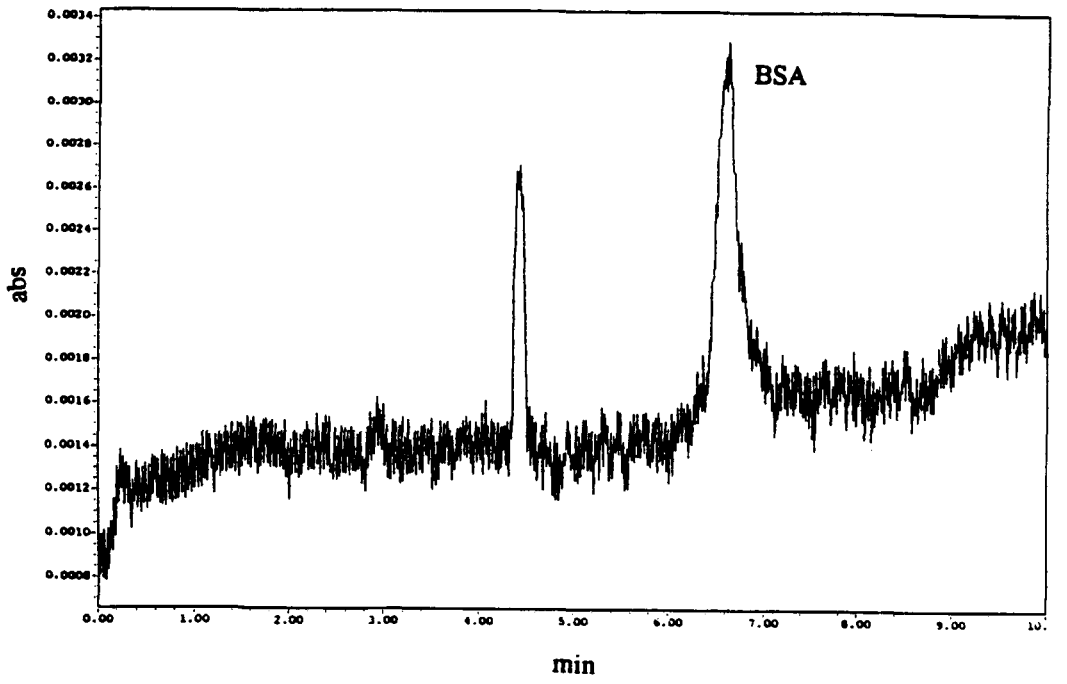

FIGURE 5.14. Electropherogram of BSA.
(TBE, 60 cm column, normal polarity, 25 kV, hydrostatic injection 20 s, 280 nm)

In Figure 5.7, the electropherogram of BSA in borate buffer where the sample was loaded hydrostatically for 20 seconds can be seen. During the run, constant voltage of 20 kV was applied and UV absorbance was followed at 214 nm. All these parameters were kept constant and the sample was introduced to the system by electromigration for 20 seconds at 20 kV to observe the effect of change of injection mode (Figure 5.15).

It was pointed out that in on-column detection the width of a peak in the electropherogram was not proportional to the width of the zone in the electrophoresis column; a slowly migrating zone would give a broader peak than a faster zone, even if the two zones had the same width when they passed the UV beam of the detector (Zhu et al., 1989). Actually, the peak width on the chart only indicates the time needed for a zone to pass the detection point.

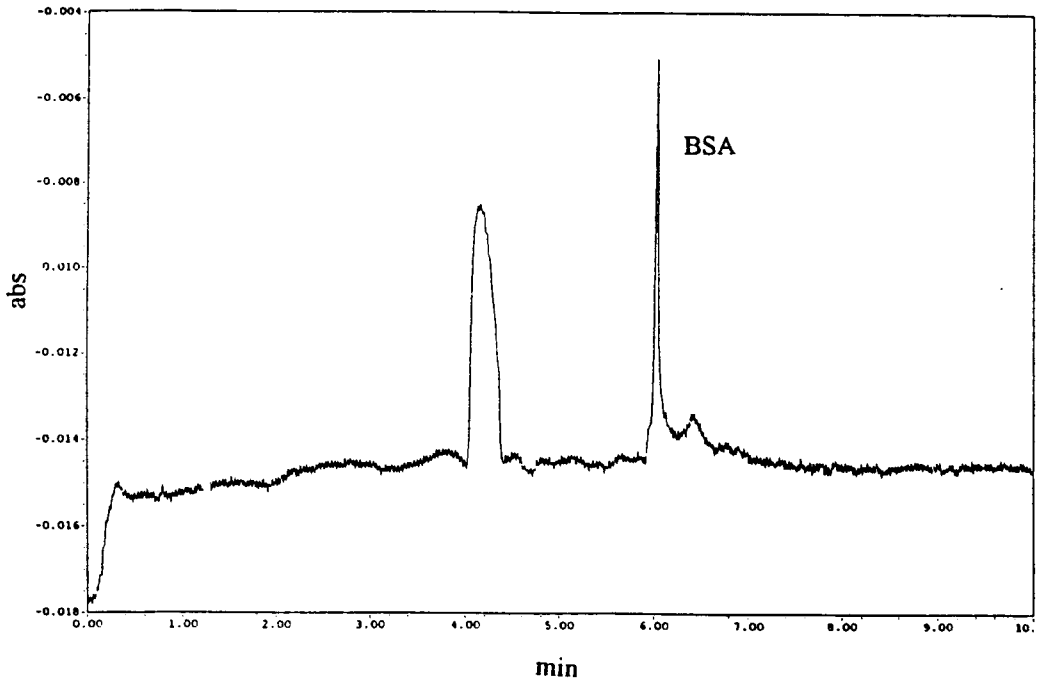

FIGURE 5.15. Electropherogram of BSA.
(Borate, 60 cm column, normal polarity, 20 kV, electromigration 20 s 20 kV, 214 nm)

Control of the differential height and the duration of the injection in hydrostatic injection technique result in accurate, reproducible injections. The amount of material injected into the capillary is fixed when hydrostatic injection mode is used, provided the sample viscosity and temperature are controlled (Weinberger, 1998).

Electromigration also produces reproducible injections, but introduces sample molecules differentially on the basis of each molecule's electrophoretic mobility. The main advantage of electromigration injection is trace enrichment. If the electroosmotic force is low, it is possible to inject only anions or cations into the capillary. On the other hand, the influence of mobility and ionic strength, which are not present in hydrostatic injection, are the disadvantages of electromigration injection. It is important to maintain a constant ionic strength for the injection solution or else, the peak width, peak shape and resolution can be affected (Weinberger, 1998). Injection by electromigration is preferred because of the fact that it introduces minimal band broadening, however, sample introduction with applied

voltage introduces substances based on their electrophoretic mobilities, which complicates the matter of quantitative analysis (Jorgenson and Lukacs, 1981).

The peak height, that is the absorbance of BSA changes; it decreases when the sample injection was done by electromigration although amount of sample loaded was not changed. The peak shape is also different in the two electropherograms obtained using different injection modes (Figures 5.7 and 5.15). A sharper peak was obtained with electromigration injection.

The effect of change in the injection mode was also analysed in the runs in TBE buffer. The electropherogram of BSA in TBE buffer at 25 kV where the sample was loaded hydrostatically for 7 seconds can be seen in Figure 5.10. The parameters such as sample time, run voltage, detector wavelength were kept constant and the sample was introduced to the system by electromigration for 7 seconds at 20 kV to observe the effect of change of injection mode (Figure 5.16). As a matter of fact, it was already mentioned that there was not much difference in peak retention times when the applied voltages are close as 20 and 25 kV.

The same consequences of changing injection mode for the run in borate buffer are also observed for the run in TBE buffer. The peak height is lower when the sample is introduced by electromigration injection.

5.1.2.7 Effect of Polarity. Capillary zone electrophoresis of BSA was also performed in the reversed polarity mode (negative potential at the injection end of the capillary) by replacing the negative high voltage power supply on the system. When the negative voltage supply was fitted on the system, the cathodic end is the injection end of the capillary and the charged components, regardless of whether a cation or an anion, migrate towards the anode at the collection end. Contrary to the case of normal polarity, anions migrate faster than the osmotic flow while cations migrate slower than the osmotic flow.

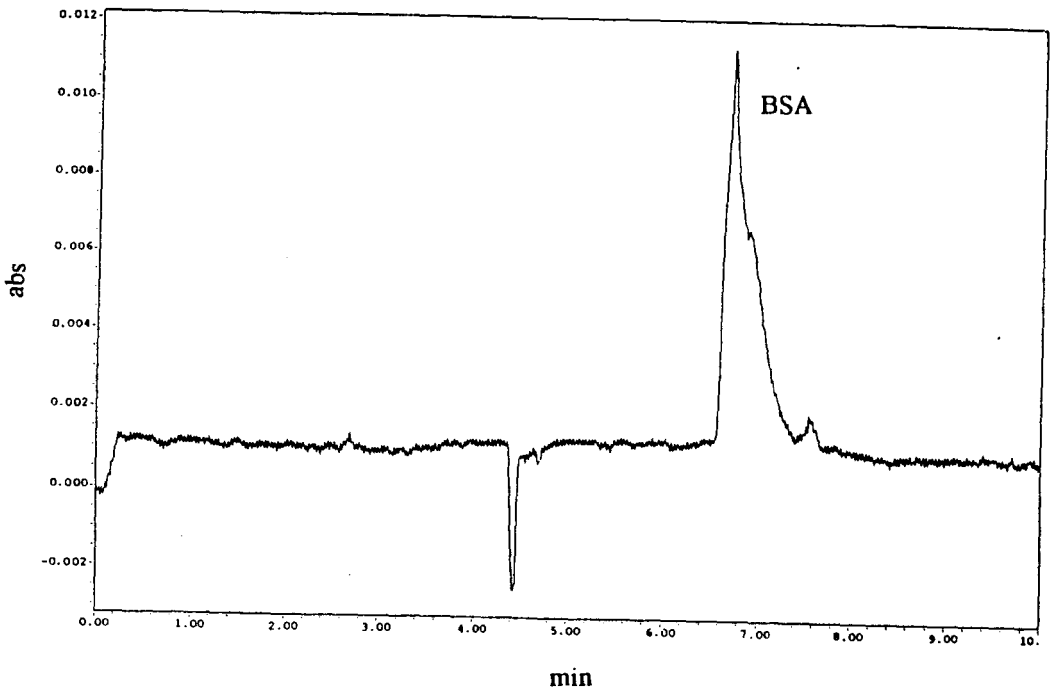

FIGURE 5.16. Electropherogram of BSA.
(TBE, 60 cm column, normal polarity, 25 kV, electromigration 7 s 20 kV, 214 nm)

Since BSA is negatively charged in the pH range of the buffer systems used, it is expected to migrate earlier in the reversed polarity mode where the detector is on the anode side. When BSA was run in borate buffer at reversed polarity, no peak was obtained at either 214 nm or 254 nm of detector wavelength. TBE buffer system was also applied to the system fitted with negative high voltage power supply and BSA was detected at 214 nm at reversed polarity. The electropherogram of BSA in TBE buffer run at normal polarity was shown in Figure 5.10. The same run in the reversed polarity mode can be observed in Figure 5.17. In both analyses, the run voltage was 25 kV, the sample was introduced hydrostatically for 7 seconds and detected at 214 nm.

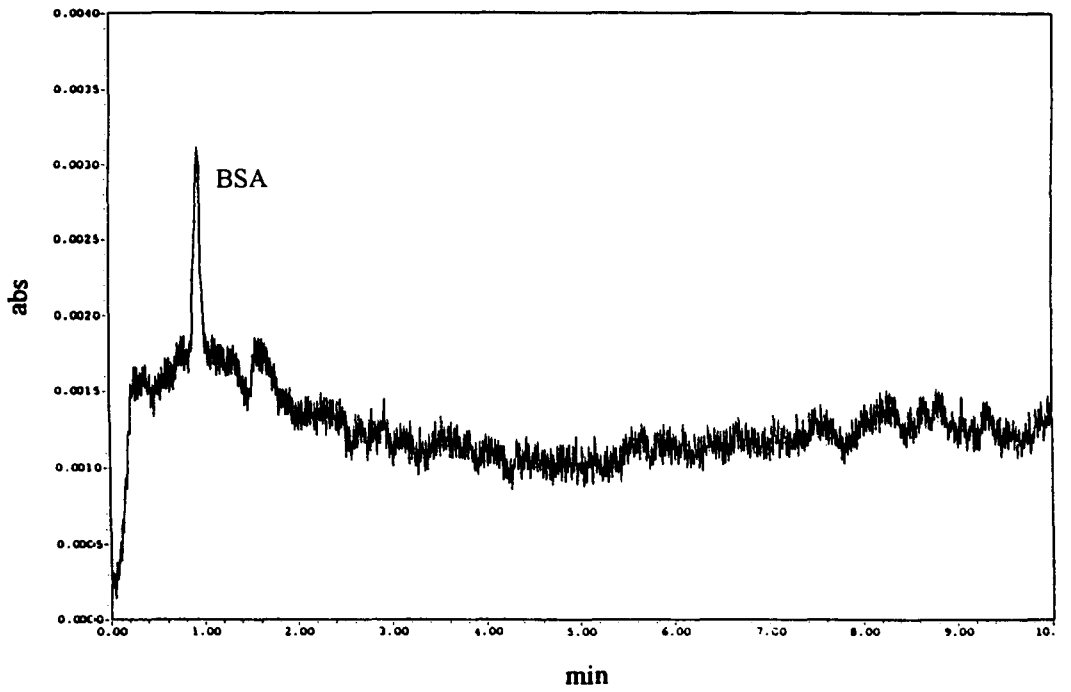

FIGURE 5.17. Electropherogram of BSA.
(TBE, 60 cm column, reversed polarity, 25 kV, hydrostatic injection 7 s, 214 nm)

While BSA migrated at about the seventh minute in the normal polarity mode, its retention time decreases noticeably as expected to about one minute in the reversed polarity mode. The early negative peak in Figure 5.10 belonging to the components in the aqueous zone cannot be observed in the reversed polarity mode (Figure 5.17).

The analysis mentioned above was repeated under the same experimental conditions in reversed polarity mode applying a run voltage of 15 kV. BSA migrated slower as a result of lower voltage (Figure 5.18).

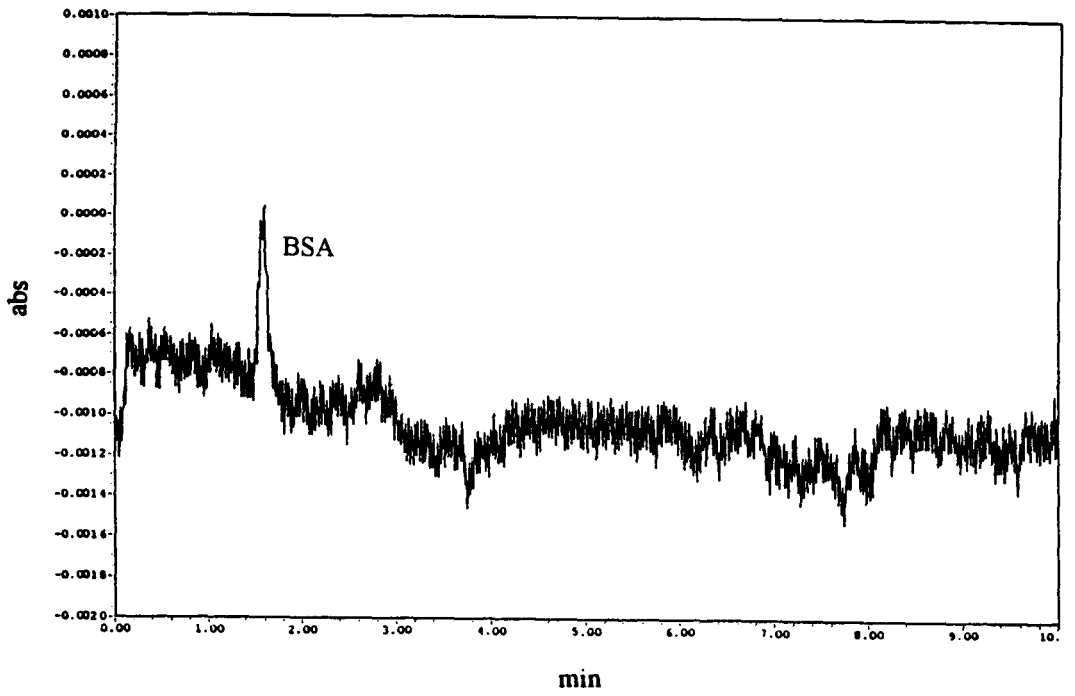

FIGURE 5.18. Electropherogram of BSA.
(TBE, 60 cm column, reversed polarity, 15 kV, hydrostatic injection 7 s, 214 nm)

5.2 Capillary Zone Electrophoresis of Restriction Enzymes

Three restriction enzymes Taq1, EcoR1 and Pst1 kept in storage buffers containing BSA were analysed by capillary zone electrophoresis. The analyses were performed in TBE buffer in normal polarity mode and the system was fitted with 60 cm long capillary with 75 μm inner diameter. The samples were loaded by hydrostatic injection for 20 seconds and UV absorbance was monitored at different wavelengths such as 214 nm, 254 nm and 280 nm. The experiments carried out are listed on Table 4.2.

The electropherograms of Taq1, EcoR1 and Pst1 can be observed in Figures 5.19, 5.20 and 5.21 respectively. The run voltage was 20 kV and the detection was carried out at 214 nm in the experiments demonstrated in these figures.

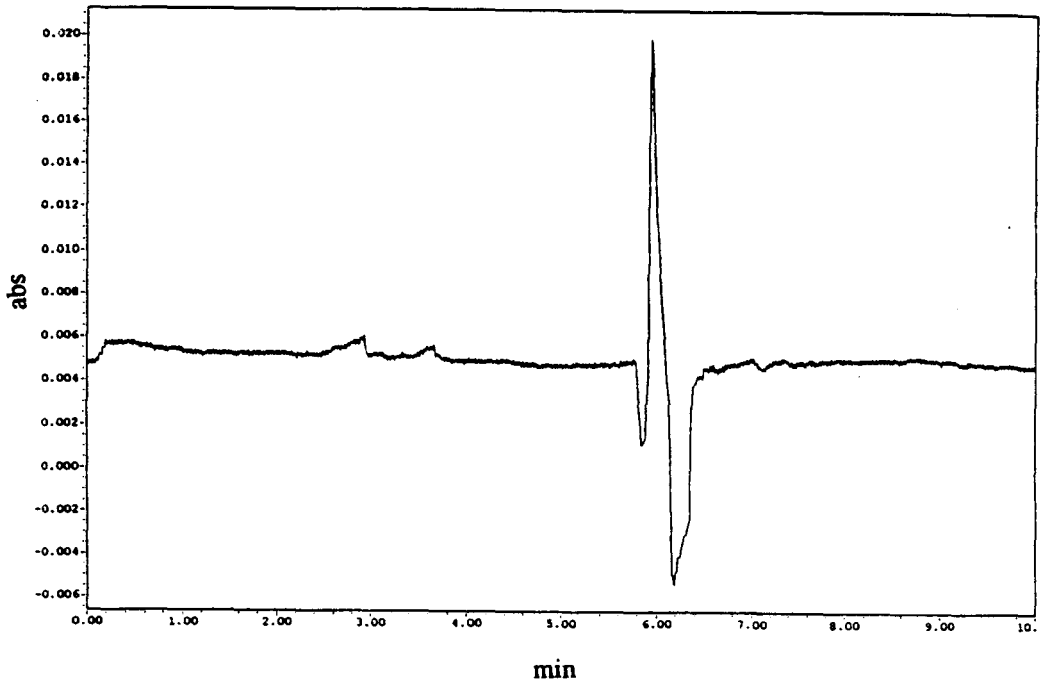

FIGURE 5.19. Electropherogram of Taq1 restriction endonuclease.
(TBE, 20 kV, hydrostatic injection 20 s, 214 nm)

The peak shapes are very similar in the runs with restriction enzymes and they have the same retention times. The small peak at about the third minute might belong to Taq1 restriction endonuclease since it is observed only in the electropherogram of Taq1 sample. A mixture of Taq1 and Pst1 was prepared and analysed at 20 kV, the electropherogram consisted of again one peak at the sixth minute (Figure 5.22). The peak having a retention time of three minutes, which might contain Taq1 restriction enzyme, can also be observed in this electropherogram.

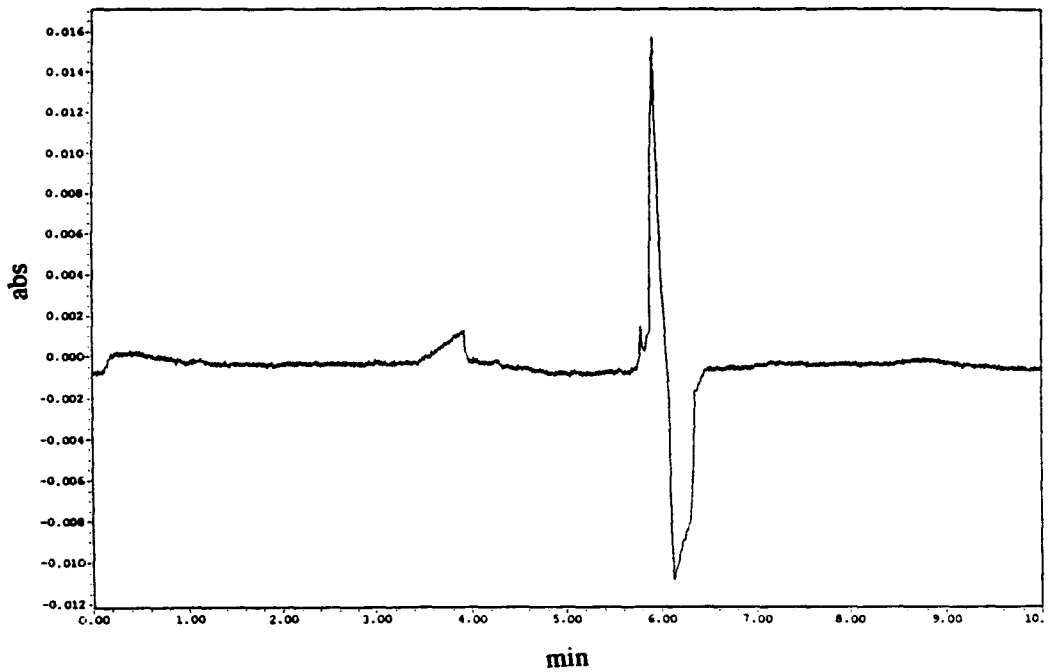

FIGURE 5.20. Electropherogram of EcoR1 restriction endonuclease.
(TBE, 20 kV, hydrostatic injection 20 s, 214 nm)

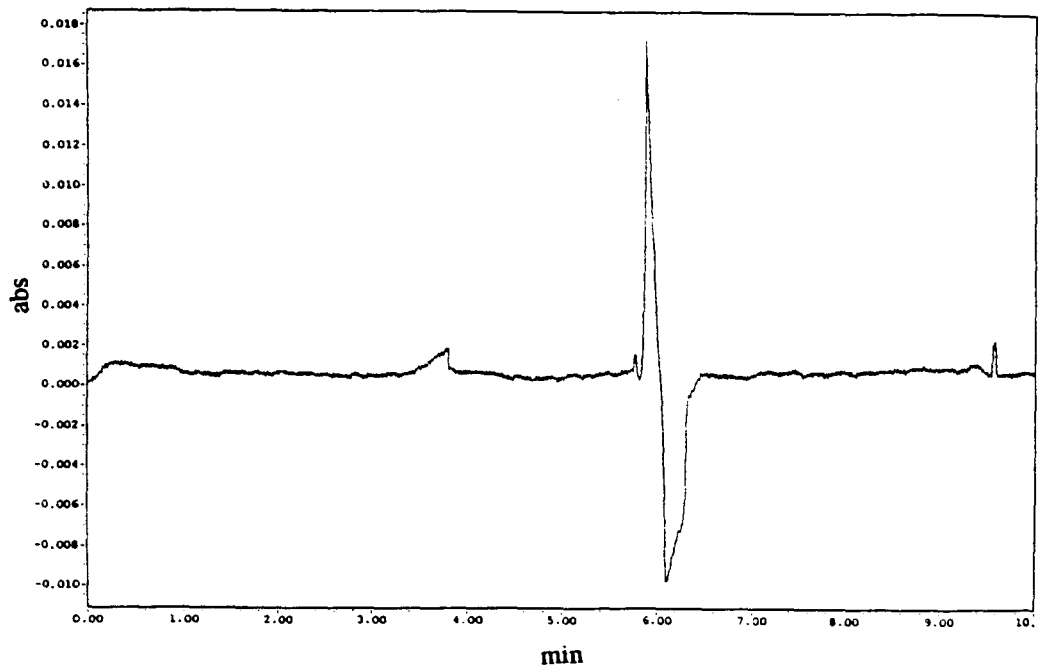

FIGURE 5.21. Electropherogram of Pst1 restriction endonuclease.
(TBE, 20 kV, hydrostatic injection 20 s, 214 nm)

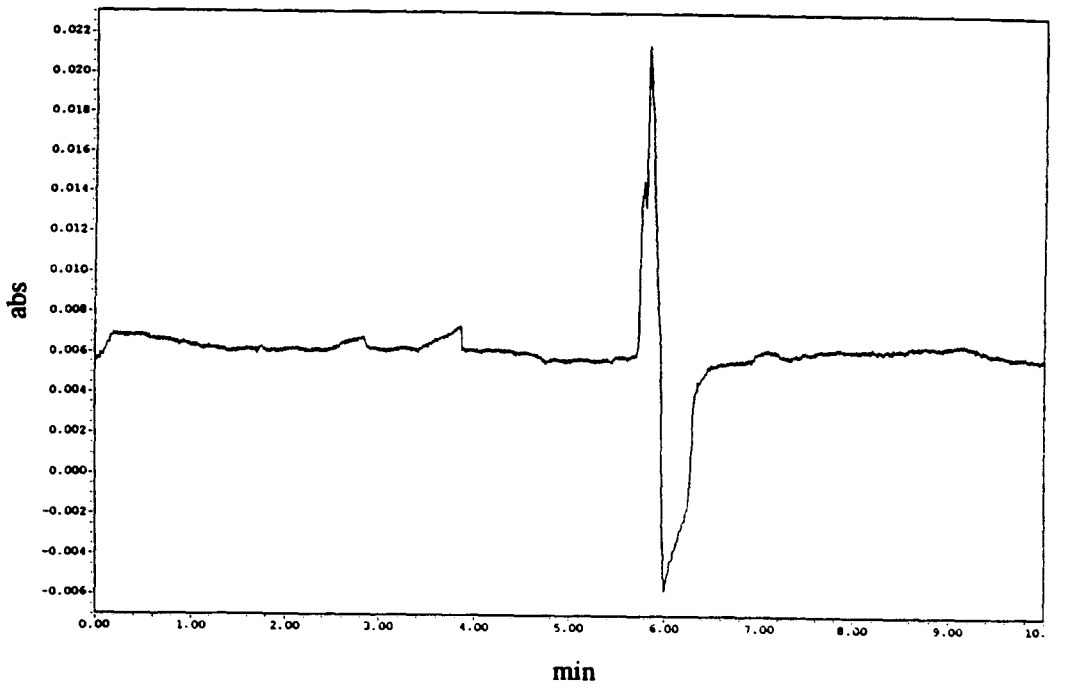

FIGURE 5.22. Electropherogram of Taq1-Pst1 restriction endonucleases mixture. (TBE, 20 kV, hydrostatic injection 20 s, 214 nm)

Since only one peak with the same retention time is observed in separate analyses with three different enzymes and with the mixture of two enzymes, this peak should not belong to any of the restriction enzymes. The storage buffers of the enzymes contain the same components, therefore one of the components in the storage buffer should have been eluted at that minute. The width of the negative peak at the sixth minute is increased in the case of the enzyme mixture, i.e. when the amount of enzyme load is higher, therefore this negative peak might contain the enzymes. If the small peak at the third minute belongs to Taq1, the Pst1 enzyme might have migrated at the sixth minute with negative absorbance.

The results of CZE of the restriction enzymes Taq1 and Pst1 were compared with those of BSA (Figure 5.23) using the same experimental conditions; run voltage was set as 11 kV (Figures 5.24 and 5.25).

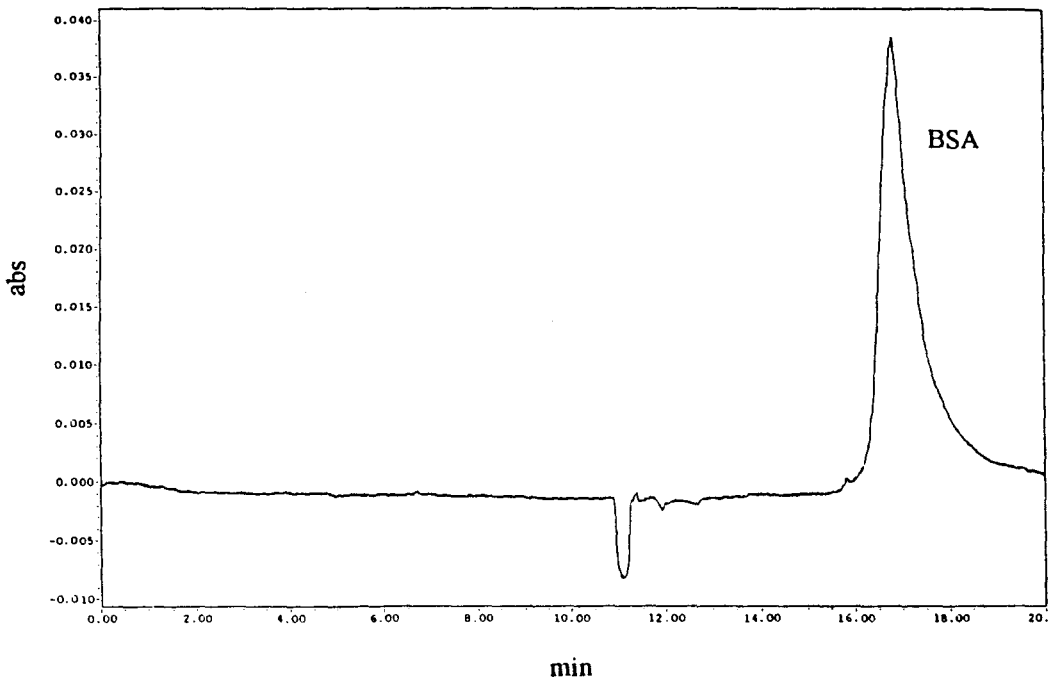

FIGURE 5.23. Electropherogram of BSA.
(TBE, 11 kV, hydrostatic injection 20 s, 214 nm)

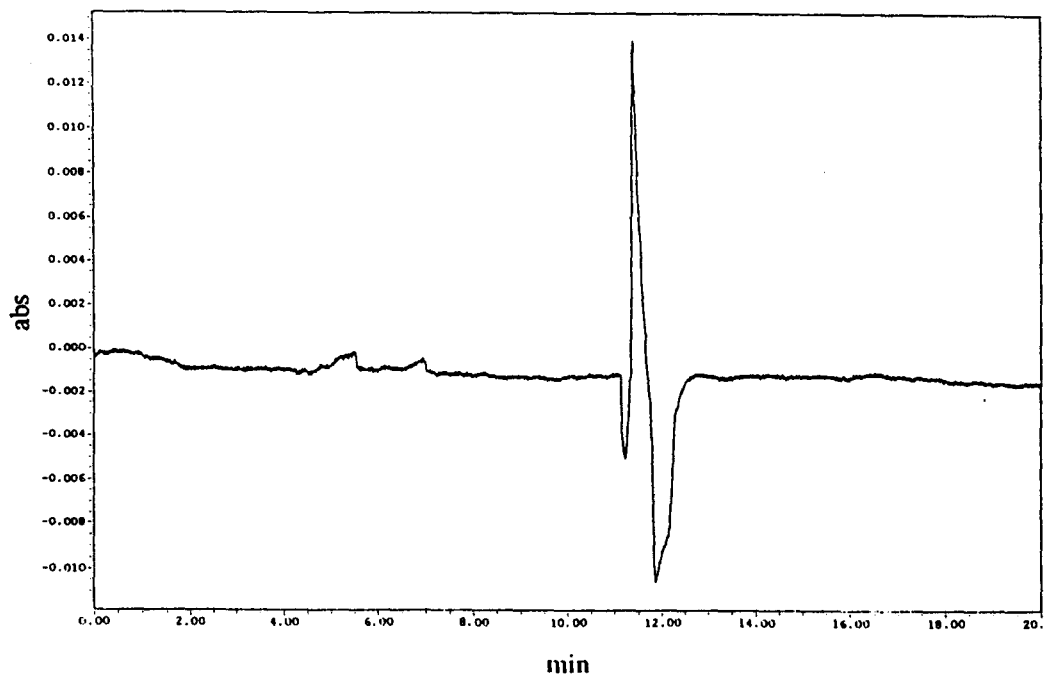

FIGURE 5.24. Electropherogram of Taq1 restriction endonuclease.
(TBE, 11 kV, hydrostatic injection 20 s, 214 nm)

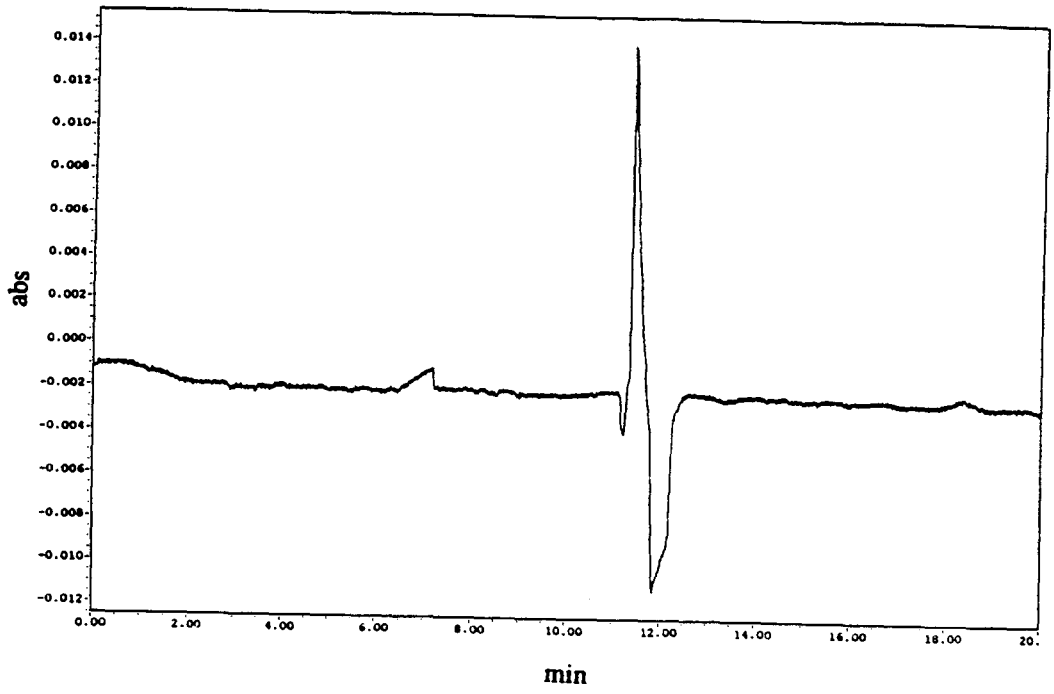

FIGURE 5.25. Electropherogram of Pst1 restriction endonuclease.
(TBE, 11 kV, hydrostatic injection 20 s, 214 nm)

The retention time of BSA is about 16 minutes at 11 kV as observed in the electropherogram in Figure 5.23 while the major peaks obtained in the analyses with the restriction enzymes at the same run voltage migrate at about the twelfth minute (Figures 5.24 and 5.25). Therefore, the peak might not belong to BSA in the storage buffer.

The storage buffer of Pst1 was prepared and CZE was carried out at 20 kV to observe the peaks obtained in the case without the enzyme. The component in the storage buffer was eluted at the sixth minute (Figure 5.26). The retention time of the major peak in the analysis with Pst1 was also six minutes (Figure 5.21), therefore it was proved that this component migrating at the sixth minute at 20 kV was not the restriction enzyme. The small peak with three minutes migration time could not be observed in the electropherogram of storage buffer (Figure 5.26) making it probable to be the peak of the Taq1 enzyme. The negative peak at the sixth minute, which was doubted to be that of Pst1, could not be observed neither.

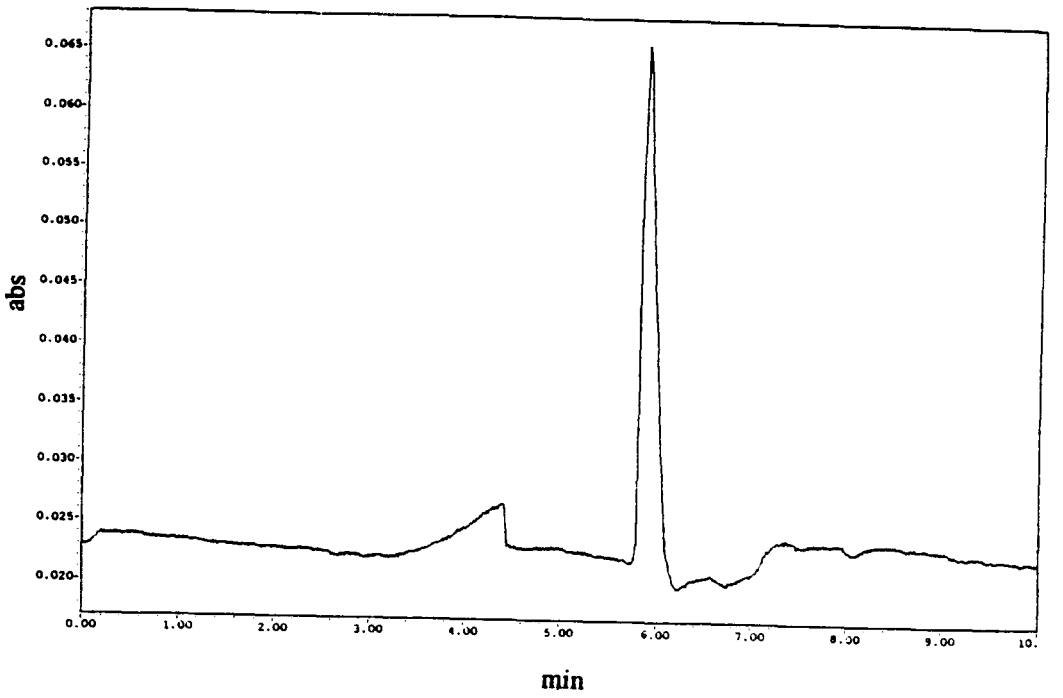

FIGURE 5.26. Electropherogram of storage buffer of Pst1 restriction endonuclease. (TBE, 20 kV, hydrostatic injection 20 s, 214 nm)

When the electropherograms in Figures 5.21 and 5.26 are compared, the absence of the negative peak just after the highest peak can be observed in the latter. The restriction enzyme might be migrating at that minute and because of the difference in the absorbance between the enzyme and the run buffer it might be observed as a negative peak. Therefore, this buffer system is not suitable for the analysis of restriction enzymes Taq1, EcoR1 and Pst1.

The restriction enzymes were also analysed by monitoring the UV absorbance at 254 nm and 280 nm. The electropherograms of Taq1, EcoR1 and Pst1 at 254 nm are shown in Figures 5.27, 5.28, 5.29 and those at 280 nm are shown in Figures 5.30, 5.31, 5.32 respectively.

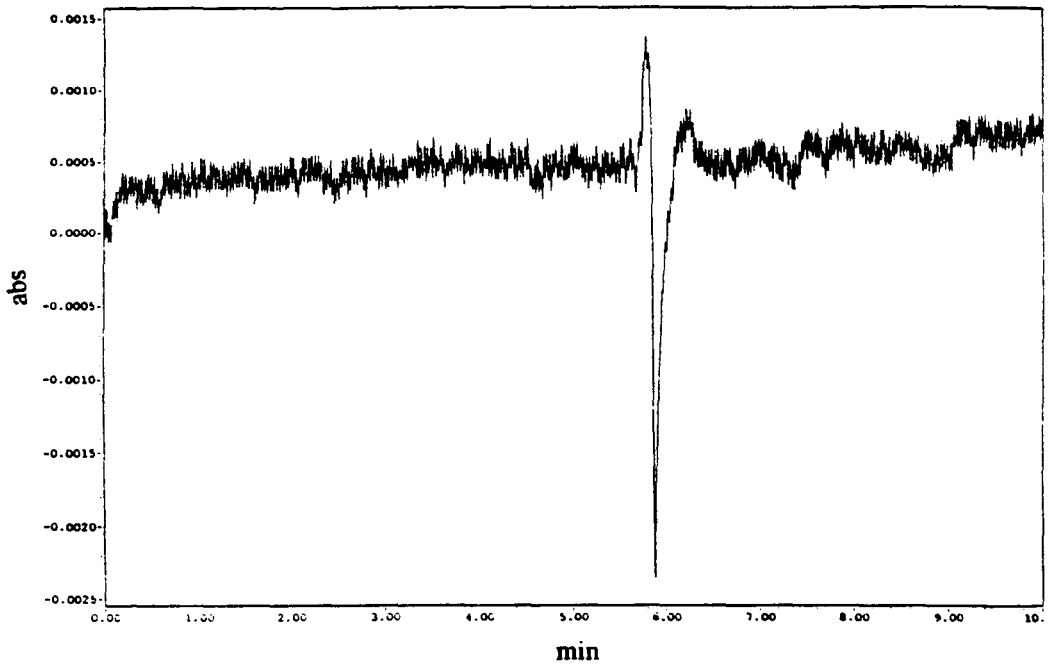

FIGURE 5.27. Electropherogram of Taq1 restriction endonuclease.
(TBE, 20 kV, hydrostatic injection 20 s, 254 nm)

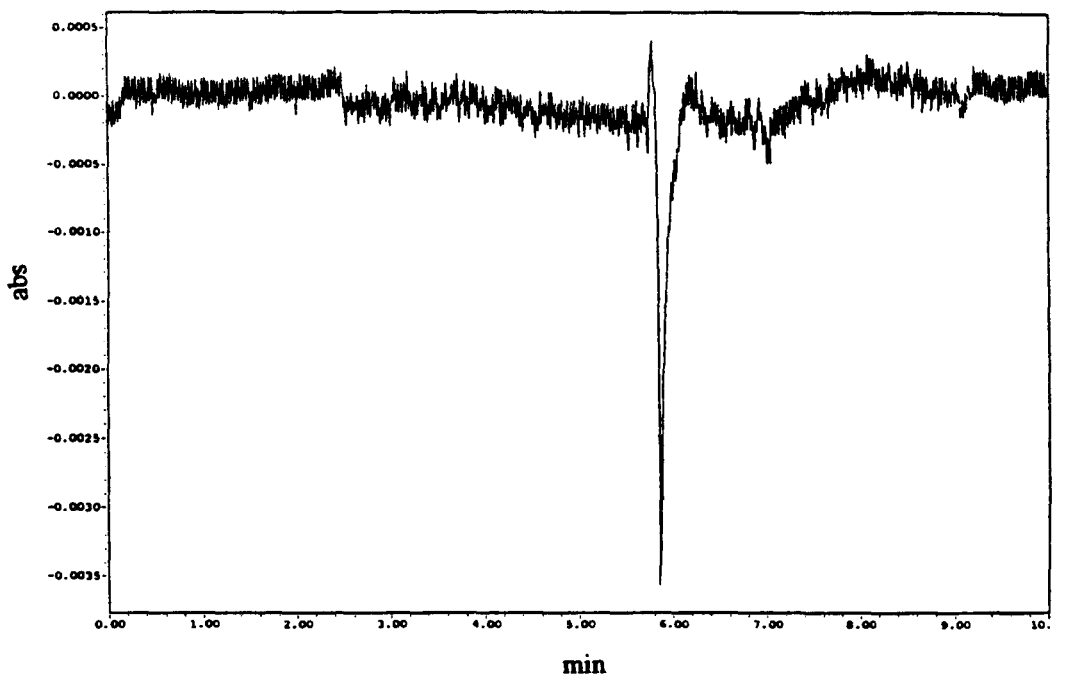

FIGURE 5.28. Electropherogram of EcoR1 restriction endonuclease.
(TBE, 20 kV, hydrostatic injection 20 s, 254 nm)

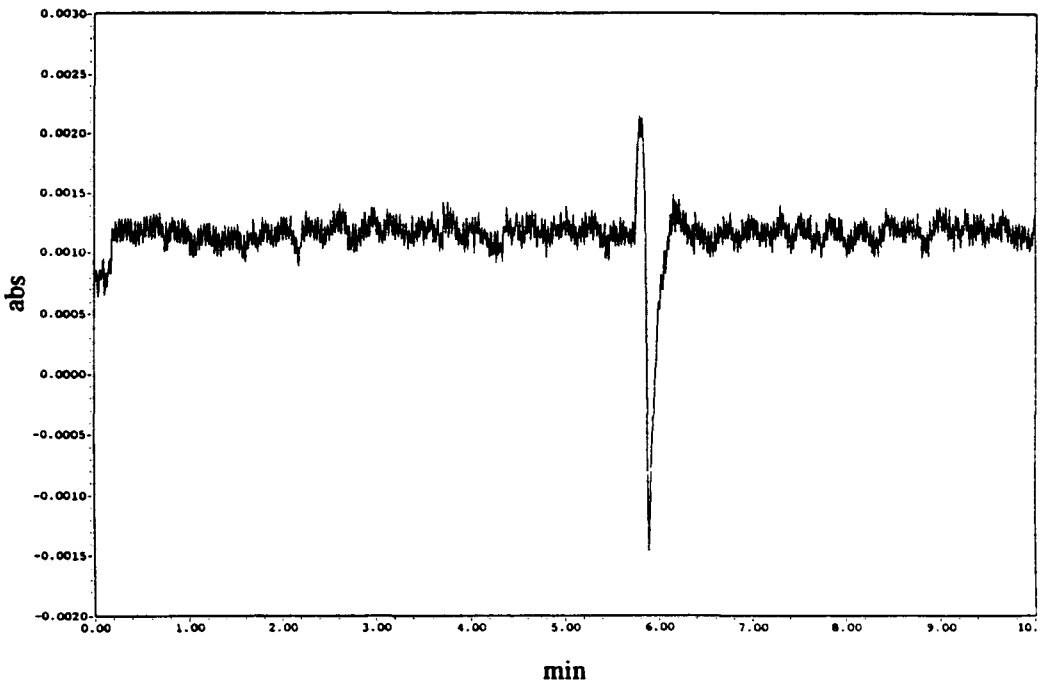

FIGURE 5.29. Electropherogram of Pst1 restriction endonuclease.
(TBE, 20 kV, hydrostatic injection 20 s, 254 nm)

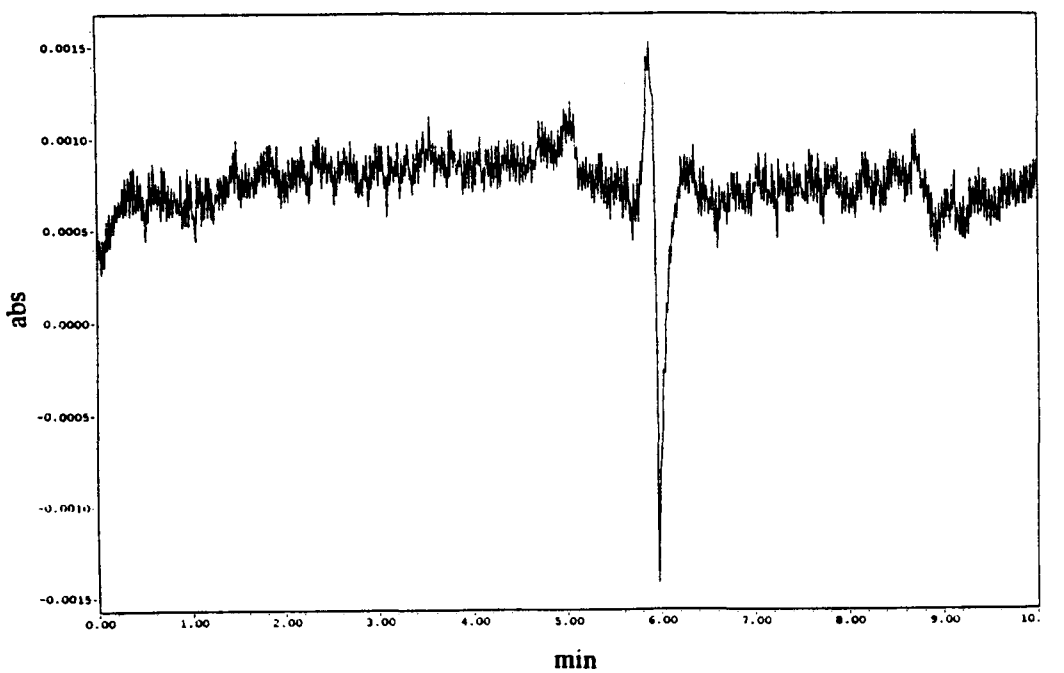

FIGURE 5.30. Electropherogram of Taq1 restriction endonuclease.
(TBE, 20 kV, hydrostatic injection 20 s, 280 nm)

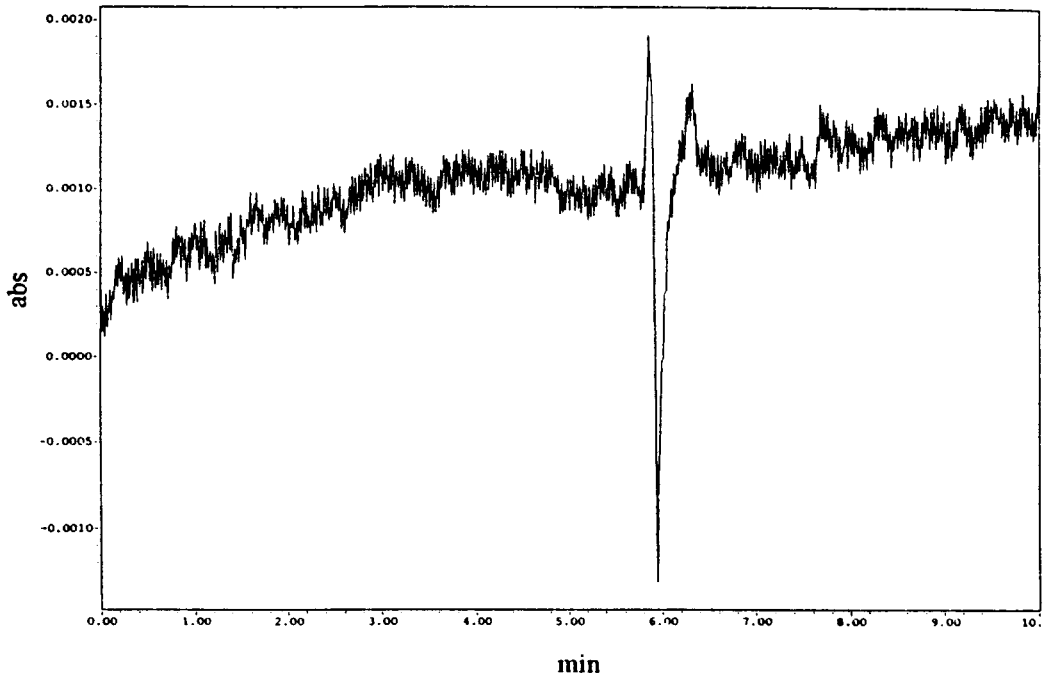

FIGURE 5.31. Electropherogram of EcoR1 restriction endonuclease.
(TBE, 20 kV, hydrostatic injection 20 s, 280 nm)

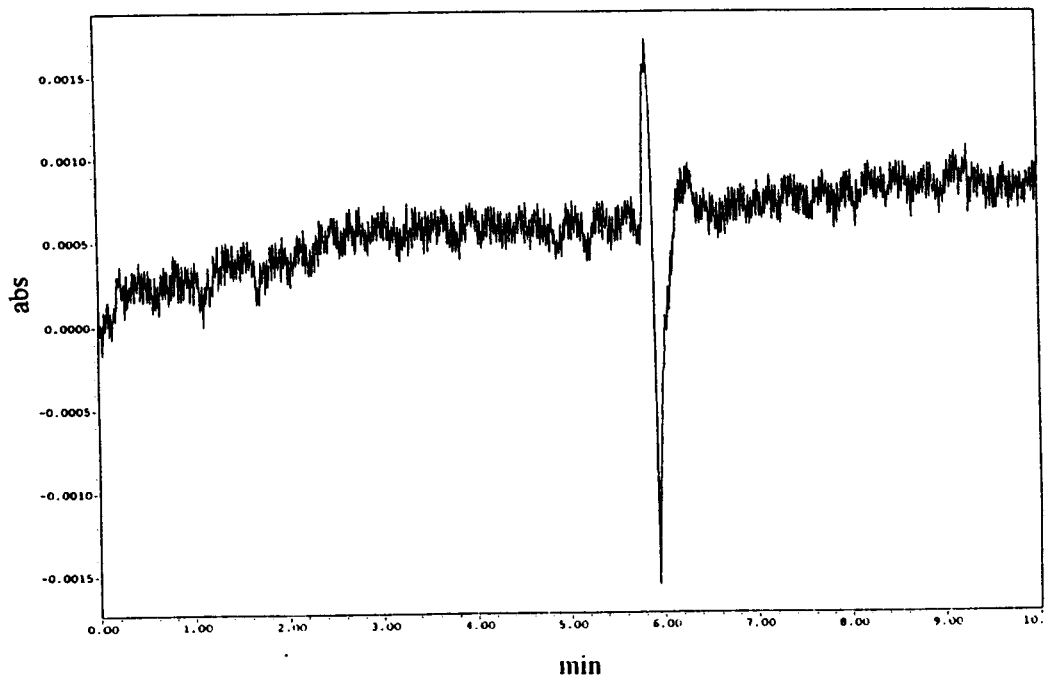

FIGURE 5.32. Electropherogram of Pst1 restriction endonuclease.
(TBE, 20 kV, hydrostatic injection 20 s, 280 nm)

The peak shapes are similar at these two wavelengths and the height of the negative peak increases compared to the analyses under 214 nm. The component eluted at that minute is absorbed more at 254 nm or 280 nm. The restriction enzymes might be analysed in a convenient buffer system with lower absorbance than that of the enzyme and the detection wavelength might be monitored accordingly.

5.3 Capillary Zone Electrophoresis of Serum Proteins

Electrophoresis of serum proteins is one of the traditional applications of zone electrophoresis. Serum proteins are separated into about five fractions: albumin, α_1-globulin, α_2-globulin, β-globulin and γ-globulin. By the modification of the method of separation, the separated zones are assigned to the individual proteins: prealbumin, albumin, α_1-lipoprotein, α_1-antitrypsin, α_2-macroglobulin, haptoglobulin, β-lipoprotein, transferrin, C_3-complement and γ-globulin (Dolnik, 1995).

Human serum proteins were analysed by CZE to check the convenience of the set of conditions developed for the bovine serum albumin. Human serum samples were kindly provided from Düzen Laboratories in Ankara and some of the analyses were performed with the Biorad capillary electrophoresis system fitted with 200 nm deuterium detector lamp in Düzen Laboratories. The serum sample of P#1 was also analysed with the Waters Quanta 4000E capillary electrophoresis system fitted with 214 nm detector lamp. A constant run voltage of 11 kV was applied to both systems and injection was carried out hydrostatically. Dolnik's buffer was used as the run buffer for the capillary zone electrophoresis of serum proteins.

For the analysis of the serum sample of P#1, sample time was adjusted to two seconds in the run performed with the Biorad system while it was increased to five seconds with the Waters system. The electropherograms of serum sample of P#1 can be compared

in Figures 5.33 and 5.34, performed with Biorad and Waters systems respectively. The serum sample was also analysed by monitoring UV absorbance at 254 nm but peaks could not be observed at this wavelength.

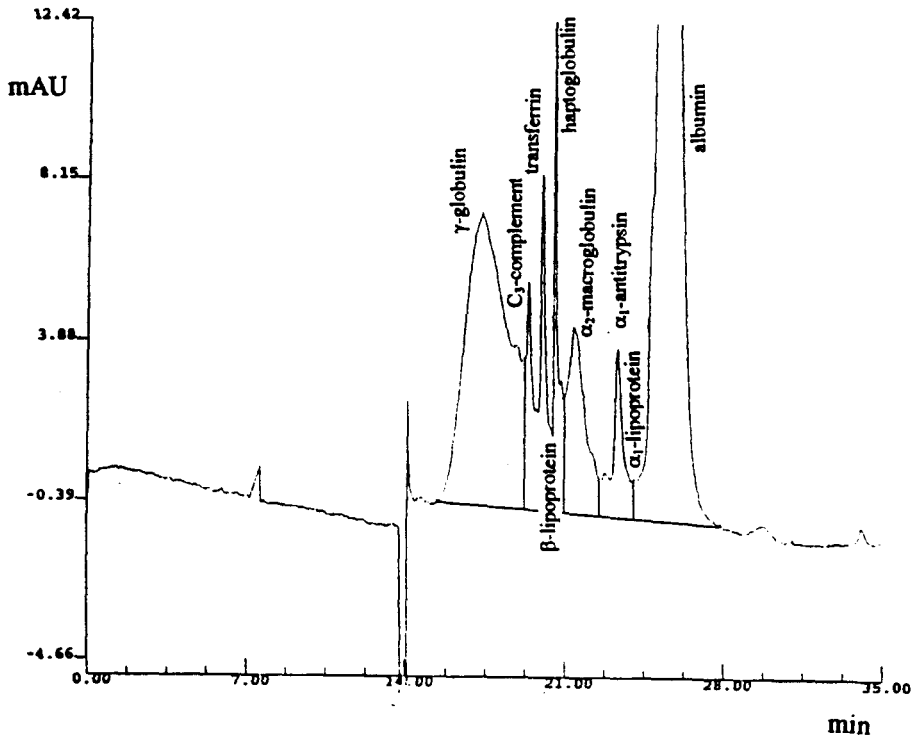

FIGURE 5.33. Electropherogram of P#1.
(Biorad CE system, Dolnik, 11 kV, hydrostatic injection 2 s, 200 nm)

The particular zones were identified according to the generally known migration order of serum proteins on agarose gels. If the fractions were resolved into several subfractions, α_1-antitrypsin, α_2-macroglobulin and transferrin were considered as the main components of α_1-globulin, α_2-globulin and β-globulin, respectively, and their mobilities were used to express the mobility of the whole fraction (Dolnik, 1995).

It is easy to determine that the Biorad system fitted with 200 nm lamp is more efficient to analyse serum proteins since the peaks of protein fractions can be observed more clearly. The highest peak belongs to the human serum albumin, other peaks migrated

before the albumin are the fractions of the serum protein. The separation zones migrate in the order of γ-globulin, C_3-complement, transferrin, β-lipoprotein, haptoglobulin, α_2-macroglobulin, α_1-antitrypsin, α_1-lipoprotein and finally albumin. The difference between the peak shapes obtained with different CE instruments show that optimization of the set of conditions for the analysis of serum proteins is needed in the Waters CE system with 214 nm lamp.

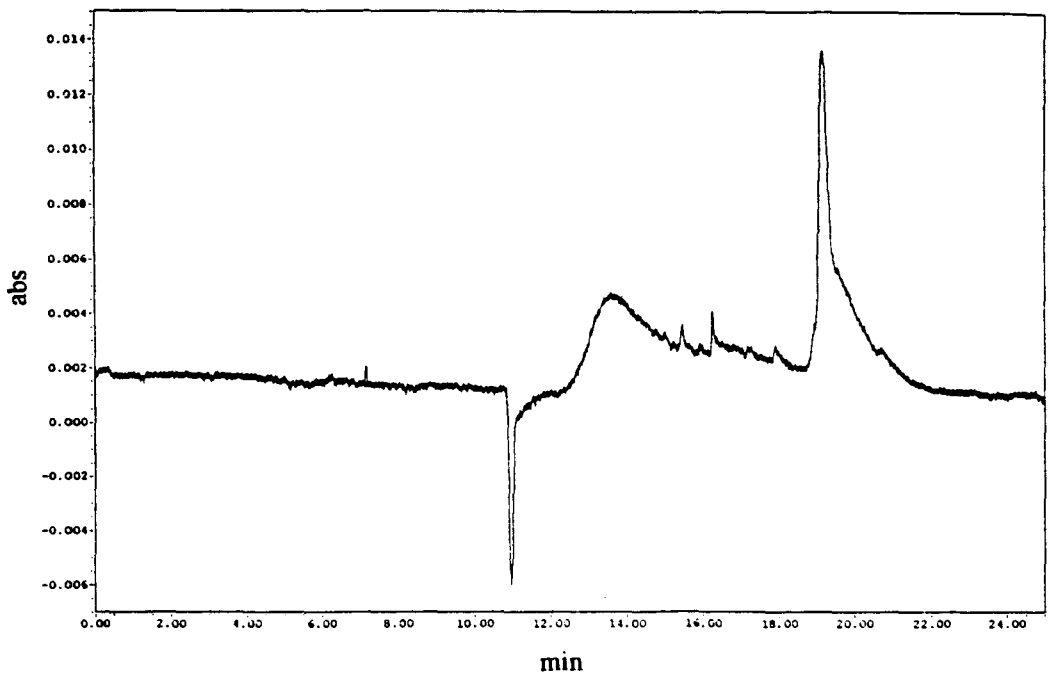

FIGURE 5.34. Electropherogram of P#1.
(Waters CE system, Dolnik, 11 kV, hydrostatic injection 5 s, 214 nm)

The electropherograms of serum samples of other healthy individuals subjected to CZE with the Biorad system are demonstrated in Figures 5.35 and 5.36. The peak heights of the α, β, γ-globulin regions of the serum protein are similar in these normal individuals.

The heights of the γ-globulin regions are higher in the pathological serum samples that belong to P#4 and P#5 (Figures 5.37 and 5.38).

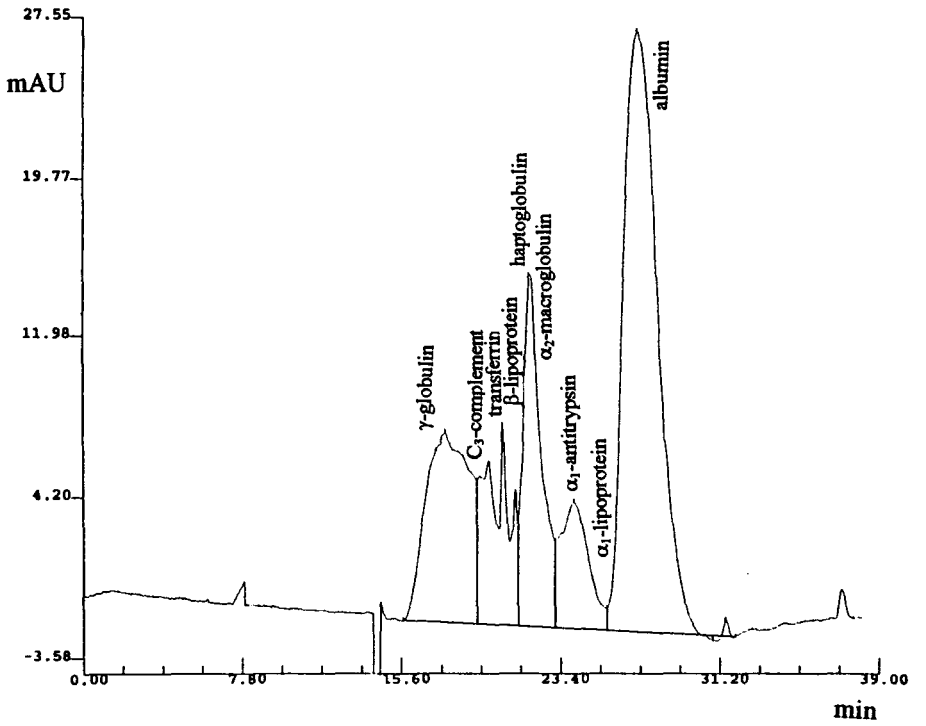

FIGURE 5.35. Electropherogram of P#2.

(Biorad CE system, Dolnik, 11 kV, hydrostatic injection 2 s, 200 nm)

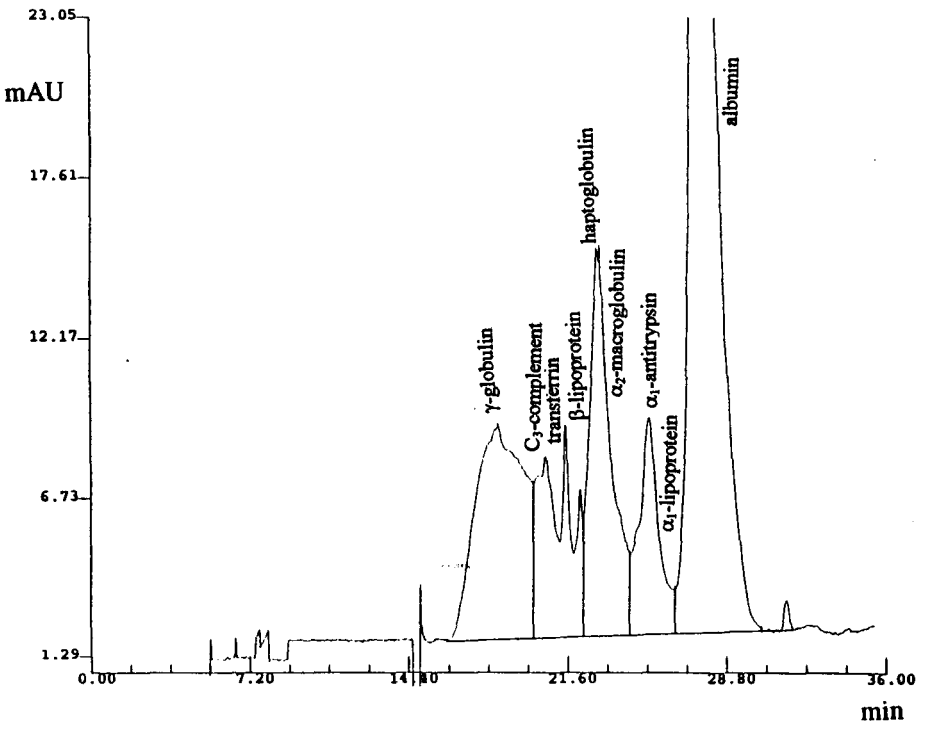

FIGURE 5.36. Electropherogram of P#3.

(Biorad CE system, Dolnik, 11 kV, hydrostatic injection 2 s, 200 nm)

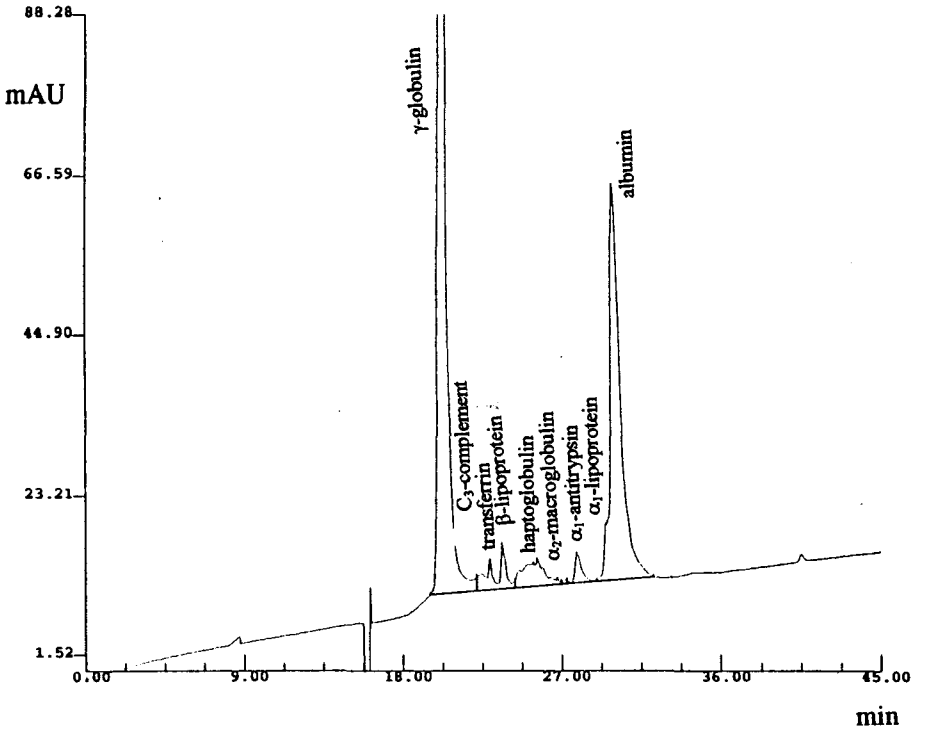

FIGURE 5.37. Electropherogram of P#4.

(Biorad CE system, Dolnik, 11 kV, hydrostatic injection 2 s, 200 nm)

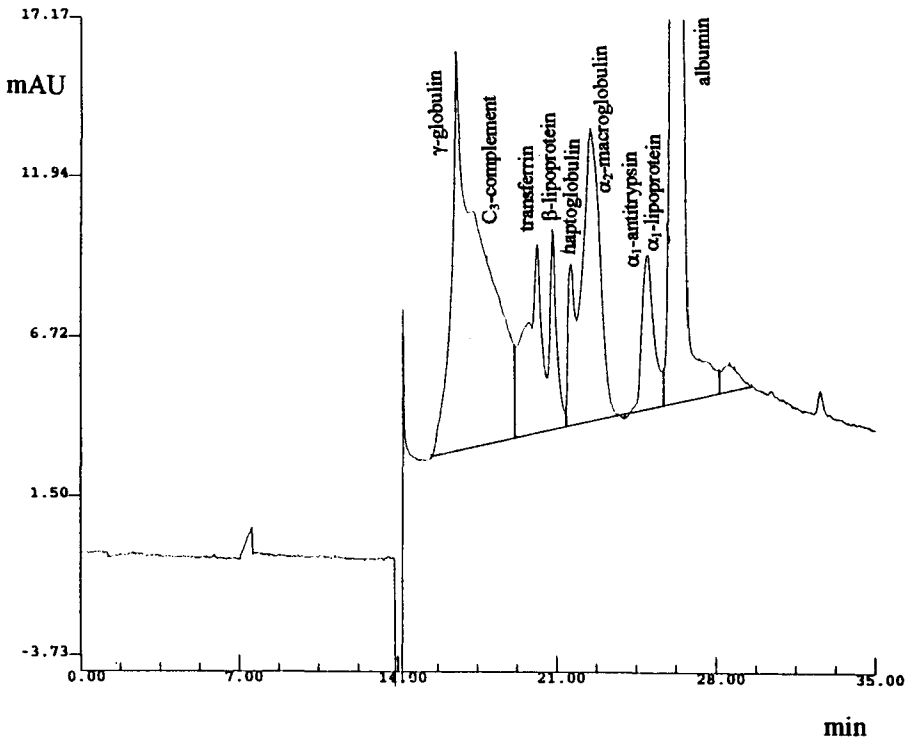

FIGURE 5.38. Electropherogram of P#5.

(Biorad CE system, Dolnik, 11 kV, hydrostatic injection 2 s, 200 nm)

5.4 Capillary Gel Electrophoresis of DNA

DNA mutation detection is important in many fields, including molecular biology, ecology, phylogenetics and medicine, and has become central to the characterization of disease-causing genes and for the diagnosis of human genetic diseases. Conventionally, mutation assays have employed submerged agarose gels and polyacrylamide-gel electrophoresis (PAGE) for separation of the mutant DNA molecule from wild-type molecules. Although agarose gels and PAGE are simple and require low cost equipment, both separation techniques are expensive in terms of time and labour, and neither are particularly amenable to automation (Mitchelson et al., 1997).

Capillary zone electrophoresis in polymer networks has recently become an important tool for size-fractionation of macromolecules, particularly in the case of nucleic acids, where the charge-to-mass ratio is constant over a large interval of molecular sizes. It consists of dissolving, in the background electrolyte, linear polymers of various sizes, above a critical threshold (entanglement threshold) which then exert sieving on macromolecular analytes just as chemically cross-linked gels do. A few reports have appeared on the use of CZE in polymer networks for the analysis of PCR fragments (Gelfi et al., 1994).

Cystic fibrosis (CF) is the most common severe autosomal recessive genetic disorder in the white population, having a carrier frequency of 1 in 25 and an incidence of 1 in 2500 liveborns. The disease is caused by mutations in cystic fibrosis transmembrane conductance regulator (CFTR) gene. The predominant mutation causing CF is a 3-bp deletion in exon 10, ΔF508, results in the loss of the phenylalanine 508 residue of the putative protein, accounting for about 24% of the molecular defects in Turkish CF patients (Onay, 1999).

In order to establish a novel mutation detection technique using capillary electrophoresis, PCR amplified fragments from normal, homozygous and heterozygous Turkish cystic fibrosis carriers harboring a defined mutation were also analysed by capillary gel electrophoresis. The presence of the mismatches within the heteroduplexes was to result in conformational changes and so they were to be detected by capillary electrophoresis due to the difference in their electrophoretic mobilities.

The DNA fragments from the CFTR gene were amplified by polymerase chain reaction and the quality of amplification was checked on the agarose gel (Figure 4.39). The samples run on the lower part of the agarose gel were amplified using primers from a different stock solution.

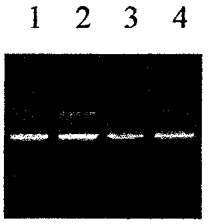

FIGURE 5.39. Agarose Gel Electrophoresis of PCR amplified DNA fragments. Lane 1: 491 bp, genotype: N/N, 1540 A/G: A/A, Lane 2: 491 bp, genotype: N/N, 1540 A/G: G/G, Lane 3: 491 bp, genotype: ΔF508/N, 1540 A/G: A/A, Lane 4: 491 bp, genotype: ΔF508/ΔF508, 1540 A/G: A/A.

For the capillary electrophoretic analysis of the PCR amplified 491 bp DNA fragments (Figure 5.39), fused silica capillaries were fitted onto the system and dynamic coating with linear polyacrylamide containing buffer was carried out. The run buffer was prepared by adding 6 per cent bis-acrylamide (6 per cent T 0 per cent C polyacrylamide solution) into the TBE buffer. The runs were performed at negative polarity using the negative power supply and detection was carried out at 254 nm.

This dynamic approach for capillary coating for the analysis of DNA fragments was not successful. However, capillary electrophoresis in non-cross-linked polymer solutions has been shown to be a promising technique for the rapid and efficient separation of DNA restriction fragments up to 23,000 bp in size. While cross-linking a homogeneous and stress-free gel within a capillary can be problematic, the use of non-cross-linked polymer solutions enables high resolution DNA separations to be carried out in an uncoated capillary. Solutions of non-cross-linked polymers have been found to have separation potential over a wide range of concentrations, from semi-dilute, low viscosity solutions to extremely concentrated, "syrupy" solutions which are so viscous that they cannot be injected into a capillary and must be polymerized in situ (Barron et al., 1993).

The two disturbing phenomena of electrophoresis, that is electroendosmosis and adsorption of solutes onto the inside of the column, are negligible in capillary electrophoresis when the capillary column is coated with a monomolecular layer of non-cross-linked polyacrylamide. There are many works in literature on the use of static coating for the analysis of DNA fragments by capillary electrophoresis (Hjerten, 1985).

Capillary gel electrophoresis of synthetic oligonucleotides on the Waters Quanta 4000E system offers reproducible separations with excellent component resolution as demonstrated by the analysis of a phosphodeoxyadenine standard mixture (Figure 5.40).

The polyacrylamide gel-filled (5 per cent T, 5 per cent C gel) columns were tested with the pd $(A)_{25\text{-}30,40\text{-}60}$ oligonucleotide standard. After cutting and conditioning the column, the standard sample was run at 12.5 kV at negative polarity using electrokinetic injection. The cutting procedure was carried out very carefully and the standard μPAGE buffer, which was specific for the column, was degassed and filtered prior to use not to allow any air bubbles into the system. Detection was at 254 nm.

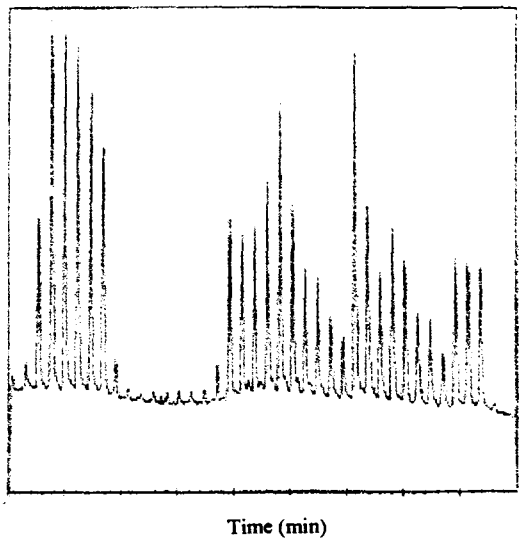

FIGURE 5.40. Elution profile of pd $(A)_{25\text{-}30,40\text{-}60}$ oligonucleotide standard (Waters Corporation, 1998).

The elution profile should have been similar to that shown on the column performance summary sheet in Figure 5.40. During the run with the oligonucleotide standard, the first group of peaks on the electropherogram was observed but about 30 minutes after injection, a sudden decrease in the current occurred. When the current reached almost zero, the absorbance also changed dramatically causing vanishing of the peaks, therefore a proper electropherogram could not be observed although conditioning of the column was carried out properly at constant current as proposed.

The decrease in the current during the run was probably caused by bubbles that had entered into the gel-filled capillary somehow. The bubble formation within the gel matrix might have occurred due to gel hydration prior to immersion in buffer or insufficient removal of gel degraded during flame sealing. A small portion near the column end, which might have been the voided portion, was cut away to recover the column. A second conditioning was applied but the current fluctuations continued. The column was discarded and another gel-filled μ-PAGE column was replaced.

The new gel-filled capillary was conditioned as proposed in the instruction manual, the current remained constant. The oligonucleotide standard was injected for five seconds at 5 kV and run at 12.5 kV as proposed but an electropherogram similar to the one in Figure 5.40 could not be observed.

In order to check the performance of the mercury lamp detecting at 254 nm fitted onto the system, sodium chromate solution, which was visible under 254 nm wavelength, was prepared and the system was purged with increasing concentrations of this solution.

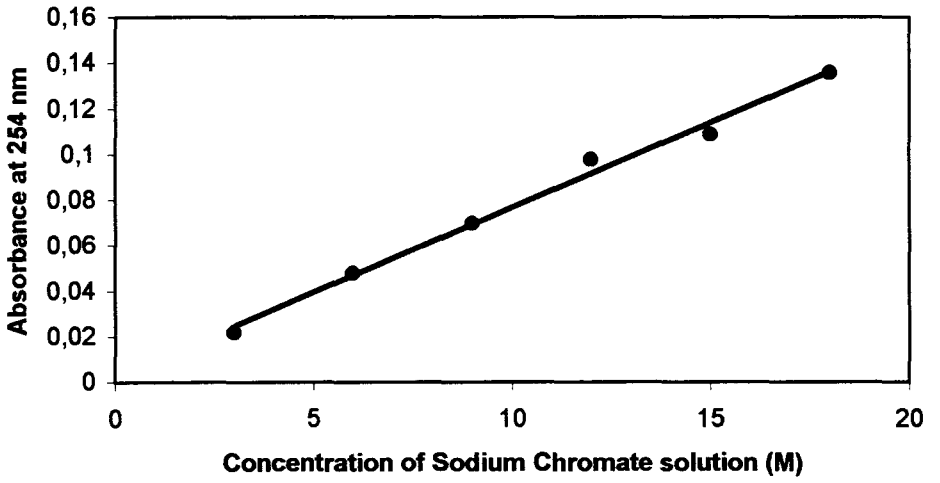

FIGURE 5.41. Detector performance check.

A linear increase in the recorded absorbance values was observed as the concentration of the solution purged was increased (Figure 5.41). The result of this check proves that the mercury lamp is properly working. Therefore, since there is no technical problem on any part of the instrument, further studies and optimization of dynamic coating of the fused silica capillaries or static coating with non-cross-linked polyacrylamide for the analysis of DNA fragments should be carried out.

6. CONCLUSIONS AND RECOMMENDATIONS

The major aim of this thesis was to develop a capillary electrophoresis method for the analysis of some proteins and DNA. Capillary zone electrophoresis was performed with mainly bovine serum albumin, some restriction enzymes, namely Taq1, EcoR1 and Pst1, and human serum proteins. For the analysis of DNA, capillary zone electrophoresis with dynamic coating and capillary gel electrophoresis were carried out. The factors affecting analytical parameters such as retention time, peak height and peak shape were studied. These factors were different buffer systems, capillary dimensions, detector wavelengths, polarity modes, applied voltage, sample injection modes and sample loading amounts.

The conclusions drawn from this study based on the results presented are summarized below followed by the recommendations for future work.

6.1 Conclusions

- For the capillary zone electrophoresis of BSA, borate, TBE and Dolnik's buffer systems were used. The smallest retention time was observed with the TBE buffer system while BSA migrated slowest in the borate buffer. The height of the major peak was the same in borate and TBE buffer systems. Peak height was lower and the peak was broader in Dolnik's buffer system.

- The optimum wavelength for the detection of BSA was 214 nm.

- When a shorter capillary column was used, migration of BSA was faster, less zone broadening and narrower peak was observed.

- An increase in the run voltage resulted in a decrease in the migration time of BSA. Highest voltages possible should be used for the fastest and most efficient separation.

- The peak height was affected mainly by the sample loading amount. The amount of sample loaded was increased by increasing the sample injection time, thus a higher peak was observed.

- The peak height was lower when the sample was introduced by electromigration. Broader peaks were obtained with hydrostatic injection mode, minimal band broadening was observed in electrokinetic injection with sharper peaks.

- Since BSA was negatively charged in the pH range of the buffer system used (TBE), it migrated earlier in the reversed polarity mode where the negative high voltage power supply was used. No peaks were observed at reversed polarity with the borate buffer system.

- The restriction enzymes Taq1, EcoR1 and Pst1 were analysed in TBE buffer system at 214 nm. One major peak with the same retention time was observed with all three enzyme samples, which was doubted to be a component in the storage buffer since the same peak was observed when the storage buffer was run in the same buffer system under the same conditions. The other peaks in the electropherograms could not be identified, therefore TBE buffer system was found to be not suitable for the CZE of restriction enzymes.

- The most appropriate buffer system for the analysis of human serum proteins was Dolnik's buffer with detection at 214 nm. The fractions of the serum protein were identified on the electropherogram in the order of γ-globulin, C_3-complement, transferrin, β-lipoprotein, haptoglobulin, α_2-macroglobulin, α_1-antitrypsin, α_1-lipoprotein and finally albumin.

- For the analysis of PCR amplified DNA fragments, capillary zone electrophoresis with dynamic coating by using polyacrylamide-containing buffer was not successful.

6.2 Recommendations

- The parameters that affect the efficiency and resolution of capillary electrophoretic separation of proteins need to be optimized carefully. Validation of the optimized method is also necessary.

- Different buffer systems need to be tested for the capillary zone electrophoresis of the restriction enzymes in order to develop a suitable method of analysis. As observed in the case of BSA analysis, care should be taken for the optimization of each set of conditions.

- For the analysis of PCR amplified DNA fragments, a polymer network capillary separation system should be developed by optimization of the dynamic coating procedure. Entangled solution capillary electrophoresis might be performed with the addition of ethidium bromide to the run buffer to improve the separation.

• Static coating of the capillary column with linear polyacrylamide as proposed by Hjerten (Hjerten, 1985) to analyse the DNA fragments is needed. The inside of the capillary wall can be coated with γ-methacryloxypropyltrimethoxysilane solution first and then by deaerated acrylamide solution.

REFERENCES

Bae, Y. C., D. Soane, "Polymeric Separation Media for Electrophoresis: Cross-Linked Systems or Entangled Solutions," *Journal of Chromatography A*, Vol. 652, pp. 17-22, 1993.

Barron, A. E., D. S. Soane, H. W. Blanch, "Capillary Electrophoresis of DNA in Uncross-Linked Polymer Solutions," *Journal of Chromatography A*, Vol. 652, pp. 3-16, 1993.

Cheng, J., K. R. Mitchelson, "Glycerol-Enhanced Separation of DNA Fragments in Entangled Solution Capillary Electrophoresis," *Analytical Chemistry*, Vol. 66, No. 23, pp. 4210-4214, 1994.

Cheng, Y. F., M. Fuchs, D. Andrews, W. Carson, "Membrane Fraction Collection for Capillary Electrophoresis," *Journal of Chromatography*, Vol. 608, pp. 109-116, 1992.

Chiu, R. W., K. L. Walker, J. J. Hagen, C. A. Monnig, C. L. Wilkins, "Coaxial Capillary and Conductive Capillary Interfaces for Collection of Fractions Isolated by Capillary Electrophoresis," *Analytical Chemistry*, Vol. 67, pp. 4190-4196, 1995.

Dolnik, V., "Capillary Zone Electrophoresis of Serum Proteins: Study of Separation Variables," *Journal of Chromatography A*, Vol. 709, pp. 99-110, 1995.

Gelfi, C., A. Orsi, P. G. Righetti, V. Brancolini, L. Cremonesi, M. Ferrari, "Capillary Zone Electrophoresis of Polymerase Chain Reaction-Amplified DNA Fragments in Polymer Networks: The Case of GATT Microsatellites in Cystic Fibrosis," *Electrophoresis*, Vol. 15, pp. 640-643, 1994.

Grossman, P. D., D. S. Soane, "Capillary Electrophoresis of DNA in Entangled Polymer Solutions," *Journal of Chromatography*, Vol. 559, pp. 257-266, 1991.

Halloran, M., *SPCE Method*, Düzen Laboratory Interoffice Memorandum, 1998.

Hjerten, S., "High-Performance Electrophoresis, Elimination of Electroendosmosis and Solute Adsorption," *Journal of Chromatography*, Vol. 347, pp. 191-198, 1985.

Jorgenson, J. W., K. D. Lukacs, "Zone Electrophoresis in Open-Tubular Glass Capillaries," *Analytical Chemistry*, Vol. 53, pp. 1298-1302, 1981.

Kuhn, R., S. Hoffstetter-Kuhn, *Capillary Electrophoresis: Principles and Practice*, Springer-Verlag, Berlin, 1993.

Mitchelson, K. R., J. Cheng, L. J. Kricka, "The Use of Capillary Electrophoresis for Point-Mutation Screening," *Trends in Biotechnology*, Vol. 15, pp. 448-458, November 1997.

Müller, O., F. Foret, B. L. Karger, "Design of a High-Precision Fraction Collector for Capillary Electrophoresis," *Analytical Chemistry*, Vol. 67, pp. 2974-2980, 1995.

Onay, Tuncer, "Spectrum of Cystic Fibrosis Mutations and Haplotype Analysis in Turkish CF Families," Ph.D. Dissertation, Boğaziçi University, 1999.

Pande, P. G., R. V. Nellore, H. R. Bhagat, "Optimization and Validation of Analytical Conditions for Bovine Serum Albumin Using Capillary Electrophoresis," *Analytical Biochemistry*, Vol. 204, pp. 103-106, 1992.

Quesada, M. A., "Replaceable Polymers in DNA Sequencing by Capillary Electrophoresis," *Current Opinion in Biotechnology*, Vol. 8, pp. 82-93, 1997.

Rose, D. J., J. W. Jorgenson, "Fraction Collector for Capillary Electrophoresis," *Journal of Chromatography*, Vol. 438, pp. 23-34, 1988.

Rush, R. S., A. S. Cohen, B. L. Karger, "Influence of Column Temperature on the Electrophoretic Behavior of Myoglobin and α-Lactalbumin in High-Performance Capillary Electrophoresis," *Analytical Chemistry*, Vol. 63, pp. 1346-1350, 1991.

Schwartz, H. E., R. H. Palmieri, J. A. Nolan, R. Brown, *Separation of Proteins and Peptides by Capillary Electrophoresis: an Introduction*, Beckman, 1992.

Srinivasan, K., J. E. Girard, P. Wiliams, R. K. Roby, V. W. Weedn, S. C. Morris, M. C. Kline, D. J. Reeder, "Electrophoretic Separations of Polymerase Chain Reaction-Amplified DNA Fragments in DNA Typing using Capillary Electrophoresis-Laser Induced Fluorescence System," *Journal of Chromatography A*, Vol. 652, pp. 83-91, 1993.

Wahlbroehl, Y., J. W. Jorgenson, "On-Column UV Absorption Detector for Open Tubular Capillary Zone Electrophoresis," *Journal of Chromatography*, Vol. 315, pp. 135-143, 1984.

Waters Corporation, *Capillary Ion Analysis Cookbook*, 1995.

Waters Corporation, *Essentials in Bioresearch, Rapid Analysis of Synthetic Oligonucleotides by Capillary Gel Electrophoresis*, 1998.

Weinberger, R., *Practical Capillary Electrophoresis*, Short Course presented during the HPLC'98 Symposium, CE Technologies, 1998.

Zhu, M., D. L. Hansen, S. Burd, F. Gannon, "Factors Affecting Free Zone Elecrophoresis and Isoelectric Focusing in Capillary Electrophoresis," *Journal of Chromatography*, Vol. 480, pp. 311-319, 1989.

REFERENCES NOT CITED

Chan, K. C., G. M. Muschik, H. J. Issaq, K. J. Garvey, P. L. Generlette, "High-Speed Screening of Polymerase Chain Reaction Products by Capillary Electrophoresis," *Analytical Biochemistry*, Vol. 243, pp. 133-139, 1996.

Cheng, J., T. Kasuga, K. R. Mitchelson, E. R. T. Lightly, N. D. Watson, W. J. Martin, D. Atkinson, "Polmerase Chain Reaction Heteroduplex Polymorphism Analysis by Entangled Solution Capillary Electrophoresis," *Journal of Chromatography A*, Vol. 677, pp. 169-177, 1994.

Chiari, M., M. Nesi, P. G. Righetti, "Movement of DNA Fragments during Capillary Zone Electrophoresis in Liquid Polyacrylamide," *Journmal of Chromatography A*, Vol. 652, pp. 31-39, 1993.

Fung, E. N., E. S. Yeung, "High-Speed DNA Sequencing by Using Mixed Poly(ethylene oxide) Solutions in Uncoated Capillary Columns," *Analytical Chemistry*, Vol. 67, pp. 1913-1919, 1995.

Gelfi, C., A. Orsi, P. G. Righetti, M. Zanussi, P. Carrera, M. Ferrari, "Capillary Zone Electrophoresis in Polymer Networks of Polymerase Chain Reaction-Amplified Oligonucleotides: The Case of Congenital Adrenal Hyperplasia," *Journal of Chromatography B*, Vol. 657, pp. 201-205, 1994.

Gelfi, C., P. G. Righetti, V. Brancolini, L. Cremonesi, M. Ferrari, "Capillary Electrophoresis in Polymer Networks for Analysis of PCR Products: Detection of ΔF508 Mutation in Cystic Fibrosis," *Clinical Chemistry*, Vol. 40, No. 8, pp. 1603-1605, 1994.

Kasper, T. J., M. Melera, P. Gozel, R. G. Brownlee, "Separation and Detection of DNA by Capillary Electrophoresis," *Journal of Chromatography*, Vol. 458, pp. 303-312, 1988.

Khrapko, K., J. S. Hanekamp, W. G. Thilly, A. Belenkii, F. Foret, B. L. Karger, "Constant Denaturant Capillary Electrophoresis (CDCE): A High Resolution Approach to Mutational Analysis," *Nucleic Acids Research*, Vol. 22, No. 3, pp. 364-369, 1994.

McCord, B. R., D. L. McClure, J. M. Jung, "Capillary Electrophoresis of Polymerase Chain Reaction-Amplified DNA using Fluorescence Detection with an Intercalating Dye," *Journal of Chromatography A*, Vol. 652, pp. 75-82, 1993.

McGregor, D. A., E. S. Yeung, "Optimization of Capillary Electrophoretic Separation of DNA Fragments based on Polymer Filled Capillaries," *Journal of Chromatography A*, Vol. 652, pp. 67-73, 1993.

Maniatis, T., E. F. Fritsch, *Molecular Cloning-A Laboratory Manual*, Cold Spring Harbour Laboratory Publications, New York, 1984.

Pariat, Y. F., J. Berka, D. N. Heiger, T. Schmitt, M. Vilenchik, A. S. Cohen, F. Foret, B. L. Karger, "Separation of DNA Fragments by Capillary Electrophoresis using Replaceable Linear Polyacrylamide Matrices," *Journal of Chromatography A*, Vol. 652, pp. 57-66, 1993.

Thorne, J. M., W. K. Goetzinger, A. B. Chen, K. G. Moorhouse, B. L. Karger, "Examination of Capillary Zone Electrophoresis, Capillary Isoelectric Focusing and Sodium Dodecyl Sulfate Capillary Electrophoresis for the Analysis of Recombinant Tissue Plasminogen Activator," *Journal of Chromatography A*, Vol. 744, pp. 155-165, 1996.

Widhalm, A., C. Schwer, D. Blaas, E. Kenndler, "Capillary Zone Electrophoresis with A Linear, Non-Cross-Linked Plyacrylamide Gel: Separation of Proteins according to Molecular Mass," *Journal of Chromatography*, Vol. 549, pp. 446-451, 1991.

Wu, D., F. E. Regnier, "Sodium Dodecyl Sulfate-Capillary Gel Electrophoresis of Proteins Using Non-Cross-Linked Polyacrylamide," *Journal of Chromatography*, Vol. 608, pp. 349-356, 1992.